Universitat Politècnica de València
Departamento de Máquinas y Motores Térmicos

DUAL-FUEL DUAL-MODE COMBUSTION STRATEGY TO ACHIEVE HIGH THERMAL EFFICIENCY, LOW NO_X AND SMOKE EMISSIONS IN COMPRESSION IGNITION ENGINES

Doctoral Thesis

Presented by:
Vicente Boronat Colomer
Directed by:
Dr. Antonio García Martínez

Valencia, September 2018

Doctoral Thesis

DUAL-FUEL DUAL-MODE COMBUSTION STRATEGY TO ACHIEVE HIGH THERMAL EFFICIENCY, LOW NO_X AND SMOKE EMISSIONS IN COMPRESSION IGNITION ENGINES

Presented by: Vicente Boronat Colomer
Directed by: Dr. Antonio García Martínez

Examining Board:

President: Prof. Raúl Payri Marín
Secretary: Prof. Juan José Hernández Adrover
Examiner: Dr. Carlo Beatrice

Reviewing Board:

Prof. Rosario Ballesteros Yáñez
Dr. Carlo Beatrice
Dr. Christopher Paul Kolodziej

Valencia, September 2018

Abstract

High thermal efficiency coupled to minimum pollutants emissions imposed by the stringent standard emissions limitations in reciprocating engines represent the main target of the engine manufacturers industry.

Conventional diesel combustion strategy is widely used worldwide due to its excellent fuel economy. This combustion strategy allows operating under lean mixtures of fuel and air that provide high thermal efficiency. In addition, this type of combustion can be applied from light-duty engines to large bore marine engines. However, the combustion process leads to high NOx and particle matter emissions, being impossible to reduce both pollutants simultaneously. Hence, manufactures have incorporated aftertreatment systems in order to meet the imposed standard emissions limitations, which are aimed to provide cleaner emissions and high efficiency. By contrast, these systems required for the emissions mitigation result in a very complex processes and an increase in the engine production and operational costs. The research community continues developing alternative solutions to the conventional diesel combustion concept keeping the benefits of this combustion process while the emissions are reduced (mainly focused on NOx and soot).

Research community have found in the low temperature combustion strategies the combustion process able to provide excellent high thermal efficiency and ultra-low NOx and smoke emissions. In this sense, the literature review states that this types of combustion processes allow the simultaneous reduction of NOx and smoke, breaking the traditional trade-off found in diesel engines. Amongst others, the most promising strategy is the reactivity controlled compression ignition. This combustion process is characterized by using two fuels and is able to solve the main challenges of the low temperature combustion processes such as combustion phasing control. Nonetheless, the reactivity controlled strategy also presents some challenges such as excessive carbon monoxide and unburned hydrocarbons

during low load operation and high pressure rise rate and in-cylinder pressure that limit the engine range operation.

The general objective of this investigation is to provide a dual-fuel strategy able to operate over the whole range providing similar or better thermal efficiency that the conventional diesel combustion and ultra-low values of NOx and smoke. In addition, the investigation also explores the particle emissions of the concept since it is regulated by the standard emissions.

The combustion process that responds to the target provided at the general objective is the Dual-Fuel Dual-Mode concept. This concept uses two fuels and switches from a dual-fuel fully premixed strategy (based on the RCCI concept) during low load operation to a diffusive nature during high load operation. In order to explore the capabilities of the concept, two hardware configurations are used and a particle size distribution exploration is performed.

Finally, considering the main findings of the investigation, the last chapter is aimed to provide the benefits of the combustion process developed as well as the main limitations or future works of the concept.

Resumen

Elevada eficiencia térmica y mínimas emisiones contaminantes impuestas por las restrictivas normativas anticontaminación en motores alternativos representan el principal objetivos de los fabricantes de motores.

La estrategia de combustión diésel convencional es ampliamente utilizada en el mundo gracias a su excelente economía en el consumo de carburante. Esta estrategia permite operar con mezclas pobres de combustible y aire proporcionando elevada eficiencia térmica. Además, este tipo de combustión puede ser aplicada desde motores tanto para vehículos ligeros como en motores marinos. Sin embargo, este proceso de combustión conlleva a la generación de elevadas emisiones de NOx y emisiones de partículas (comúnmente llamado hollín en los diésel), siendo imposible reducir ambos contaminantes de forma simultánea. Por tanto, los fabricantes han incorporado sistemas de post-tratamiento con el objetivo de cumplir con las normativas de emisiones, cuya intención es la de proveer emisiones más limpias y elevada eficiencia. Por el contrario, este tipo de sistemas para mitigar las emisiones contaminantes incrementan la complejidad del motor dado el complejo proceso llevado a cabo durante el post-tratamiento y una aumento en los costes tanto de producción como operativos a lo largo del ciclo de vida del motor. La comunidad científica continua desarrollando soluciones alternativas a la combustión diésel convencional manteniendo los beneficios de este proceso de combustión mientras que las emisiones son reducidas (principalmente NOx y hollín).

La comunidad científica ha encontrado en las estrategias de combustión de baja temperatura un proceso de combustión capaz de proporcionar elevada eficiencia térmica y emisiones ultra bajas de NOx y humo. En este sentido, la revisión bibliográfica dice que estos tipos de combustión permiten la reducción simultánea de ambas emisiones, rompiendo así el tradicional *"trade-off"* existente en la combustión diésel convencional. Sobre todas las estrategias, la que muestra un potencial superior es la estrategia conocida como combustión dominada por la reactividad del combustible. Este proceso

de combustión se caracteriza por emplear dos combustibles, siendo capaz de solucionar los principales problemas de las estrategias de baja temperatura tales como el fasado de la combustión. Sin embargo, esta estrategia de combustión también presenta algunos inconvenientes como el elevado nivel de monóxido de carbono e hidrocarburos inquemados a baja carga y elevado gradiente de presión y presión en cámara a elevada carga que limitan el rango de operación.

El objetivo general de la presente investigación es proveer de una estrategia de combustión *"dual-fuel"* capaz de operar sobre todo el rango de operación de un motor proporcionando igual o mejores eficiencia térmica que el diésel convencional y emisiones ultra bajas de NOx y humos. Adicionalmente, esta investigación implica una exploración delas emisiones de las partículas del concepto de combustión ya que el número de partículas se encuentra actualmente regulado por la normativa anticontaminante.

El proceso de combustión que responde a este objetivo es *"Dual-Mode Dual-Fuel".* Este concepto de combustión emplea dos combustibles y cambia de combustión premezclada a baja carga a combustión de naturaleza difusiva a plena carga. Con el deseo de explorar las capacidades de la estrategia de combustión, se han empleado dos configuraciones de *"hardware"* y se ha realizado un estudio de la distribución por tamaños de las partículas.

Finalmente, considerando los principales resultados de la investigación, el último capítulo pretende resumir las principales bondades del concepto de combustión así como sus limitaciones y trabajos futuros.

Resum

Elevada eficiència tèrmica i mínimes emissions contaminants impostes per les normatives anticontaminants en motores alternatius representen el principal objectiu dels fabricants de motors.

La estratègia de combustió diésel convencional es àmpliament utilitzada per tot el mon gracies al excel · lent consum de carburant. Esta estratègia permet operar el motor amb dosatges pobres que resulten en elevada eficiència tèrmica. A més, aquest tipus de combustió pot ser aplicada tant a els motor mes lleugers con als motor per aplicacions marines. No obstant això, aquest procés de combustió implica la generació de elevats nivells de emissió de NOx i sutja, que no es poden reduir simultàniament. Per tant, els fabricants han incorporat sistemes de post-tractament amb el objectiu de acomplir les normatives anticontaminació, que pretenen obtindre motors en emissions mes netes i mes eficients. Per el contrari, aquest tipus de sistemes per a reduir les emissions incrementen la complexitat del motor i els costos tant de producció com operatius al llarg del cicle de vida del motor. La comunitat científica continua desenvolupant solucions alternatives a la combustió dièsel mantenint els beneficis d´aquest tipus de combustió però reduint les emissions (principalment NOx i sutja).

La comunitat científica ha trobat a les estratègies de combustió de baixa temperatura un procés de combustió que te elevada eficiència tèrmica i extremadament baixes emissions de NOx y partícules. En aquest sentit, la revisió bibliogràfica constata que aquests tipus de combustions permeten la reducció simultània dels contaminants NOx i sutja, trencant el tradicional *"trade-off"* existent a la combustió dièsel. De entre totes les estratègies proposades de baixa temperatura, la estratègia combustió dominada per la reactivitat del combustible presenta mes potencial que les altres. Aquest procés de combustió es caracteritza per utilitzar dos combustibles, lo que li permet solventar els principals problemes que han aparegut al llarg de la investigació de les estratègies de baixa temperatura com el control de la combustió. No obstant, aquest concepte de combustió també presenta algunes

limitacions com el excessiu nivell de monòxid de carbó e inquemats a baixa càrrega i el elevat gradient de pressió i elevada pressió en càmera a elevada càrrega que limiten el rang de operació del motor.

El objectiu de la investigació es proposar un concepte de combustió *"dual-fuel"* que puga operar en tot el rang de operació de un motor proporcionant el mateix o millorant la eficiència tèrmica que el dièsel amb emissions ultra baixes de NOx y partícules. A més, aquesta investigació també implica realitzar una exploració de les partícules emitides per el concepte ja que actualment està regulat per les normatives anticontaminants.

El procés de combustió que compleix el objectiu es diu *"Dual-Mode Dual-Fuel".* Aquest concepte de combustió utilitza dos combustibles de diferent reactivitat y modifica la combustió de totalment premesclada a baixa càrrega a combustió de natura difusiva a plena càrrega. Amb el desig de explorar les capacitats del concepte, s´han arribat a provar dos configuracions de pistons diferent per a adequar la relació de compressió i també un anàlisi per tamanys de les partícules.

Finalment, considerant els principals resultats obtinguts, el últim capítol pretén resumir les principals avantatges del concepte ací com les principals limitacions y , per tant, els treballs futurs.

Per aspera ad astra

Acknowledgments

I would like to acknowledge those individuals that have contributed directly or indirectly to the elaboration of the present thesis investigation.

Firstly, I would like to thank the management board of the CMT-Motores Térmicos formed by Francisco Payri, José María desantes, Jesús Benajes and Vicente Macián the opportunity to join the PhD. program in propulsive systems as well as the different equipment provided to carry out the investigation. In particular, the opportunity provided by Jesús Benajes to allow me to join the combustion group is really appreciated.

With special affection, I want to express my gratitude to my thesis director, Antonio García. He provoked the ignition of this project and he has been always encouraging me to pursuit this work. I have learned a lot during these years enhancing my personal and professional skills. Thanks again!

During the PhD period, I have received support from other professors at the CMT that I would like to thank as well. In particular, I would like to thank José Ramón Serrano, Andrés Tiseira, Pedro Piqueras, José Galindo and Héctor Climent from the air management group. Also very important contribution of Jaime Martín, Pablo Olmeda, José María García, Ricardo Novella, José Javier López and José Vicente Pastor from the combustion group and Raul Payri and Francisco Javier Salvador from the injection group. Without their help, this work would have been much more difficult.

The present investigations is characterized by having many tests performed on a single-cylinder engine, which was fitted in a fully instrumented test cell. Hence, I would like to thank the labor of the technicians that have taken part of this project and also have shared time with me along this 4 years at CMT. Hence, Gabriel Alcantarilla, Daniel Lérida, Raúl Lujan, José Gálvez, Juan Antonio López, Bernardo Planells, Sergi Soro, Miguel Ortiz, Valentín Ucedo, Ali and Jorge Moya, thanks so much for everything.

Juan Antonio Yustas, Norma Molina and all the administration staff, your patience and help is really appreciated, thanks.

I could not forget to remember the colleagues and friends from CMT. I would like to mention Javier Monsalve-Serrano, David Villalta, Lian Soto, Rafael Lago and María Baviera for the uncountable number of hours that we have been working together and sharing our daily experiences. Not less relevant the other colleagues that I have interacted at CMT such as Alba Andreina García, Leonardo Pachano, Felipe Lewinsky, Jorge Valero, Dani Vaquerizo and other many individuals. You are part of it as well.

Volvo Trucks Technology has been a key point for the present investigation since it has funded the investigation carried out in this thesis. I would like to express my gratitude to Iyad Balloul as well for following the project closely from Volvo. It has been challenging and we have worked really hard in order to obtain such as outstanding results. I am really grateful about the Volvo Powertrain from Malmö, where I performed my internship last year. I really appreciated this internship and I am really delighted with the Volvo company and the Volvo team. I would like to mention Martin Bauer, Ulf Arronsson and Johan Persson for their kind attention.

Finally, I would like to express my gratitude to my family and close friends. I would like to express to you that without your continue encourage, I would not have been the same person nor the same professional. I wish you could be proud of me some day.

I would also like to thank the Universitat Politècnica de València for supporting the predoctoral contract (FPI-S2-2016-2882) during the current investigation. The predoctoral contract belongs to the program known as Programa de Apoyo para la Investigación y Desarrollo (PAID).

Table of Contents

Index of Figures

Index of Tables

Nomenclature

AIM: Aerosol Instrument Manager

aTDC: After Top Dead Center

CAD: Crank Angle Degree

CA10: Crank angle at 10% mass fraction burned

CA50: Crank angle at 50% mass fraction burned

CA90: Crank angle at 90% mass fraction burned

CDC: Conventional Diesel Combustion

CI: Compression Ignition

CO: Carbon Monoxide

CPC: Condensation Particle Counter

CR: Compression Ratio

DI: Direct Injection

DMA: Differential Mobility Analyzer

DMDF: Dual Mode Dual Fuel

ECU: Engine Control Unit

EGR: Exhaust Gas Recirculation

EOI: End of Injection

EU: European Union

EVO: Exhaust Valve Open

GF: Gasoline Fraction

FSN: Filter Smoke Number

uHC: Unburned Hydro Carbons

HCCI: Homogeneous Charge Compression Ignition

IMEP: Indicated Mean Effective Pressure

IVC: Intake Valve Close

IVO: Intake Valve Open

LHV: Lower Heating Value

LTC: Low Temperature Combustion

MON: Motor Octane Number

OEM: Original Equipment Manufacturer

ON: Octane Number

PCCI: Partially Charged Compression Ignition

PFI: Port Fuel Injection

PPC: Partially Premixed Charge

PRR: Pressure Rise Rate

PSD: Particle Size Distribution

RCCI: Reactivity Controlled Compression Ignition

RoHR: Rate of Heat Release

RON: Research Octane Number

SCE: Single Cylinder Engine

SMPS: Scanning Mobility Particle Sizer

SOC: Start of Combustion

SOI: Start of Injection

TDC: Top Dead Center

Chapter 1

Introduction

Content

1.1 Introduction

The motivation of the present chapter is to introduce the scope of the investigation. Hence, this chapter will provide a general overview of this research performed as well as the structure of the document. The general framework starts on compression ignition engine operated under dual-fuel strategies. This combustion concept presents several challenges regarding the emissions. It is widely known the trade-off existing between NOx and soot emissions. This trade-off makes not possible to reduce both emission simultaneously. Therefore, low temperature strategies are aimed to overcome those shortcomings from the conventional combustion concept. Dual-fuel strategies arise as the most promising concepts that are able to reduce the emissions while the overall efficiency is maintained. The structure of the document will provide a general view of the work carried out.

1.2 Reciprocating engines framework

Compression ignition (CI) engines operated under conventional diesel combustion (CDC) are widely used nowadays. It has passed more than hundred years since the first compression ignition engine was patented by Gottlieb Wilhem Daimler in 1884 [1]. This patent generated by Daimler, described the engine operation in a very particular way. However, Daimler is well known by the creation of the famous car brand Mercedes-Benz. In addition, the Daimler Dream was his famous engine, which was developed to be a high-speed engine able to be installed in any locomotion vehicle creating, what many people consider, the first motorcycle.

However, the first diesel compression ignition engine was created by the German engineer Rudolf Diesel in 1892 and first prototype was ready in 1898 [2]. This new concept presented a revolutionary engine concept that was more efficient that the steam engines that operated at the end-nineteenth century. In addition, this engine was able to provide motive power in an

extensive different ways [3]. Diesel proposed a work cycle that was aimed to behave as much as possible the high efficiency cycle developed by Carnot [4]. Main difference with the strategy proposed by Daimler was that Diesel concept injected the fuel during the burning process. The injection rate raised by Diesel maintained constant the temperature due to the compensation between the increase of the temperature during the combustion and the cooling effect produced during the expansion. Diesel developed up to three prototypes helped by the financial support from the steam engine manufacturers. Therefore, the third prototype reached up to 26% of efficiency (Diesel claimed that diesel engines would reach up to 50% of efficiency), which was much better that the efficiency reached by the steam engines. Indeed, Diesel identified the boiler as the weakest element of the steam engines and thereby, the idea to introduce the fuel and burn it at the combustion chamber. Another important goal achieved at the early of the diesel engines belongs to the fuel supply. First prototypes of the diesel engine were fueled with coal powder. Thus, it was decided to move the fuel into a liquid petroleum-based fuel in order to improve the manageability. At this point, during this first phase of the diesel engines, liquid fuel injection was unreliable due to there was not experience in containing the high pressure of the fuel prior to the injection event. The problem got solved by Robert Bosch, when invented his fuel injection system [3]. Finally, the industry took in account the benefits of this type of engine and manufactured in different sizes.

Since then, the compression ignition engine fueled with diesel has been evolving up to the present day. As it was described in [3], the diesel engine has evolved as a collection of subsystems and each of these subsystems belongs to a dedicated group of specialized industries. Hence, the improvement of every subsystem concerns to the fuel injection systems, metallurgy of the hardware engine components, boosting systems, cooling, electronic controls, engine variable distribution or piston design. All of these improvements are aimed in improving the overall efficiency and reliability of the engines. Nowadays, it is possible to find high speed diesel engines that achieved high power density during a short period of time and large engine

capable to operate at high load during more than 8.000 hours per year. This development has been also observed at the investigation field. New techniques have allowed the research community to investigate deeper the conventional diesel combustion concept and transfer the knowledge acquired to the industry in order to speed up the evolution process.

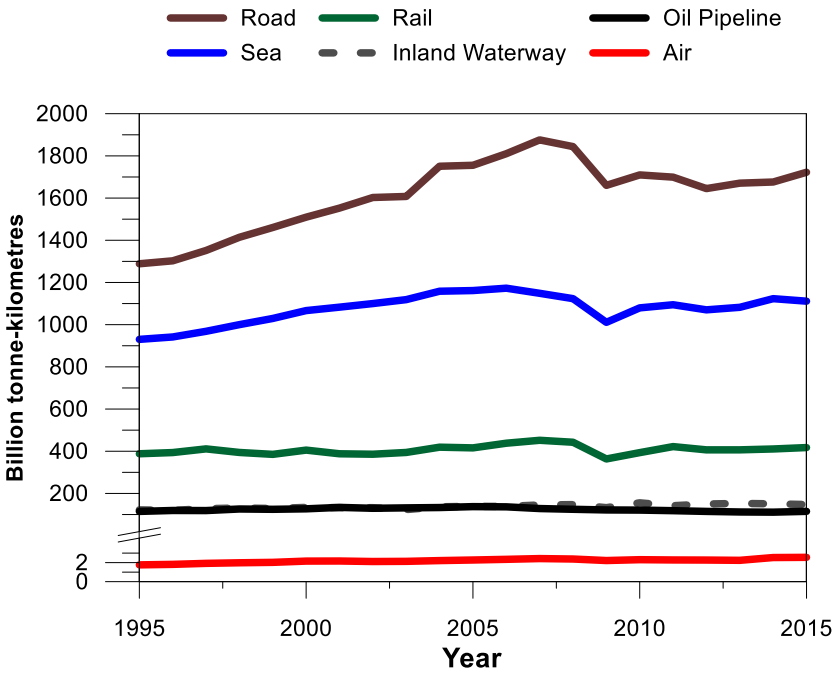

Figure 1.1. Evolution of the goods of transportation in Europe between 1995 and 2015 by modes. Adapted from [5].

This evolution observed in internal combustion engines (ICE) has allowed increasing the road transportation much more the rest of transportation modes. Figure 1.1 shows the evolution of the transportation of goods in Europe between 1995 and 2015. As it can be observed in the figure, most of the modes depicted have been kept almost constant during those years. Only sea and road transportation have noticed a remarkable upgrowth. Not only the road transport for goods has been increasing since 1995. As it is presented in Figure 1.2, the total passenger-kilometer

transportation is completely dominated by cars. In addition, an auxiliary y-axis has been used for the other modes of passenger transportation. The car mode exceeds by far the air mode, which represents the second more used transportation mode.

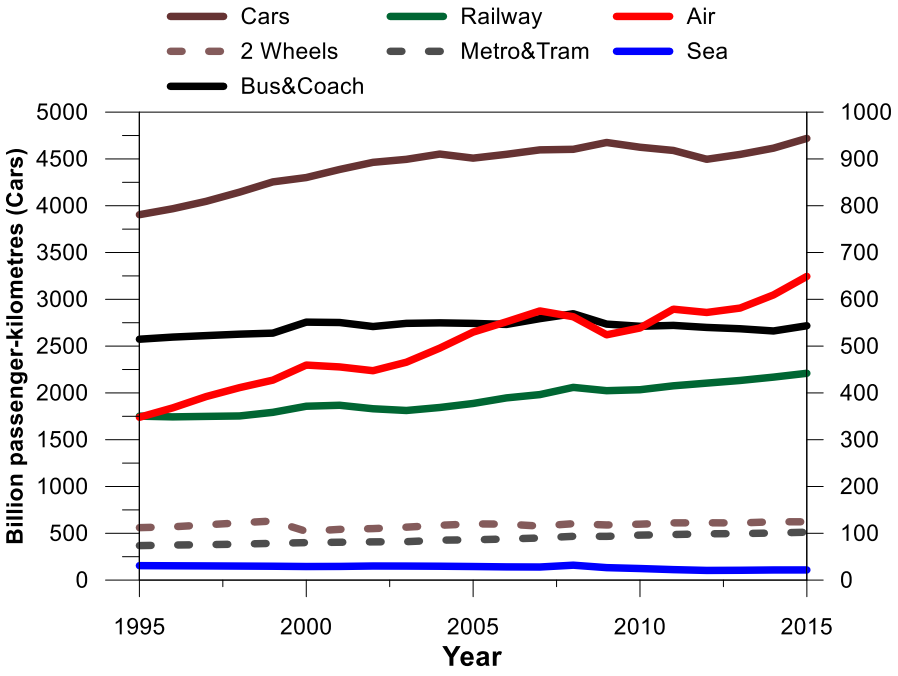

Figure 1.2. Evolution of the passenger transportation in Europe between 1995 and 2015 by modes. Adapted from [5].

Hence, Figure 1.1 and Figure 1.2 show that the most part of the goods and passenger transportation is carried out by using road transport vehicles such as passenger cars or trucks. In addition, sea and air modes also represent an important part of the total transportation modes. Hence, summarizing the most important conclusions of these pictures, it is possible to state that most part of the transportation is performed by using internal combustion engines. In particular, focusing mainly in goods and passenger transportation most part of the vehicles uses compression ignition engines. As it has been

mentioned along the present subsection, this evolution has been produced in parallel with the engine development.

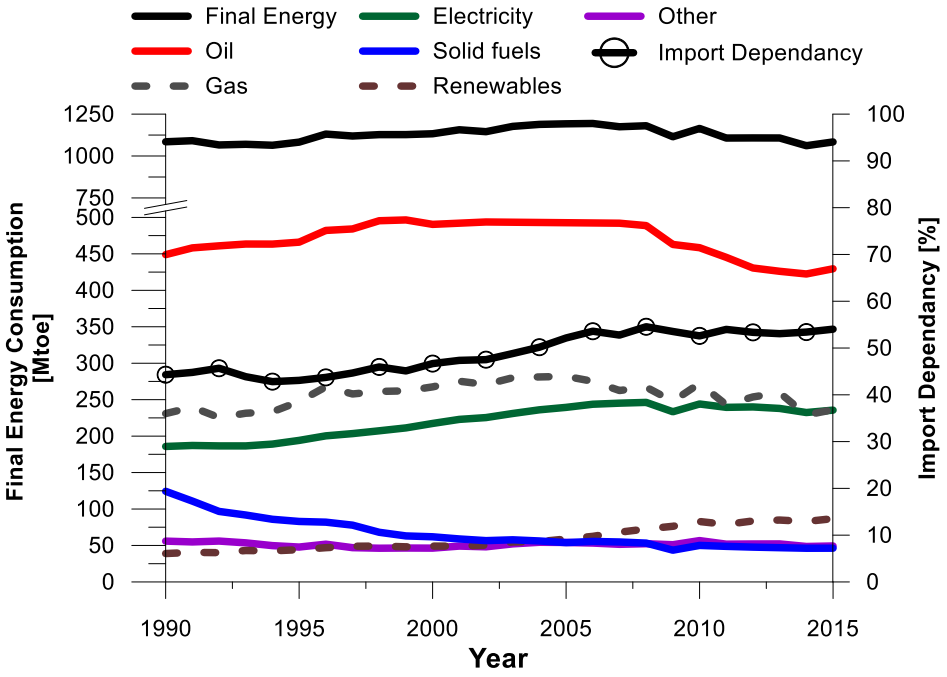

Figure 1.3. Evolution of the final energy consumption and energy consumption classification by sources of energy in Europe between 1990 and 2015. Adapted from [5].

Another point of view about the current situation corresponds to the final energy consumption distribution. In other words, how this evolution of the road transportation impacts into the total energy consumption in Europe. As it is observed in Figure 1.3, shows the energy consumption evolution since 1990 up to 2015. Despite the total energy consumed remains quite constant for the last 25 years, it is possible to observe some trends variations regarding the source of the energy. In this case, solid fuels such as coal has decreased a 45% since 1990. However, the electricity and the energy from renewable sources has increased in order to balance the overall energy consumption. Another important reduction in terms of energy supply is observed in the oil

demand. During the last 5 years has experienced an important reduction remaining below the levels reached during the early 90's. Thus, most relevant conclusion of this evolution is that the energy sources have been redistributed being possible to reach the same level of energy consumption. By contrast, the import dependency of the energy has been increasing during these years. Despite the fact that it is not clear at the picture the source of energy that is causing this increment, it reveals the requirements of energy of Europe. In this sense, Europe requires a huge amount of energy that is not possible to obtain by itself forcing to import an important amount of energy every year.

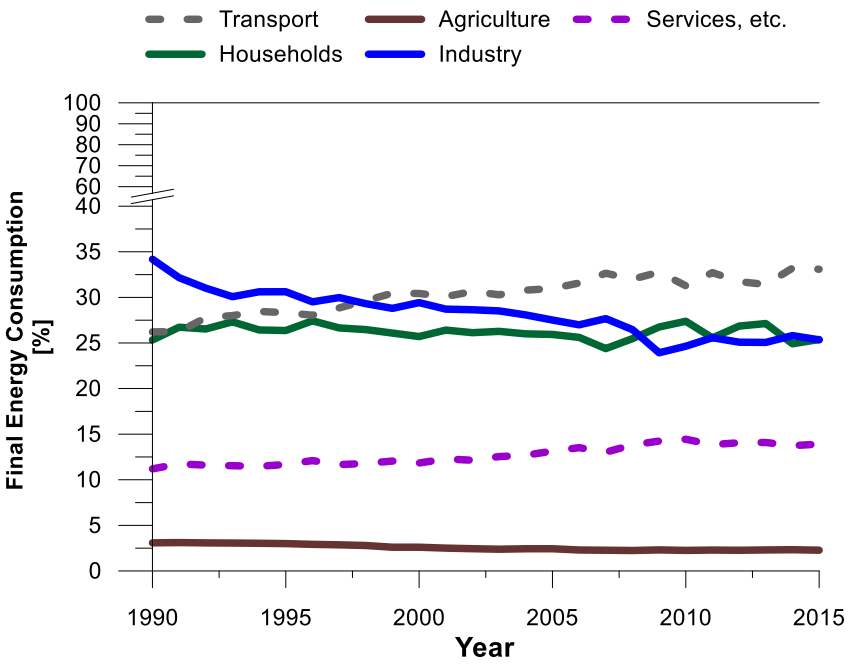

Figure 1.4. Evolution of the energy share consumption in Europe between 1990 and 2015 by sectors. Adapted from [5].

Considering the final energy distribution by sectors, the Figure 1.4 presents how the energy is shared in function of the sector. As it can be observed, sectors as industry or agriculture have decreased the energy consumption during last years. The households sector remains almost

constant and the transport sector presents the biggest increase since 1990. This trend is obvious due to the increase at the goods and passenger transportation observed in Figure 1.1 and Figure 1.2. However, the oil consumption presented in Figure 1.3 shows that this type of transportation has become more and more efficient due to its traditional oil dependency.

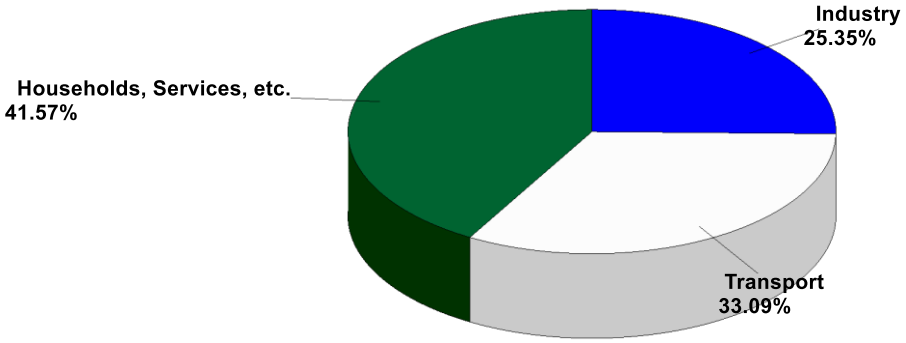

Figure 1.5. Energy consumption by sectors in Europe in 2015. Adapted from [5].

Regarding the overall energy distribution by sectors, the most recent study presents a picture of the energy distribution in Europe for the 2015, Figure 1.5. It is possible to consider the current situation as the depicted in the figure. Hence, the energy dedicated for the transportation only represents around a third part of the total energy consumption. Figure 1.6 represents the distribution of the energy dedicated to the transportation sector. As it is possible to observe, most part the energy consumed for transportation comes from the road transport (82% of the total). It is followed by the air transportation with a 14% of share and behind, Railways and Domestic navigation represents a share of around a 3% of the total. It can be considered that most part of the energy consumed in this sector comes from the oil. Indeed, the road transportation is dominated by the compression ignition engines.

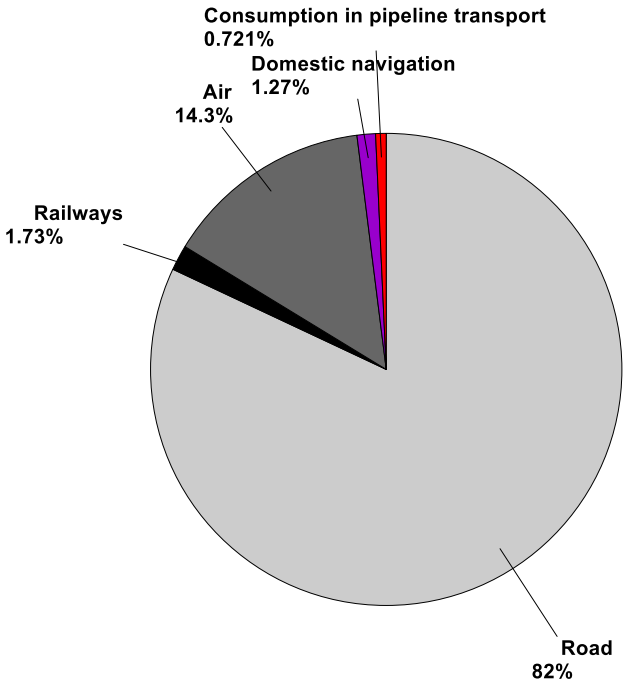

Figure 1.6. Transport energy consumption in Europe in 2015 by modes. Adapted from [5].

A brief summary of the information provided is that despite the continuous increase of the transportation requirements, this sector has been adapting with an increase of the road transportation due to its flexibility and quality in terms of logistics. Despite the huge dependency on the oil energy source, during the last 25 years a relevant reduction in the oil consumption has been observed. This reduction is even a surprise because of the road transportation has been increasing more than other transportation modes. Thus, it is clear that the internal combustion engines and, in particular, compression ignition engines have played a key role during the evolution of our society since they appeared and with more impact during the last 25 years. This leading position of the compression ignition engines over the spark ignition (SI) engines rely on the efficiency. CI engine reach better efficiency than SI provoking that only CI engines can be found on road transportation for goods haulage purposes. In addition, the share of CI engines in Europe

passenger cars fleet has increased during the recent years [6]. One of the reasons of the CI domination at the passenger cars sector was the EU policy aimed in the lower CO_2 emissions promoted. These emissions are directly related with the fuel consumption. The lower the fuel consumption, the lower the CO_2 emissions.

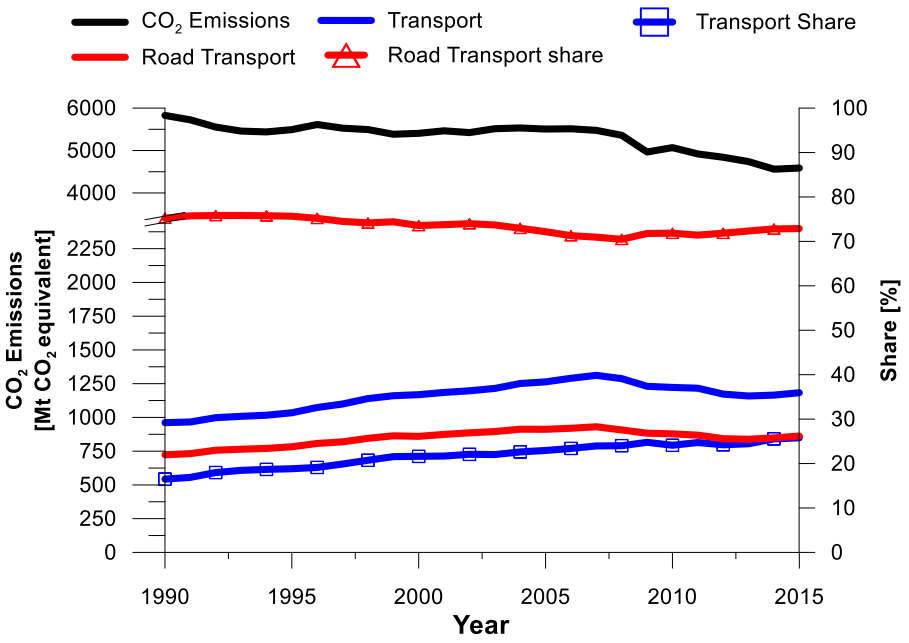

Figure 1.7. Evolution of the total CO_2 emissions in Europe between 1990 and 2015. Adapted from [5]. (Including International Bunkers and Indirect CO_2 but excluding LULUCF)

In this sense, Europe is really concerned about the greenhouse effect gases such as CO_2. CO_2 represents the most important greenhouse gas and Europe has been involved in its reduction for more than 20 years as it can be observed in Figure 1.7. Thus, despite of the similar levels of final energy consumption during the last 25 years, the increase in transportation demand and the increase also in population and production the emissions have decreased. The figure also presents the impact of the transport sector in these emissions and in particular the road transport. As it is observed, the

transport share has been increasing since 1990, as well as the transportation demands. Hence, the main reduction of the CO_2 is due to a combination of different phenomena, but all related with the efficiency. Hence, the energy production, in general, has become more efficient and thereby, despite of the continuous increase in activity and population, there is not a substantial increase in final energy consumption. As a society, we have become more efficient. Regarding the transportation, the more efficient the engines, the lower CO_2 emissions. These continuous improvement of efficiency has mitigated the impact on the emissions. Indeed, transport sector only produces the 25% of the total CO_2 emissions. The other 75% corresponds to the industry, power generation, households, etc.

However, aimed with the desire to provide more fuel efficient engines, CI engines are considered one of the first responsible of the current air pollution, moreover in big cities. The main reasons are found in the other emissions associated to the combustion process. These pollutants are described next:

- Nitrogen oxides (NO_x): These pollutants are one of the most relevant contributors to acid deposition and eutrophication, which worsen drastically the quality of the water and the soil. Additionally to the mentioned problems, the nitrogen oxides form ozone ate ground level by reacting with volatile organic compounds. The ozone resultant causes health problems such as respiratory illness [7]. This type of pollutants are produced by means of thermal mechanisms during the combustion process, being a consequence of high temperatures and lean environments. Thus, CI are completely affected by these pollutants compared with the SI engines.
- Particulate matter (PM): The particulate matter is mainly formed by soot, hydrocarbons (HC) from the fuel and lubricants and other minor products found during the combustion process. The most important health problems, that cause this pollutant, affect to the respiratory organs. As it has been presented in the

previous pictures, the transport sector is mainly contains ICE, which promote the 11% of the PM_{10} (particles with a scanning mobility diameter lower than 10µs) and the 16% of the $PM_{2.5}$ [8].

- Carbon monoxide (CO): This toxic gas is characterized by its odorless and colorless. CO is capable to pass through the lungs to the bloodstream reducing the oxygen content. This reduction of the oxygen affects the organs of the body causing the death. This gas is produced during the combustion process due to a lack of oxidation caused by low combustion temperatures. This lack of oxidation produces CO instead of CO_2. At CI engines, it is not usually a relevant issue due to the excess of oxygen and the high local temperatures achieved during the combustion event.
- Hydrocarbons (HC): In particular, unburned hydrocarbons are produced due to an incomplete process of combustion. A low temperature during the combustion usually promotes high values of unburned HC. Thus, this type of emissions are usually found at SI engines due to rich mixtures and low temperatures at low load operation and at CI engines while running at low load. However, unburned HC does not represent a big issue for CI engines.

As it is observed, these pollutants are potentially harmful for the humans and thereby, stringent regulations have been imposed since the early 90's. In this sense, the most stringent regulations have been focused on CI engines due to the harmfulness of the pollutants. In Europe, these regulations are known as EURO regulation. EURO regulations were set up for light-duty and medium or heavy-duty engines. As the present investigation is based in medium and heavy-duty purposes, the EURO regulations that apply are the heavy-duty standard limitations. Hence, EURO emissions standard started in 1992 with the EURO I. Since then, they have become more and more stringent up to the most recent EURO VI standard emissions limitation.

Table 1.1. European emissions standards for heavy-duty engines operated under steady-state conditions. Data from [9].

Regulation	Year	NOx	PM	CO	HC	PN
			[g/kWh]			[1/kWh]
EURO I	1992,(<85kW)	8.0	0.612	4.5	1.1	-
	1992,(>85kW)	8.0	0.36	4.5	1.1	-
EURO II	10/1996	7.0	0.25	4.0	1.1	-
	10/1998	7.0	0.15	4.0	1.1	-
EURO III	10/2000	5.0	0.1	2.1	0.66	-
EURO IV	10/2005	3.5	0.02	1.5	0.46	-
EURO V	10/2008	2.0	0.02	1.5	0.46	-
EURO VI	10/2013	0.4	0.01	1.5	0.13	$8.0x10^{11}$

As it is observed in Table 1.1, the transition from EU V to EU VI presented a new challenge to the research community as well as the engine manufacturers due to the huge reduction in terms of NO_x emissions and particle number emitted. Hence, the engine manufacturers developed bigger and more complex after-treatment devices with the capability to reduce the engine-raw emissions below the limits at the exhaust tail pipe [10]. In this sense, the engine manufacturers have implemented two types of aftertreatment elements in order to mitigate the particle matter and the NOx emissions. Despite of being considered separately for the explanation, these elements actuate as a unique system due to the benefits of working together. The element used to reduce the NOx emissions is the two-stage NOx reduction element. As it can be observed in Figure 1.8, the two-stage element consists of a combination of a Diesel Oxidation Catalityc (DOC) and a Selective Catalytic Reduction (SCR). Between those elements is usually set the diesel particulate filter (DPF) and the Diesel Exhaust Fluid (DEF). The SCR is a complex active emissions control device that injects a liquid-reductant agent through the exhaust stream. The reductant or DEF is automotive urea commercially known as AdBlue [12]. The AdBlue sets off

the chemical reaction in charge of converting nitrogen oxides into diatomic nitrogen, water and small quantities of CO_2.

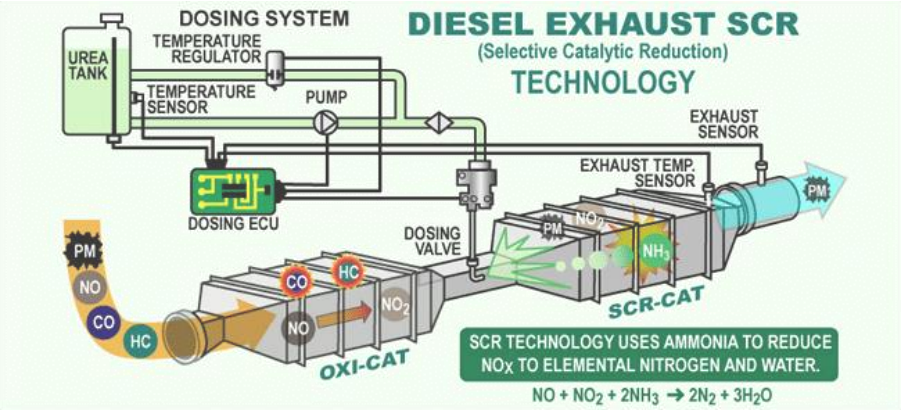

Figure 1.8. Selective Catalytic Reduction (SCR) system typically used in diesel engines [11].

It is called "selective" due to it reduces the NOx emissions using ammonia as a reductant within a catalyst system. Hence, the AdBlue is the reducing agent that reacts with the NOx components. This DEF can be broken down at the exhaust stream producing the oxidizing ammonia instantaneously. SCR technology reduces up to 90% of the NOx components. In addition, the current technologies allows using two variations of SCR. The standard SCR by using ammonia and the SNCR (Selective Non-Catalytic Reduction) by using ammonia and Fuel Reburning (FR).

The second element is the DPF. It is usually located between the DOC (oxi-cat) and the SCR-cat before the dosing valve for the DEF. The DPF is the device in charge of capturing physically the diesel particle elements content in the exhaust flow. Diesel particulates filter usually contain flow-through walls made of ceramics which provide excellent filtration efficiencies (more than 90% of efficiency) and mechanical and thermal properties that offer excellent durability. Ceramic walls facilitate the carbon content to adhere to the surface. Hence, these deposition mechanisms provoke that this type of filters are specifically dedicated to control the solid fraction of diesel

particles (such as elemental carbon). However, the particle filters also capture non-solid fractions (soluble organic fractions (SOF) and sulfate particles. The reason is that the filter device can filter by using other mechanisms such as impaction, interception or diffusion. By contrast, the DPF devices might be ineffective (or with a very reduced efficiency) with the non-solid particles.

Once the PM exceeds a certain value the pressure differential between the inlet and the outlet is excessively high affecting the overall efficiency. Hence, the engine detects that the DPF needs a *"regeneration"*. The regeneration is improved with the DOC action. Late post-injections, or the auxiliary injector in heavy-duty engines, are activated allowing to provide diesel fuel to the DOC. The diesel fuel also regenerates the DOC reacting and increasing the exhaust flow temperature. This temperature reaches up to 800°C, allowing the carbon burning accumulated at the DPF. The *"active regeneration"* is periodically scheduled and it is forced to start when the differential pressure is high. By contrast, if the active regeneration are interrupted systematically by the user, the DPF can get completely clogged. In this case, the DPF needs to be cleaned in a dedicated service center or replaced by a new one. Heavy-duty engines usually incorporate these aftertreatment elements with a lay-out similar to the scheme depicted in Figure 1.9.

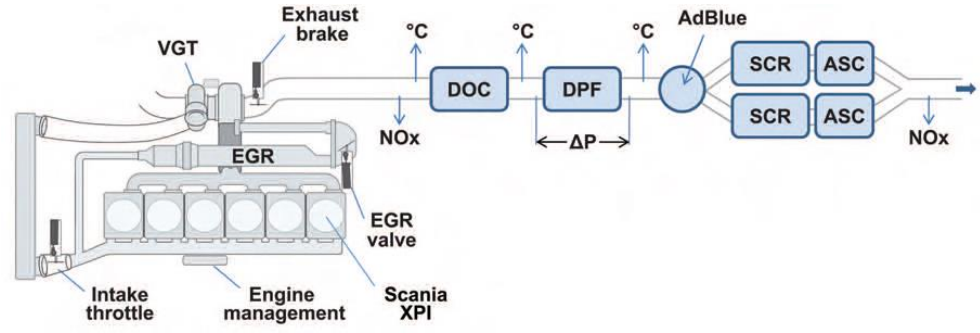

Figure 1.9. Scheme of the typical lay-out of the aftertreatment systems in heavy-duty engines [13].

As it is observed in Figure 1.9, the mandatory fulfillment of the emissions standards limitations implies the aftertreatment elements. Hence, the impact of these elements affect to the volume and weight of the powertrain elements. A new packaging of the exhaust pipe is required to place the aftertreatment devices as close the engine as possible in order to avoid wasting temperature to the ambient. A second impact concerns the overall efficiency of the engine due to the extra backpressure provoked by the different in series elements added at the exhaust downstream the turbine that increase the outlet turbine pressure. Another impact is observed at the costs of these elements. Due to the complexity of the process and the materials required, the overall costs of these elements increase considerably respect the first EURO engines. Posada et al. [14] investigated the economic impact of the aftertreatment devices required to meet the different EURO standards from EU II to EU VI. The study stated that for a 12 liter engine the total cumulative costs raises up to around 6.000€.

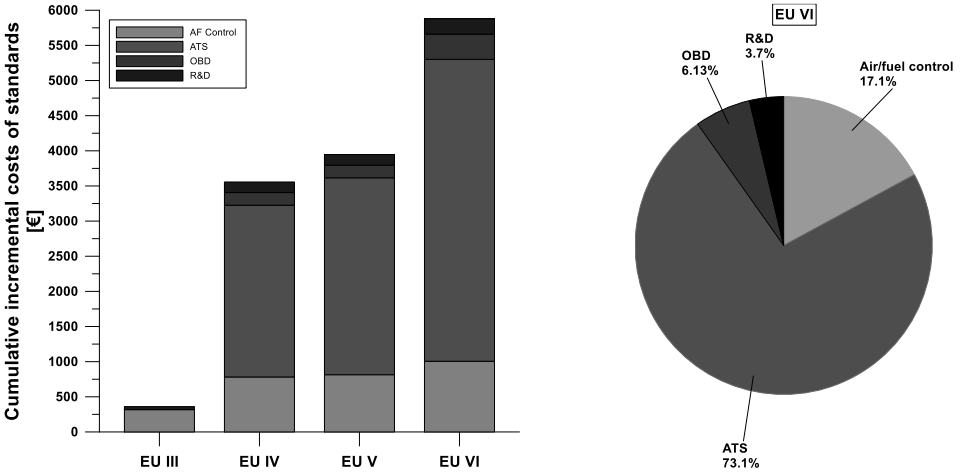

Figure 1.10. Cumulative incremental costs of the different standard emissions limitations [14].

Figure 1.10 shows the cumulative costs of the different standards from EU III to EU VI. As it can be observed, the costs have been multiplied by 10. At the left side of the picture, it is depicted the percentage of the different

costs of the EU VI technology. The biggest budget is dedicated to the aftertreatment system (ATS). The ATS represents more than the 70% of the overall costs dedicated to fulfill the EU VI standard limitations. The increase at the ATS costs observed denotes the more and more stringent emissions limitations regulations. In addition, most part of the ATS costs correspond to the SCR element, as depicted in Figure 1.11. SCR element results to be a key element for the NOx emissions compliance, moving from 5.0 g/kWh (EU III) to 0.4 g/kWh (EU VI).

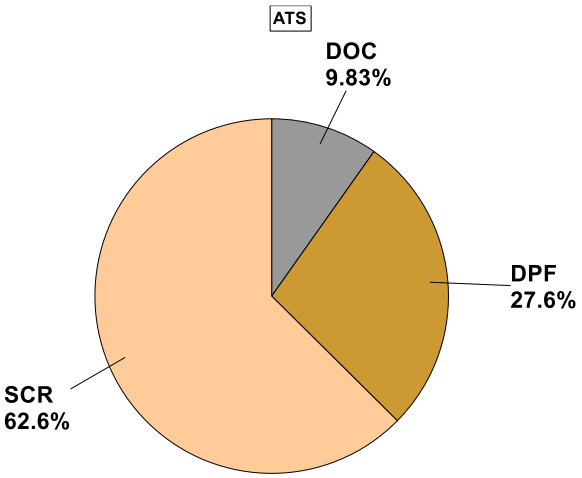

Figure 1.11. Impact on the costs of the aftertreatment elements required to meet the EU VI standard.

In addition, not only the direct costs of engine production are increased but the engine operation costs during the lifetime also do. In this sense, the DEF consumption required by the ATS, the extra diesel fuel consumption required for the DPF regeneration and the increase in price of the maintenance implies additional costs during engine lifetime [15][16].

Additionally to the technical issues found at the conventional diesel combustion (CDC), during the recent years, the diesel fueled cars have become very unpopular due to the Volkswagen scandal and the Dieselgate [17][18]. The Dieselgate discovered with VW, uncovered a scandal at the

automotive industry due to the difference between the theoretical emissions and the real driving conditions emissions. The scandal affected mainly the passenger cars vehicles but it has been extended to all the diesel-fueled vehicles (light, medium and heavy-duty vehicles included). The Dieselgate started in 2015 when Dr. John German[1] helped to expose VW emissions scandal [19]. First study was performed due to Dr. Peter Mock[2] had the idea to carry out the test in order to improve the comprehension of the discrepancies observed between the emissions promoted by the VW Passat and the VW Jetta. Indeed, he decided to perform the study in the US because of the more stringent US standard at the moment. This study was aimed in that the expected results were that the cars could meet the current standard emissions limitations in US and use it as a proof to the European market that it was possible to provide diesel fueled vehicles with cleaner emissions. Dr. Peter Mock[2] and Dr. John German[1] belonged to the International Council of Clean Transportation (ICCT). Unfortunately, the results obtained were unforeseen, causing the biggest scandals of the German automotive industry. The VWs nitrogen oxide emissions exceeded the US standards by more than 30 times. As a consequence, the authorities of US and Europe have pursued this type of fraud in order to force the industry to provide the market with clean vehicles. Other brands such as Renault were also involved in such scandal [20]. Even some executives from VW in US were sent to prison [21].

Since 2015, the industry has been forced by the public opinion and the politics to intensify the resources in offering electric vehicles and removing the diesel engines of their catalog. In fact, big cities such as London or Madrid were positive to ban diesel passenger cars in a close future [22].

1- Engineer who is the US co-lead of the International Council on Clean Transportation (ICCT). Senior Fellow.

2- Engineer who is the coordinator of the International Council on Clean Transportation (ICCT) activities in Europe. EU Managing Director.

Hence, the regulations used to control the passenger car emissions has shown their weaknesses when referring to NOx emissions in real driving. Even the total CO_2 shows discrepancies between the automakers values and the real driving ones. By contrast, despite the NOx emissions are typically found in diesel engines, Europe policy has been favouring diesel engines for decades since diesel fuels promote less CO_2 due to their better efficiency makes them to provide a lower fuel consumption compared with the spark ignited engines. This politics have conducted Europe to be dominated by diesel fueled engines at the passenger cars market.

In this sense, the Europeans authorities are really concerned about this problem and have forced the automakers to evaluate the cars under real conditions. Hence, they have to pass with all the vehicles a Real Driving Emissions (RDE) testing by using a Portable emissions measurement system (PEMS). Not only the basic model offered but the different car configurations that affect the aerodynamics or the overall efficiency such as different tire sizes, wheels, etc. With the RDE the idea is to avoid the discrepancies between the results obtained at the laboratory and the results obtained by the users at the road.

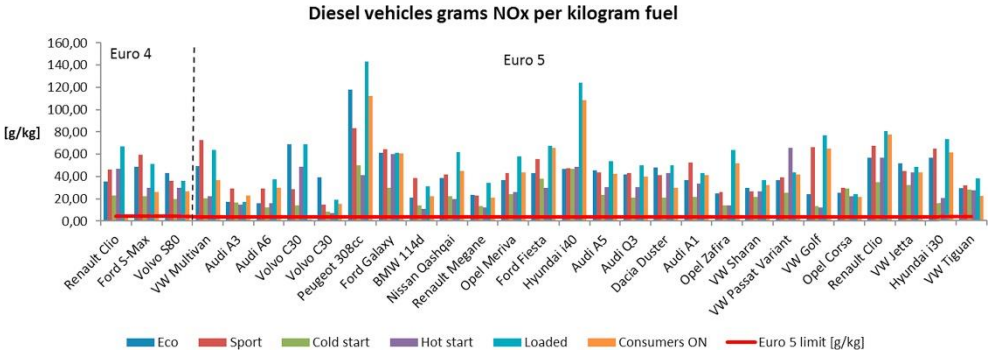

Figure 1.12. Diesel vehicles emissions comparison [20].

Despite the potential of this new testing procedure, the politics have relaxed the emissions assessment in order to provide an extra-time to the manufacturers to move from the lab to the road. In other words, diesel cars

will continue over-emitting NOx until 2020 at least. Nonetheless, several stages have been applied in order to revise the type-approval Directive [23] and additional systems for the incompliant vehicles recalls [24]. As it has been observed during these years since the RDE application, the RDE compliance application has been full of difficulties, especially at the passenger car sector, compared with the heavy-duty vehicle one. In this sense, heavy-duty vehicles reduced the NOx emissions from 4.5 g/km during EU V regulation to 0.2 g/km when the EU VI regulation was introduced in 2014 [25]. Indeed, the HDV was forced to incorporate an in-service testing to monitor the emissions since 2014.

Hence, it is possible to conclude that the European standards emissions limitations framework requires an update as well as more ambitious targets further than 2020 will be set in order to preserve the competitive position of the automotive industry in the global market.

1.3 Low temperature combustion strategies

As it has been mentioned in previous subsection, NOx and particle matter emissions limits imposed by the regulations are getting more severe over the years and, in particular, since the recent emissions scandal. Hence, the automotive industry is extremely concerned about the current situation [26]. The main solution used for the NOx and soot emissions consists on the aftertreatment of the exhaust gases, mitigating the emissions in order to meet the regulations. Alternatively, other options are being studied such as the low temperature combustion (LTC) strategies. LTC strategies are proposed as a way to reduce simultaneously both pollutants during the combustion process [27]. This achievement is possible due to the use of high rates of exhaust gas recirculation (EGR) and longer mixing times comparing with the CDC strategy [28], which lead to lower combustion temperatures [29] and avoidance of local rich fuel equivalence ratios [30]. In addition, LTC characterizes by breaking the trade-off existing in CDC mode while thermal efficiency is maintained or even improved. Thus, thermal efficiency is

improved due to the fast heat release of the combustion process and the reduction of the heat transfer (HT) because of the lower combustion peak bulk gas temperatures [31]. Amongst others, the most promising LTC is the Reactivity Controlled Compression Ignition (RCCI) concept proposed by Inagaki et al. [32]. Later, RCCI concept was developed by Kokjohn et al. [33]. Despite of the benefits provided by LTC and, in particular, by the RCCI, they still present several challenges that have to be solved such as high pressure rise rate during high engine load operation or excessive CO and unburned HC during low load operation which limit the range of operation of the concept. Thus, chapter 2 will provide a better background of the LTC techniques and their limitations. In this sense, the work presented in this thesis hopes to provide a new combustion strategy based in the RCCI concept that uses Dual-Fuel combustion over the whole engine map trying to overcome the main limitations of the actual RCCI concept. In addition, an approach of the PM study will be carried out in order to answer future considerations of the Dual-Fuel concepts.

1.4 Document content and structure

Finally, the present subsection is aimed to introduce the main structure of the thesis as well as a brief description of each chapter of the document. The thesis document is formed by six chapters including the present chapter.

Chapter 1 presents a brief outline of the social, technological and economic framework of the investigation. It also introduces the structure of the document.

Chapter 2 is dedicated to the background of the investigation. In this sense, a dedicated bibliography review has been performed about the diesel engines and their main challenges and the novel LTC techniques that are proposed to overcome the shortcomings found at the traditional diesel engines. Finally, the objectives, motivation and methodology of the investigation are defined.

Chapter 3 describes the different tools used to performed this investigation. A set of experimental tools will permit to conduct the test campaign in which most remarkable element is the Single-Cylinder Engine (SCE). The SCE will be fully described along the chapter. Additional elements required for the operation of the engine such as air management control, fuel supply and data acquisition. Theoretical tools will be used to obtain the combustion diagnosis from the experimental data, which are mainly based in the in-cylinder pressure.

Chapter 4 shows the results obtained regarding the Dual-Mode Dual-Fuel (DMDF) concept developed in order to solve the main challenges of the RCCI concept. The concept has been applied to the SCE by using two different compression ratios and they were evaluated in terms of performance and emissions. Best results were compared against the CDC concept to state the benefits of the DMDF concept.

Chapter 5 evaluates the particle size distribution (PSD) analysis over the whole engine map under the DMDF concept. It is also explored the PSD under RCCI operation. Then, the PSD were compared with the PSD under CDC mode. Finally, particles maps were defined for the DMDF concept.

Chapter 6 summarizes all the results achieved during the thesis work and establishes the most important conclusions of the investigation. Additionally, some suggestions regarding future works are provided.

Finally, Figure 1.13 shows the scheme of the contents followed during the thesis document. This scheme allows establishing and reaching the objectives as well as discussing about the results obtained.

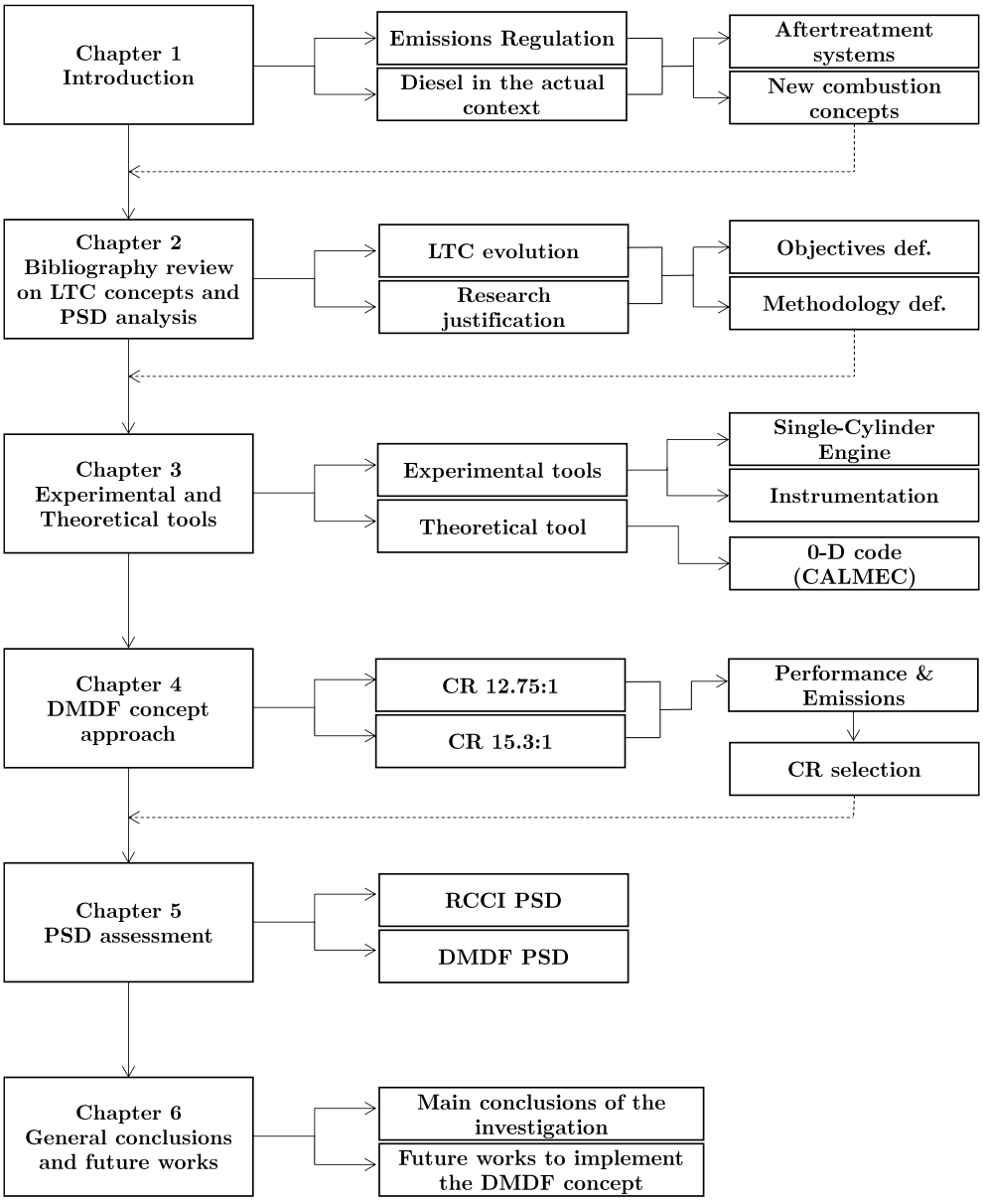

Figure 1.13. Information flow of the present thesis.

1.5 Bibliography

[1] Amengual Rubén. "Bielas y álabes 1826-1914. Evolución histórica de las primeras máquinas térmicas a través de las patentes españolas". Oficina Española de Patentes y Marcas, 2008.

[2] Diesel R. "Internal combustion engine". US Patent Number 608845, 1898.

[3] Shrinivasa, U. "The evolution of diesel engines". Resonance. 2012.

[4] Carnot S. "Reflections on the Motive Power of Fire: And Other Papers on the Second Law of Thermodynamics". Dover Publications, 2005.

[5] European Commission. Transport. Statistical pocketbook, 2017. https://ec.europa.eu/transport/facts-fundings/statistics/pocketbook-2017_en.

[6] European Automobile Manufacturers' Association. "The Automobile Industry Pocket Guide 2014-2015". Technical report.

[7] Environmental Protection Agency. "Nitrogen Oxides (NOx), Why and How They Are Controlled". Technical report, 1999.

[8] Environmental European Agency. "Emissions of primary PM2.5 and PM10 particulate matter". Technical report.

[9] Regulation (EC) No 595/2009 of the European parliament and of the council of 18 June 2009 on type-approval of motor vehicles and engines with respect to emissions from heavy duty vehicles (Euro VI) and on access to vehicle repair and maintenance information and amending Regulation (EC) No 715/2007 and Directive 2007/46/EC and repealing Directives 80/1269/EEC, 2005/55/EC and 2005/78/EC.

[10] Engineer Commercial Vehicle. "Euro 6 the inside story". Technical report, March 2012.

[11] Selective Catalytic Reduction (SCR). Researchgate. More information in www.researchgate.net.

[12] AdBlue®. More information at https://www.vda.de/en.

[13] Commercial Vehicle Engineer, January 2010.

[14] Posada F., Chambliss S. and Blumberg K. "Costs of emission reduction technologies for heavy- duty diesel vehicles". ICCT, 2016.

[15] Johnson T.V. "Vehicular Emissions in Review". SAE Int. J. Engines, Vol. 5, 216-234, 2012.

[16] Gense N.L.J., Riemersma, Such C. and Ntziachristos L. "Euro VI technologies and costs for Heavy Duty vehicles". Technical report, Delft: TNO Science and Industry report, 56, 2006.

[17] Guide to the Volkswagen Emissions Recall. https://www.consumerreports.org/cro/cars/guide-to-the-volkswagen-dieselgate-emissions-recall-

[18] Dieselgate: Who? What? How? A study by Transport and Environment, 2016.

[19] Rupert Neate. "Meet John German: the man who helped expose Volkswagen's emissions scandal". The Guardian. 2015. More information at: https://www.theguardian.com/business/2015/sep/26/volkswagen-scandal-emissions-tests-john-german-research

[20] Hooftman N., Messagie M, Van Mierlo J and Coosemans T. "A review of the European passenger car regulations – Real driving emissions vs local air quality". Renewable and Sustainable Energy Reviews, 1-21, 2018.

[21] O'Kane S. "VW executive given the maximum prison sentence for his role in Dieselgate". The Verge. More information at: https://www.theverge.com/2017/12/6/16743308/volkswagen-oliver-schmidt-sentence-emissions-scandal-prison

[22] Luke John Smith. "Petrol and diesel car ban will go ahead in London this year - Ignore it and face £130 fine". Express. More information at https://www.express.co.uk/life-style/cars/944461/petrol-diesel-car-ban-London-UK-2018-fine.

[23] EC. Proposal for a regulation of the European Parliament and of the Council on the approval and market surveillance of motor vehicles and

their trailers, and of systems, components and separate technical units intended for such vehicles. Brussels; 2016.

[24] ICCT. Proposed new type-approval system for motor vehicles in the European Union. Berlin; 2016.

[25] ICCT. European vehicle market statistics. Berlin; 2016.

[26] European Parliament, Council of the European. Regulation (EC) No 595/2009 of the European Parliament and of the Council on type-approval of motor vehicles and engines with respect to emissions from heavy duty vehicles (Euro VI). Official Journal of the European Union 2009;188:1–13.

[27] Imtenan S, Varman M, Masjuki H, Kalam M, Sajjad H, Arbab M, et al. "Impact of low temperature combustion attaining strategies on diesel engine emissions for diesel and biodiesels: a review". Energy Convers Manage 2014;80:329–56.

[28] Splitter D, Wissink M, Hendricks T, Ghandhi J, Reitz R. Comparison of RCCI, HCCI, and CDC operation from low to full load, THIESEL 2012 conference on thermo- and fluid dynamic processes in direct injection engines; 2012.

[29] Neely G, Sasaki S, Huang Y, Leet J, Stewart D. "New diesel emission control strategy to meet US Tier 2 emissions regulations". SAE technical paper, 2005- 01-1091; 2005.

[30] Garcia A, Monsalve-Serrano J, Heuser B, Jakob M, Kremer F, Pischinger S. "Influence of fuel properties on fundamental spray characteristics and soot emissions using different tailor-made fuels from biomass". Energy Convers Manage, 108, 243–54, 2016.

[31] Bittle J.A., Knight B.M. and Jacobs T.J. "Heat Release Parameters to Assess Low Temperature Combustion Attainment". SAE Technical Paper, no 2011-01-1350, 2011.

[32]Inagaki K, Fuyuto T, Nishikawa K, Nakakita K, Sakata I. Dual-fuel PCI combustion controlled by in-cylinder stratification of ignitability. SAE technical paper, 2006-01-0028, 2006.

[33]Kokjohn S, Hanson R, Splitter D, Reitz R. "Fuel reactivity controlled compression ignition (RCCI): a pathway to controlled high-efficiency clean combustion". Int JEngine Res., 12, 209–226, 2011.

Chapter 2

Non-conventional combustion strategies in compression ignition engines

Content

2.1 Introduction

Second chapter provides a literature review of the main problems found at the conventional diesel combustion (CDC) and possible solutions such as low temperature combustion (LTC) strategies. It also provides the overall approach of the investigation carried out at the present thesis.

The first part of the literature review performed in this chapter focuses on the main drawbacks found at the CDC strategy. Therefore, it would include a description about the trade-off between NOx and soot which force the concept to require an aftertreatment system mandatory during its operation. In order to overcome these drawbacks, new combustion concepts appear as a plausible solution for compression ignition engines, providing similar values in terms of performance but reduced emissions compared with CDC.

New combustion concepts such as low temperature concepts (LTC) allow to reach the performance provided by the CDC concept with ultra-low levels of NOx and smoke. The second part of the literature review focuses on the main characteristics of the most interesting LTC strategies such as homogeneous charge compression ignition (HCCI). Amongst others, reactivity controlled compression ignition (RCCI) results the most interesting LTC due to its wide operating range. However, it requires a low compression ratio to be operated in a compression ignition engine. Thus, Dual-Mode Dual-Fuel concept appears as a strategy that can be operated from low to full load with higher compression ratios compared with RCCI.

Finally, the last part of the chapter consists of a presentation of the thesis approach. This approach contains the motivation of the study, the objectives pursued through the investigation and the methodology applied in order to reach the objectives proposed.

2.2 Drawbacks of the conventional diesel combustion

The present subsection describes the conventional diesel combustion (CDC) concept and presents the main challenges that the concept needs to solve. CDC, according to Dec [1] definition, *is a complex, turbulent, 3-D and multiphase process that occurs in an environment with high temperature and high density.* As a raw approach to the combustion process, CDC is governed by the diesel fuel injection timming. Thus, diesel fuel is injected in the combustion chamber when the cylinder is around the top dead center (TDC). Diesel fuel penetrates radially into the combustion chamber with a high velocity that allows to reach a proper atomization of the fuel jet. This process follows with evaporation of the fuel and fuel and air mixing (exhaust gas recirculated (EGR) and fresh air). The air/fuel mixture reaches ignition conditions that provokes a heat release. Unfortunately, during this process, several air pollutants such as NOx and soot are formed. Hence, from this approach to the CDC concept, it highlights that injection process and combustion process are directly related.

In this sense, CDC has been deeply studied by the research community. Main fields of investigation have been the mixture formation studies from García [2] and Musculus *et al.* [3] or the traditional study of the combustion process by comparing the heat transfer and the injection rate [4][5][6].

Figure 2.1 shows temporal evolution of the diesel combustion process. Several temporal stages have been depicted in the figure. Aditionally, the rate of heat release (RoHR), the in-cylinder pressure, the injection pulse and the bulk gas temperature have been depicted.

From the Figure 2.1, the first stage or phase considered is the ignition delay. The ignition delay is determined by the start of injection (SoI) and the start of combustion (SoC). This phase consists of the fuel atomization and vaporization inside the combustion chamber during the injection process. With the evaporated fuel appears the first chemical reactions prior to the

autoignition [7]. These reactions can be observed at the RoHR curve, very small variations appear while the in-cylinder presure curve is not reflecting these reactions. The reason is that these reactions are very low exothermal. Therefore, these reactions are called *"Cool flames"*. These pre-reactions usually conclude with the autoignition [8].

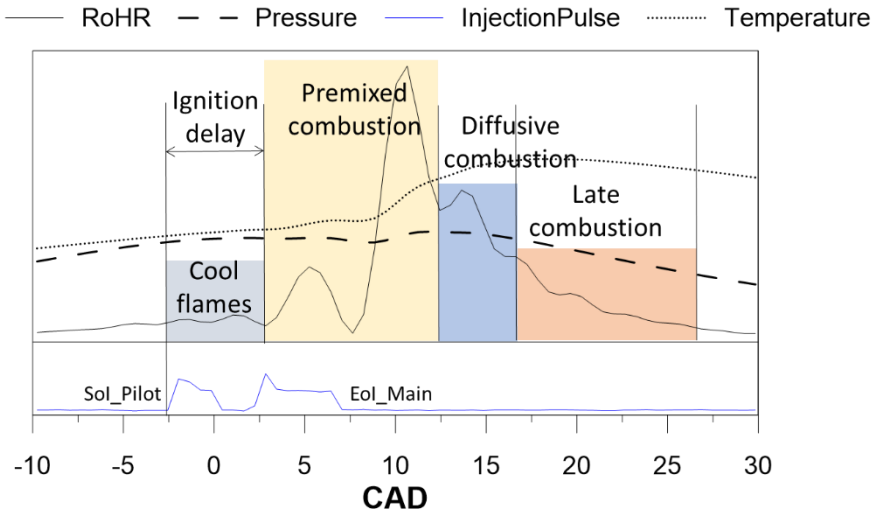

Figure 2.1. Phases of the conventional diesel combustion.

The second phase is the premixed combustion. This stage is characterized by the oxidation of the fuel injected during the ignition delay because it has not reached the proper conditions to autoignite [9]. During this phase, the RoHR achieves a maximum peak and then the curve decreases up to a relative minimum, which determines the next combustion phase. Next phase is known as diffusive combustion. The RoHR of the diffusive combustion phase is governed the by the mixture of the evaporated fuel and the air process. In addition, it is possible to assume that the equivalence ratio at the reaction zone is close to the stoichiometric values [10]. Indeed, the process of fuel/air mixture is conducted by the fuel jet momentum introduced to the combustion chamber. During this phase, most part of the pollutants are formed. Considering a quasy-steady fuel jet conditions for the fuel jet

stream, the main structure that form it is depicted in Figure 2.2. Regarding the figure, the inner zone consist of unburned fuel (or partially oxidated) and the soot formed at the premixed flame zone. Oxygen is consumed outside the flame, at the periphery of the jet where is located the diffusive combustion.

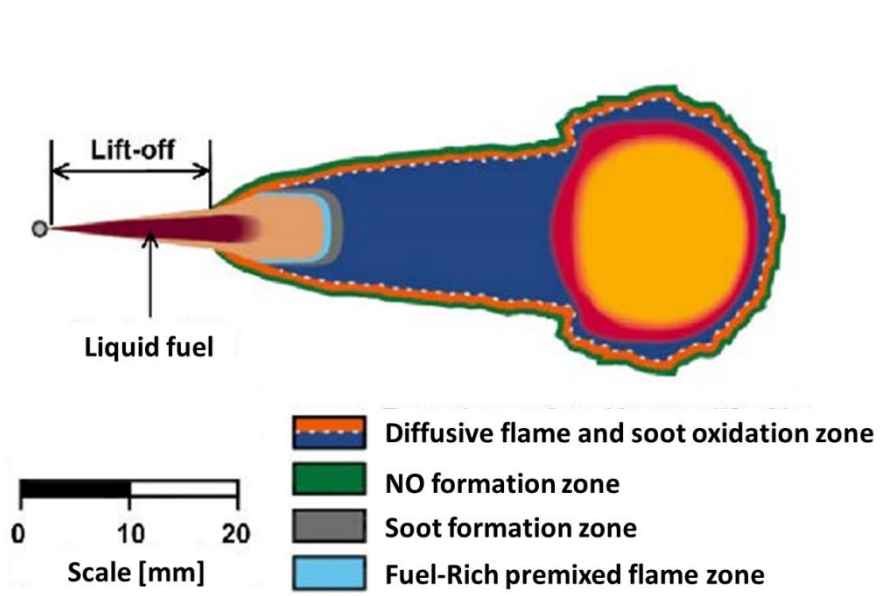

Figure 2.2. Diffusive diesel flame structure under quasi-steady state conditions, according to the model proposed by Dec [1].

As the injected fuel advances to the periphery of the flame from the inner zone, the fuel increases the temperature due to the proximity of the flame front provoking an increase at the soot particles [11]. Nearby the flame front, the size of the particles is maximum, but once the particles go through the reaction zone, the particles are oxidized and the particle concentration reduces close to cero. Regarding the NOx formation, outside the diffusive flame there is a lean fuel zone with high temperature and oxygen that provokes the NOx formation due to thermal mechanisms [12].

The last phase of the diffusive diesel combustion is called late combustion. During this phase, the fuel mass that it has not burnt continues

mixing with the air at the combustion chamber due to the existing turbulence. Due to the NOx formation process is slow, around 33% of the NOx formed during the combustion process takes part at this phase of the combustion [12]. From the soot emissions standpoint, soot formation reduces after the diesel injection event. However, the process of particle oxidation stops when the temperature decreases, permitting that particles go through the exhaust pipes [13].

Hence, soot formation appears at the inner zones of the diffusive flame where fuel rich equivalence ratios occur due to a lack of air (oxygen than can oxidize the fuel). On the other hand, NOx formation takes place outside the diffusive flame with leaner fuel zones that are burnt in presence of high rates of oxygen and high temperatures. This relation between NOx and soot observed at diesel combustion is a trade-off between both pollutants. This trade-off does not allow to reduce both pollutants simultaneously [15]. This phenomenon is also called "*Diesel dilemma*".

Figure 2.3 presents the ϕ – T diagram for the diesel combustion for different combustion concepts (LTC, PCCI, HCCI and CDC) [15]. The figure shows the local equivalence ratios (ϕ) at the y-axis and the temperature (T) at the x-axis. Inside the graph, Kamimoto and Bae [16] plotted the NO and soot formation regions. Soot region was obtained by using their own experimental results. NO formation region was obtained by means of the Zeldovich equations. As it can be observed at the figure, CDC includes much of the soot peninsula and part of the NO peninsula. This fact states the trade-off existing. Recent CDC strategies may reduce the soot by increasing the injection pressure and thereby, lowering the local equivalence ratio. But, due to the trade-off, increasing the injection pressure might result in higher NOx emissions what forces to use other options such as aftertreatment solutions in order to mitigate both pollutants. However, aftertreatment solutions such as diesel oxidation catalyst (DOC) to mitigate NOx emissions and diesel particulate filter (DPF) to remove carbonaceous particles from the exhaust gas allow the CDC concept to meet the current stringent standard emissions limitations (EU VI, EPA, …). These systems

imply an increase in the engine cost and the operational life along the engine life.

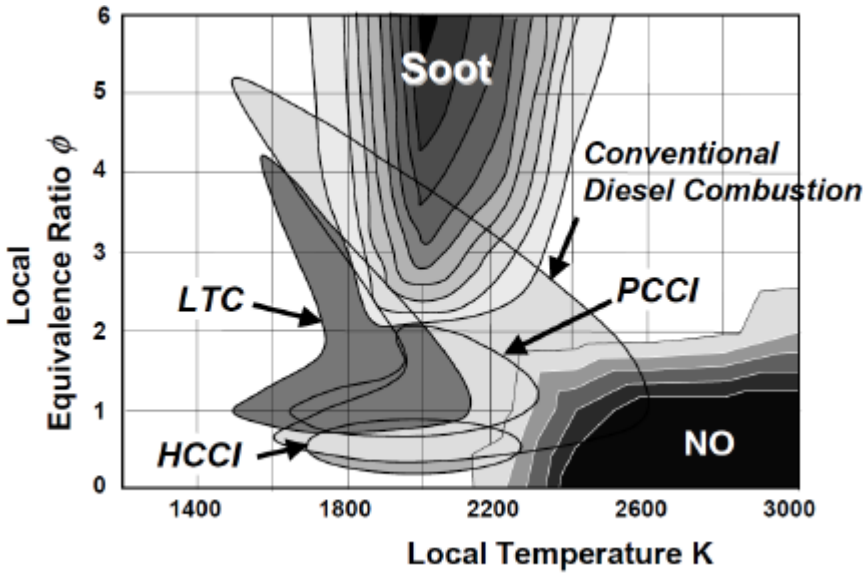

Figure 2.3. Φ–T *map for NO*x *and soot emissions in diesel combustion [15].*

Thus, in order to solve the main challenges of the diesel fueled engines, several new compression ignition combustion strategies have been proposed to reduce NOx and soot emissions simultaneously while the thermal efficiency is maintained or improved [17][18]. These advanced strategies will be briefly reviewed during the next subsections of the present chapter, which would generate the background required to define the motivation and the main objectives of the thesis.

2.3 Low temperature combustion strategies as a solution to Soot/NOx trade-off.

In order to overcome the trade-off between the NOx and soot emissions, different pathways of investigations were carried out several years ago. Most

part of these studies were focused on low temperature combustion strategies [19]. These works were aimed to split the injection process from the combustion process in order to avoid local rich equivalence ratios. In parallel, other strategies such as EGR use were aimed to reduce the local combustion temperatures. These strategies were pioneer in homogeneous LTC. Recently, premixed strategies applied in compression ignition engines appeared presenting a new pathway to solve the *"diesel dilemma"* towards Dual-Fuel combustion strategies.

A vast number of strategies have been developed being assigned different names such as Active Thermo Atmospheric Combustion (ATAC), Toyota Soken (TS), Homogeneous Charge Compression Ignition (HCCI), Controlled Auto Ignition (CAI), Premixed lean Diesel Combustion (PREDIC), Modulated Kinetics (MK) and so on. But most part of these strategies can be divided in two groups, those which are totally homogeneous (HCCI) and those which are partially premixed (PPCI). As it has been aforementioned, both concepts are aimed to reduce NOx emissions due to the reduction of the temperature during combustion which avoids NOx formation by thermal mechanisms. In addition, increasing the delay between the SoI and the SoC, the mixing time increases, which results in a reduction of the local fuel rich equivalence ratios and thereby, soot formation is mitigated [20].

Hence, as it can be observed in Figure 2.3, CDC and LTC combustion zones are depicted. Thus, it is observed that LTC strategies usually are operated outside the soot and NO regions. In addition, not only provide the possibility to break the existing trade-off, but they can reach similar or even better efficiency than the CDC due to a low heat transfer. The following subsection will describe the main LTC concepts and the most important LTC developed, presenting the main benefits and challenges of these concepts.

2.3.1 Mixing-controlled LTC

Mixing-controlled strategies are characterized by controlling the combustion phasing with the mixing process and the combustion process occurs with a low local temperatures range.

One of the benefits of the mixing-controlled strategy is that it maintains the combustion phasing controlled from the CDC mode. This represents a key point for the present strategy. It is widely known that one of the key points of the CDC strategy is the combustion phasing control. CDC controls the combustion phasing with the fuel injection system. Thus, it allows to increase the engine load keeping the combustion phasing under control as well as the rate of heat release.

On the other hand, in order to avoid the NO zone, as it is observed in Figure 2.3, the temperatures during the combustion process have to be lower than 2100K. Mixing controlled strategy has been deeply investigated by the research community [21][22]. Picket and Siebers proposed several guidelines to achieve LTC conditions under mixing controlled concept [23]:

- Massive EGR rates and better atomization of the diesel fuel.
- Massive EGR rates and the use of oxygenated fuels.
- Combustion chamber temperature reduction.

Hence, the research community studied the potential of this concept by applying different strategies in a compression ignition engine. The most important strategies are:

- **Massive EGR rate use in order to reduce the Y $O_{2,IVC}$:**

  This strategy is the most commonly investigated [24]. Benajes *et al.* [25] investigated the use of massive refrigerated EGR rates and high injection pressures. Figure 2.4 shows the main results of the investigation carried out. As it can be observed, three diferent levels of EGR were tested, resulting on three different levels of oxygen at the

intake. Despite the reduction of the oxygen, the use of high fuel injection pressure allow to avoid NOx and soot formation, as it can be observed at the figure. However, the excessive dilution rate achieved due to the massive EGR rate implies a drastic reduction at the combustion efficiency, which results in a high fuel consumption.

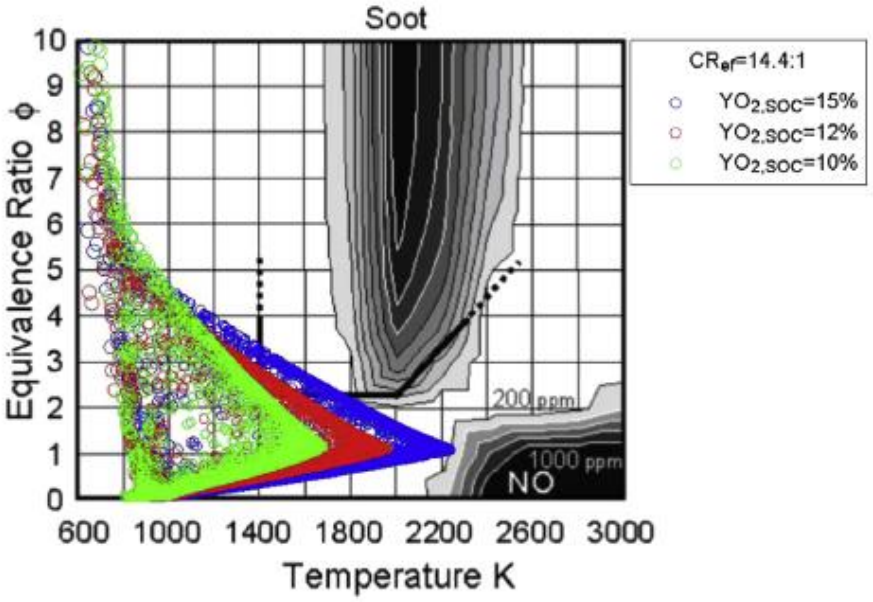

Figure 2.4. Φ–T map for NOx and soot emissions in diesel combustion for different Y_O2,IVC [25].

- **Miller cycle in order to reduce the in-cylinder temperature:**

In order to reduce the in-cylinder temperature is to apply a Miller cycle. Miller cycle reduces the in-cylinder temperature during the compression stroke [26]. Benajes *et al.* [26] studied the effects of using a Miller cycle and a high pressure fuel injection system. The main results provided by the study are presented in Figure 2.5.

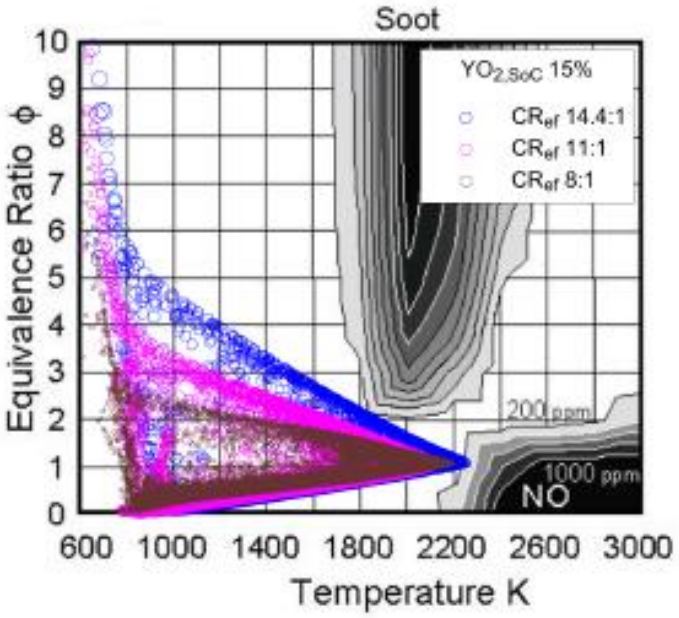

Figure 2.5. Φ–T map for NOx and soot emissions in diesel combustion for different effective compression ratios tested [27].

As it can be observed in Figure 2.5, this technique allows the simultaneous reduction of NOx and soot emissions. The possibility to operate with low fuel equivalence ratios and low in-cylinder temperatures avoids NOx and soot formation. Compared to the previous strategy, this concept maintains good levels of combustion efficiency. By contrast, the pumping work required to satisfy the air management requirements worsens the break specific fuel consumption.

2.3.2 Premixing strategies

Premixing strategies emerge as a solution to the LTC problems found at mixing-controlled strategy. Premixing strategies are focused on the objective of breaking the trade-off between NOx and soot and improve the

thermal efficiency in order to maintain or improve the fuel consumption compared with the CDC.

Therefore, decoupling the injection timing with the trigger of the combustion is the base on the success of these strategies. Hence, the delay between the end of injection (EoI) and the start of combustion (SoC), called "mixing time", will increase reducing the local fuel equivalence ratio which avoids soot formation [20]. In addition, this type of strategies presents a fast combustion process due to the premixing nature which yields in a reduced heat transfer losses. Therefore, this strategy achieves similar or lower fuel consumption than CDC concept. Several investigations endorse these premises [28][29][30][31][32][33].

Amongst other LTC premixed strategies, the present thesis will consider those strategies which have shown more potential such as HCCI, PCI and RCCI. Thus, a brief explanations of the concepts and a summary of the main benefits and drawbacks is presented along the next subsections.

2.3.2.1 Homogeneous charge compression ignition

Homogeneous charge compression ignition (HCCI) consists of having an excellent mixture of air and fuel prior to the auto ignition. HCCI is usually achieved by injecting the fuel at the intake port (using PFI injectors) or directly at the combustion chamber. Injection timing represents a key point due to it should guarantee enough mixing time to premix the fuel and air well enough to reach a quasi-homogeneous mixture. Once the premixed mixture is compressed, it auto ignites because of the chemical kinetics.

HCCI has been widely investigated by the research community and was originally described by Alperstein *et al.* [34]. Alperstein used PFI with diesel fuel in order to create a complete premixed mixture with diesel and air.

This type of combustion with fully premixed mixture provide a fast combustion process. This combustion process is characterized by a short

combustion heat release with a high peak reducing the heat transfer. Therefore, HCCI usually achieves high thermal efficiency during the combustion process. In addition, due to the premixing of the air/fuel, the local fuel equivalence ratios are lean which avoids soot formation. From the NOx emissions, HCCI combustion nature provides a stabilized flame front, which reduces the combustion temperature and thereby, mitigates the NOx formation. Hence, HCCI provides a high thermal efficiency combustion strategy that reduces NOx and soot emissions simultaneously. This behavior can be observed in Figure 2.3, where the HCCI region has been also depicted outside the soot and NO zones.

However, the mixture of fuel/air located at the crevices volume is usually not burnt during the combustion process due to the low temperatures achieved. Thus, this strategy is characterized by promoting such excessive levels of CO and unburned HC [35] which worsen the combustion efficiency increasing the fuel consumption. Another issue is that the combustion process is dominated by the chemical kinetics. This phenomenon difficults the combustion phasing control and the operation during cold start which limit the operation to partial load range [36]. This lack of combustion phasing control also increases the pressure rise rate when the load increases which can cause severe damage on the engine.

Finally, these shortcomings of the concept made to mitigate the interest on this strategy as a possible solution to the CDC despite the potential shown in terms of thermal efficiency and the low NOx and soot emissions. In order to overcome the main drawbacks of this concept, Bessonette *et al.* [37] proposed that low loads would require the use of higher reactivity fuels and high loads would require low reactivity fuels.

Several strategies such as Partially Premixed Combustion (PPC) focused on gasoline-like fuels. The PPC strategy improves the control of the heat release while decreases low NOx and soot emissions. However, this strategy presented several issues regarding the low load operation. Main problems related with the burning of the gasoline were increased when RON

was higher than 90, causing an excessive cycle-to-cycle variation. Some investigations were performed in order to mitigate the dispersion between cycles by adding a spark assistance. The spark assistance allows to operate with higher RON gasolines. By contrast, the spark plug requires local rich equivalence ratios at the combustion chamber in order to enhance the conditions at the start of the spark timing increasing the fuel consumption. Using different ignitability fuels was also studied achieving up to 50% of gross indicated efficiency while low levels of NOx and soot emissions were obtained.

2.3.2.2 Premixed compression ignition

Premixed compression ignition (PCI) appears as a solution for the weaknesses observed under HCCI operation. PCI differs from HCCI at the air/fuel mixture. The mixture resultant in PCI is premixed and it is not completely homogeneous. Hence, it is possible to improve the combustion control by varying the injection timing, which affects directly to the chemical kinetic that conducts the combustion process. Therefore, PCI uses direct fuel injection and injects during the compression stroke, thus the premixed mixture obtained due to the more heterogeneous equivalence ratios distributions obtained instead of completely homogeneous mixture found at HCCI concept.

PCI has been deeply studied by the research community [38][39]. PCI uses a fuel with high reactivity such as diesel. In addition, it is not needed to condition the temperature at the intake when operated in HCCI, due to the conditions of density and temperature reached at the cylinder allow to operate with lower temperatures at the intake. This combination improves the engine operation during low load because of the auto ignition has been improved.

By contrast, the benefits in terms of NOx and soot emissions are worst compared with the HCCI concept, as it can be observed in Figure 2.3. The more heterogeneous mixture provided by the equivalence ratio distribution generate soot. On the other hand, the benefits in terms of in-cylinder

temperature at low load increase the NOx formation when the load increases. Therefore, PCI requires massive EGR rates as the load increases [40]. Additional shortcomings of the concept were found regarding the injector and the piston bowl geometry. These elements need to be redesigned in order to operate under PCI mode. Stock CDC configurations may cause damage to the engine due to the impact of the diesel jets to the cylinder liner. This impact washes the oil that lubricates the piston surface and the cylinder liner resulting in an increase at the friction between them and, the engine oil gets contaminated with diesel fuel also. As a result, the engine lubrication efficiency decreases [41]. In order to overcome these problems, numerous investigations were carried out focusing on the hardware and injection strategy. Several studies developed new combustion strategies aimed in the HCCI and PCI load range extension such as premixed lean diesel combustion (PREDIC), multiple stage diesel combustion (MULDIC), uniform bulky combustion system (UNIBUS), multiple injection bumped combustion (MULINBUMP) and so on.

Park et al. [42] studied the effects of the fuel blends formed with diesel and gasolines. Inagaki et al. [43] proposed the dual-fuel PCI combustion concept feeding the engine with two fuels of different reactivity by means of separated injection systems. The different reactivity of the fuels was found to be a key factor for triggering the combustion phasing, also showing very promising results in terms of performance and emissions. Kokjohn et al. [44] continued this investigation and referred the combustion concept as reactivity controlled compression ignition (RCCI).

2.3.2.3 Reactivity controlled compression ignition

Amongst others, reactivity controlled compression ignition concept is the most promising LTC, achieving simultaneously low NOx and smoke emissions and high thermal efficiency under different fueling strategies [45][46] and hardware conditions [47][48]. RCCI presents excellent capabilities in order to overcome the challenges found with traditional LTC strategies

allowing to increase engine load range while the combustion phasing is under control [49].

2.3.2.3.1 Reactivity controlled compression ignition concept on a compression ignition engine

This subsection explains briefly how RCCI is implemented in a CI engine. Several variations have been used to introduce more than one fuel at the combustion chamber, but the traditional structure is depicted in Figure 2.6.

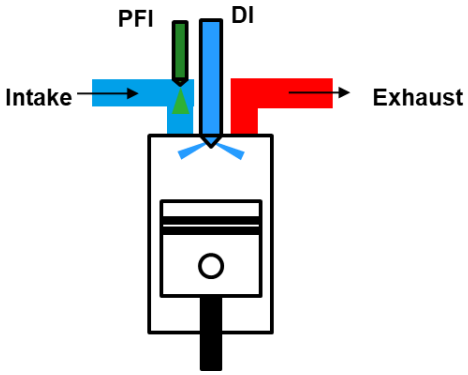

Figure 2.6. Separated fuel system scheme proposed by Inagaki [43] to implement RCCI in a CI engine.

The system proposed by Inagaki, shown in Figure 2.6, presents a dual fuel injection system. A port fuel injection (PFI) is used to inject the low reactivity fuel (LRF) at the intake manifold in order to create a homogeneous mixture of air and fuel. In this case, it is obvious that the air is the resultant combination of fresh air and EGR. Hence, the homogeneous mixture formed is compressed by the piston during the compression stroke. During this phase, the high reactivity fuel (HRF) is injected through the direct injector (DI) placed at the cylinder head. HRF can be injected in more than one event. HRF is usually injected around 50 to 60 CAD bTDC in order to premix as much as possible the HRF with the existing mixture at the combustion chamber. Once the mixture is compressed, the conditions at the combustion

chamber will determine the auto ignition of the mixture between HRF, LRF, fresh air and EGR [44]. This particular phenomenon was investigated by Splitter *et al.* [50] using optical techniques in order to visualize the ignition process. In addition, the study concludes that the ignition follows the reactivity gradient at the combustion chamber, moving from the more reactive zones to the low reactive ones.

Other hardware configurations have been used by adding a secondary direct injector. But these configurations require additional space at the cylinder head which difficult its implementation.

2.3.2.3.2 Benefits of the reactivity controlled compression ignition concept over other premixed strategies

According with the hardware configuration disposed to operate under RCCI combustion strategy, this combustion strategy opens the possibility to manage different fuel blends on demand. In this sense, it is possible to adjust the reactivity of the fuel blend depending on the engine load desired. Hence, the proper reactivity for each operating point provides an optimized combustion phasing. As a consequence, the rate of heat release (RoHR) provided by the concept results in an optimized curve that minimizes the heat transfer losses, achieving better fuel consumption efficiency that previous LTC concepts [51].

In addition, it is worthy to note that the reactivity of the air/fuel mixture is modified with the EGR and the fuel blend. Thus, this concept requires also massive use of EGR rates and the control of the HRF timing.

Concluding with the RCCI concept, the main benefits of this strategy are summarized as follows:

- Allows to reduce NOx and soot simultaneously.
- Presents great fuel efficiency such as other LTCs.
- Combustion phasing is controlled by the reactivity of the air/fuel mixture.

- It can be operated from low to full load by using a dedicated SCE capable to operate up to 30 bar/CAD, depending of the CI hardware configuration [51].

2.3.2.3.2.1 Gaseous emissions and performance achieved with RCCI

In order to explore the potential shown by the RCCI concept, Monsalve-Serrano explored the capabilities of the concept in a CI engine [51]. Monsalve-Serrano used a SCE engine with a compression ratio (CR) of 14:1. His first approach to the concept was to test two different strategies to achieve RCCI operation. First strategy was focused on the effect of the EGR and the gasoline fraction over the emissions and fuel consumption and the second strategy was focused on the effect of the intake temperature and the gasoline fraction over the emissions and fuel consumption. Main conclusions of the study were that both strategies allow to increase the combustion efficiency and GIE. Both strategies also provide ultra-low levels of NOx emissions below EU VI standard emissions limitations. However, compared to CDC, excessive values of CO and unburned HC emissions were obtained. The comparison made is depicted in Figure 2.7.

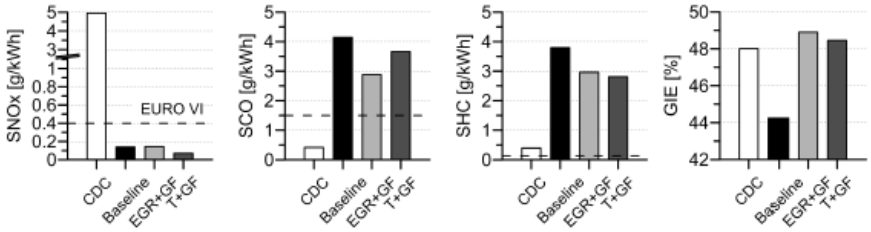

Figure 2.7. Comparison of both strategies studied by Monsalve-Serrano and the CDC strategy at medium engine load operation [51].

Following with the study carried out by Monsalve-Serrano [51], he stated that the control of the injection pattern (single or double) and the SoI of the direct injection could reduce simultaneously NOx and smoke emissions in a limited range of operation, if the combustion phasing is obtained in order to improve the gross indicated efficiency.

Hence, the concept efficiency can be also optimized by adjusting the local reactivity by means of the fuel-blending ratio. In this sense, the low reactivity fuel usually represents most part of the total fuel mas injected. This balance between the high reactivity fuel and the low reactivity fuel has been demonstrated as a key point in order to achieve the simultaneous reduction of NOx and smoke emissions. Thus, not only the reactivity of the fuel blend is important, the properties of the fuels also play a key role at the combustion process. Therefore, Monsalve-Serrano studied different LRFs which provide a variety of reactivity gradients between both high and low reactivity fuels. Monsalve-Serrano concluded that despite of the different LRF tested, the ignition of the combustion occurs due to the HRF reactions. However, the more reactive LRF, the more energy released during this combustion phase. Also the oxygen concentration showed a key role at the onset of the combustion. In this sense, it states that octane number (ON) of the LRF affected to the combustion duration. Thus, as the ON is lowered, the combustion duration decreases, presenting the main differences at the SoC.

Focusing on the fuels that show potential to operate from medium to high engine load, Figure 2.8 presents a comparison between biofuels and petroleum-based fuels. Main conclusions showed the necessity to reduce the compression ratio in order to operate at high engine load and a linear relation between the HRF SoI and the combustion phasing (CA50).

And considering the comparison performed at Figure 2.8, the different fuel blends used provide ultra-low values of NOx and smoke emissions while the efficiency was increased and the pressure rise rate was kept below the self-imposed mechanical constraint of 15 bar/CAD.

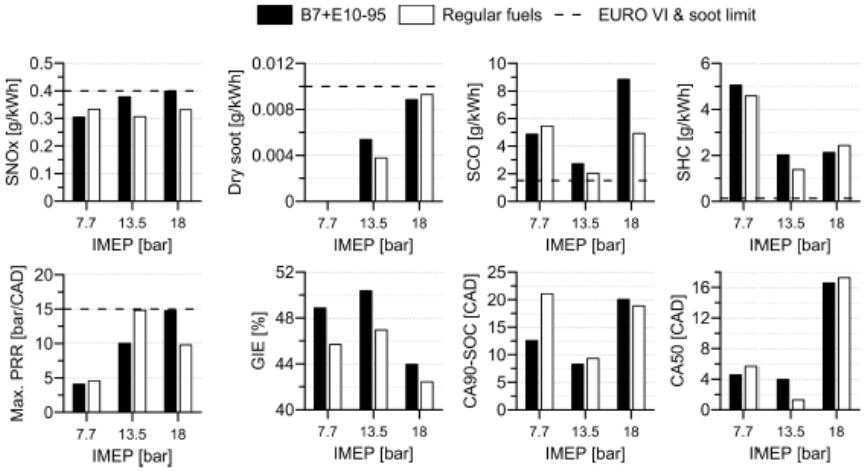

Figure 2.8. Results provided of the comparison of standard fuels such as gasoline and diesel and biofuels such as E10-95 and B7 by Monsalve-Serrano [51].

From these results, it is stated that RCCI has great potential as a flexi-fuel concept.

After these considerations, Monsalve-Serrano [51] decided to test B7 as a high reactivity fuel and E20-95 as a low reactivity fuel in a medium-duty engine. This investigation was motivated by the use of the CI engines at the transportation sector fitted with high costly aftertreatment systems in order to mitigate the engine-out emissions and meet the stringent standard emissions such as EURO VI. The engine used derived from a commercial production engine which was developed under EU VI specifications. Thus, the engine used was completely equipped with the stock hardware.

Figure 2.9 presents the main results provided by the investigation in terms of engine-out emissions and pressure rise rate and maximum in-cylinder pressure. As it can be observed, the engine load is limited up to 35% due to the excessive pressure rise rate achieved during the engine operation. At 35% engine load, the pressure rise rate reach 15 bar/CAD and the in-cylinder

pressure almost reach the maximum of 190 bar. Overpassing those values could damage the engine dramatically.

From the emissions standpoint, RCCI concept applied to a medium-duty engine by using the stock configuration shows its capabilities to promote NOx and Soot emissions below the imposed emissions constraints. It is worthy to note that the emissions constraints are EURO VI limits based without taking in account the transient operation.

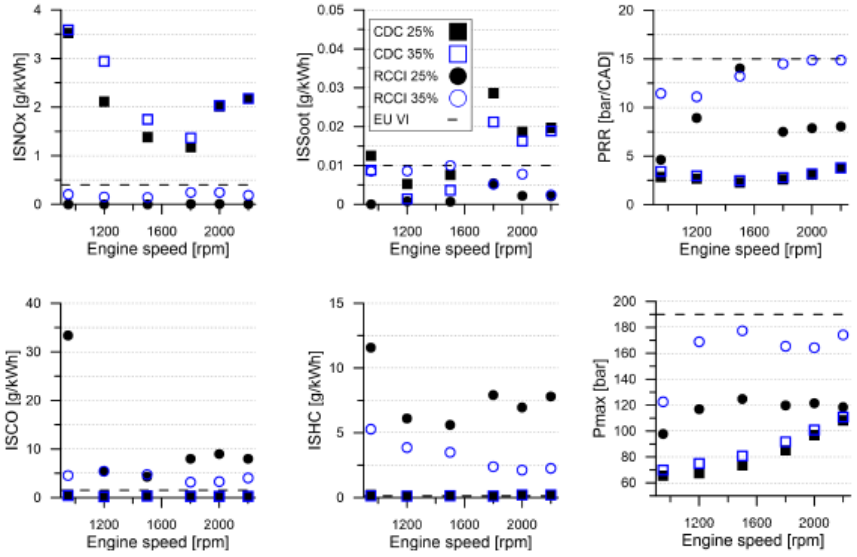

Figure 2.9. ISNOx, ISSoot, ISCO and ISHC emissions and PRR and maximum in-cylinder pressure comparison between RCCI and CDC provided by Monsalve-Serrano[51].

Main conclusions of this work state that considering the restrictions imposed in terms of NOx and soot emissions, the engine load operation was limited to 35%. Indeed, the turbocharger was capable to supply the boosting pressure demanded by the concept as well as the stock EGR loop provided the required EGR. Indeed, the stock compression ratio of 17.5:1 provided high enough exhaust temperatures to provide energy to the turbocharger as

well as energy to the catalytic converter which ensure the catalytic conversion without major problems.

By contrast, Monsalve-Serrano proposed a Dual-Mode concept in order to extend the engine load range up to full load with such a high compression ratio without exceeding the mechanical constraints of in-cylinder pressure and pressure rise rate.

2.4 Drawbacks of the RCCI concept

As demonstrated, RCCI is one of the most promising LTC concepts which is able to reduce simultaneously NOx and smoke emissions while the performance provided reaches the level achieved by the CDC. Compared with the rest of LTC modes, the engine range operation is wider and it is possible to operate from low to full load. However, RCCI concept also presents several drawbacks that have to be considered in order to consider its real implementation in stock production engines. Hence, the present subsection is focused on describing these drawbacks which can be divided in mechanical limitations that limit the engine range operation, emissions limitations that limit the efficiency of the concept and total number of particles emitted by the concept.

Regarding the mechanical limitations, pressure rise rate and maximum in-cylinder pressure become extremely high as the load increases. Thus, the maximum engine load achievable needs to be limited, compared with the CDC concept, in order to provoke severe damage to the engine.

The emission limitations in terms of NOx and smoke also limit the high engine load operation. Thus, in order to increase the engine load massive EGR rates and boosting conditions are mandatory to reach full load while ultra-low values of NOx and smoke are maintained. These requirements need to be studied to provide a turbocharging system as well as an EGR loop design capable to provide such conditions. On the other hand, excessive CO and unburned HC emissions are usually found at RCCI concept when it is

operating at low engine load. These emissions are related with the compression ratio used and the amount of gasoline injected through the PFI.

Finally, current stringent standard emissions limitations are taking in account the total number of particles emitted. The particles emitted by the concept have not been widely investigated by the community research, but the studies found state that the RCCI concept usually provides a higher number of particles but with a smaller scanning mobility diameter that the particles emitted under CDC mode.

2.4.1 CO and uHC emissions: Issue at aftertreatment efficiency

Regarding the main challenges of the RCCI concept, this subsection focuses on the CO and unburned HC emissions. Both pollutant emissions presents one of the biggest weaknesses of the concept due to the low load operation. In this sense, as it can be observed in Figure 2.10, the studies carried out over the whole engine operation load and speed states that CO and uHC emissions are excessively high during the low load operation. From the figure, CO emissions achieve up to 90 g/kWh below 4 bar of BMEP and uHC emissions achieve up to 55 g/kWh at the same engine load operation. Compared with the EU VI limitation, the emissions promoted by the concept exceed by far the limits. Hence, in order to meet the stringent emissions limitations, the need of an aftertreatment system is mandatory to obtain engine emissions at the tail pipe below the imposed limits.

In order to reduce both pollutants simultaneously, a diesel oxidation catalyst (DOC) is the aftertreatment element required. However, DOC also presents some issues due to the low combustion temperatures characteristics of the LTC strategies in general and the RCCI concept in particular.

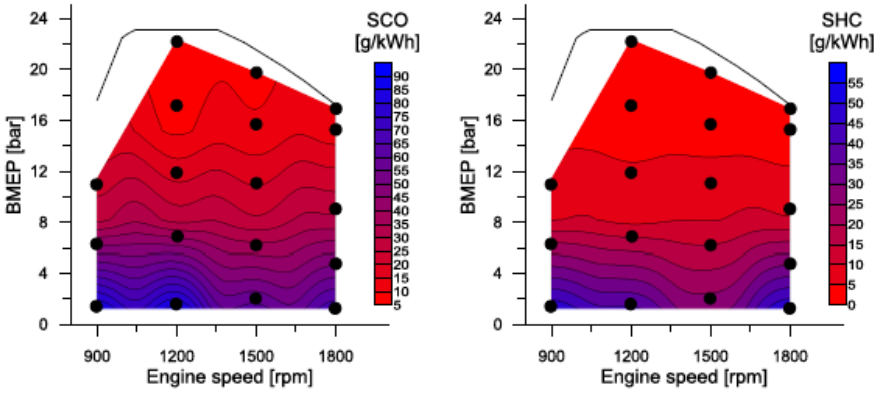

Figure 2.10. Engine-out emissions in terms of CO and uHC for the RCCI concept operated under a CR11:1 [51].

Prikhodko et al. [52] investigated the effectiveness of different DOC consistent of different substratums in order to reduce both, CO and uHC, emissions under RCCI strategy operation. In order to face the issues observed during the low load conditions, the study was performed with engine conditions that provided a range of temperatures between 160°C to 260°C. main results from this study state that there was no catalytic conversion activity below 200°C and above 300°C were effective removing CO and uHC emissions. Contrary to CDC mode, DOC provide around 80 to 100% of CO and uHC conversion at 190°C. Hence, light-off temperatures for DOC operated under RCCI mode are crucial to fulfill current emissions limitations, which are found around 200°C during RCCI operation.

Considering the results provided by Prikhodko and the adaptation of Monsalve-Serrano in [51], combined results have been depicted in Figure 2.11. As it can be observed, during low load operation and even up to medium load at low engine speeds, the temperature provided by the exhaust flow are below 200°C. Therefore, the conversion efficiency in this area is 0% due to the lack of catalytic conversion activity.

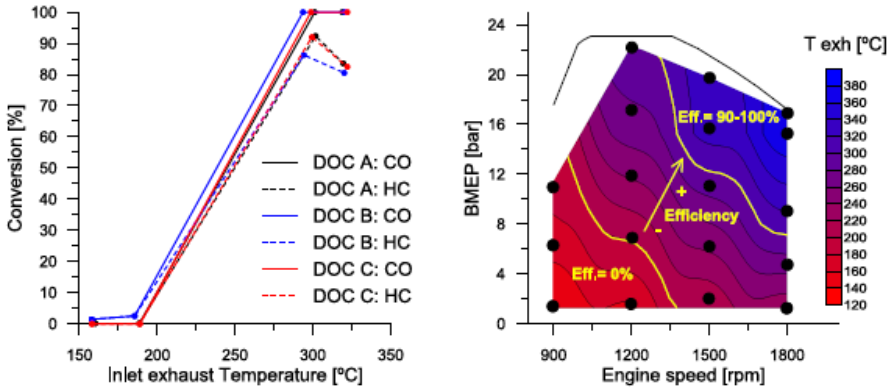

Figure 2.11. HC and CO conversion efficiency for different DOC under RCCI operation and the exhaust temperatures obtained at RCCI mode under a CR11:1 [51].

From the figure, the area with no conversion activity is located at the low left side of the engine map. This area starts at 900 rpm up to 1400 rpm with a triangle shaped depicted zone that reaches 14 bar of BMEP at the lowest engine speed. On the other hand, the work carried out by Monsalve-Serrano [51] was using a CR of 11:1, which might be excessively low to provide enough temperature at the exhaust due to the poor combustion afficiency achieved, as concluded in his thesis work.

2.4.2 Pressure gradient at high engine load

Another challenge present at the RCCI concept is the variation of the in-cylinder pressure respect to the variation of crank angle degree. Hence, excessive pressure rise rate (PRR) possibilities mechanical damage to the engine that limits the engine operation life.

RCCI concept usually achieves high PRR peaks during high engine load operation. However, CR plays a key role in this topic. When using high CR, the achievable load is decreased due to this PRR. In other words, the higher

the CR, the higher the PRR. Therefore, the maximum PRR appears earlier in load, limiting the maximum engine load achievable.

Monsalve-Serrano [51] carried out an investigation on a SCE derived from a production engine, which PRR was limited to a 15 bar/CAD in order to impose realistic mechanical constraints, provide ultra-low NOx, and smoke emissions that fulfill EU VI limitations under RCCI operation mode. E85 was used as a low reactivity fuel with the aim to enhance the benefits of the low reactivity fuel and increase the engine load operation under RCCI.

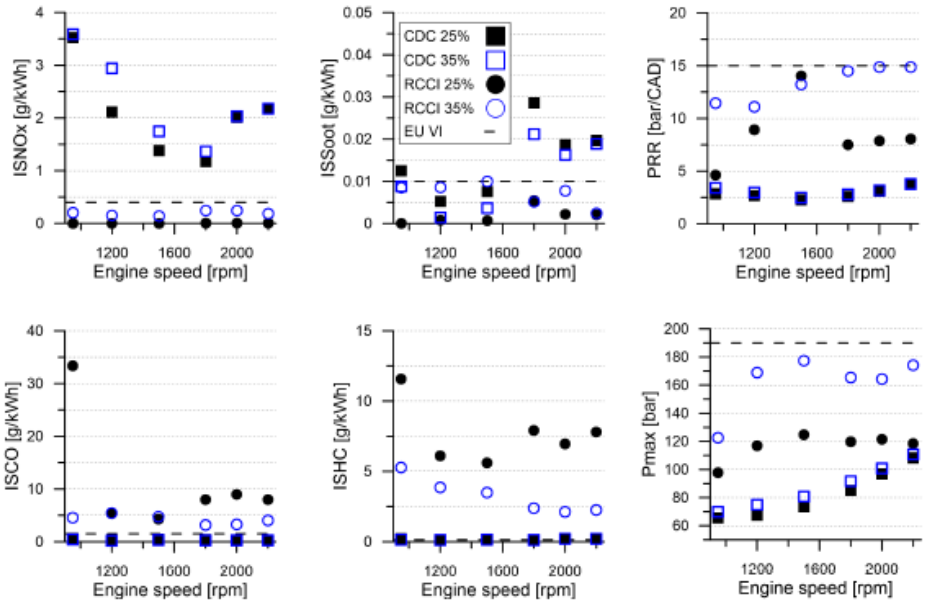

Figure 2.12. Comparison of RCCI and CDC emissions, maximum in-cylinder pressure and PRR at 25% and 35% load for all the engine speeds [51].

Main results of such study are presented in Figure 2.12. As it can be observed, a CI engine can be operated with the stock hardware configuration under RCCI providing NOx emissions below EU VI limits up to 35% engine load. However, the limitation of the concept come from the PRR, which

reached 15 bar/CAD for that engine load. Therefore, in order to overcome this issue different options could be feasible:

- Reduce the compression ratio decreases the peak PRR. This option would present some issues such as lower exhaust temperatures, higher CO and uHC emissions and fuel consumption increase.
- Emissions constraints can be modified and increase NOx and smoke emissions. Hence, by adjusting the EGR, combustion phasing and some other combustion parameters a higher engine load could be achieved. However, the benefits of ultra-low values of pollutants would be lost.
- Monsalve-Serrano proposed a Dual-Mode combustion strategy. In this sense, the engine would operate at low load under RCCI and at medium and high load under CDC mode. The main benefits of the Dual-Mode are that the engine could operate on the whole engine map. At low load operation, ultra-low NOx and smoke emissions will provide interesting results at the WLTC cycle, where low load points have a big impact over the total amount of NOx and soot emissions. Moreover, at high engine load operation the engine would maintain the performance of the stock diesel engine.

2.4.3 Air-loop requirements: Massive EGR demands

As it has been in 2.3.1 and 2.3.2, the use of EGR plays a key role in order to reduce the combustion temperatures avoiding the NOx formation. Particularly, RCCI concepts is characterized by using massive EGR rates over the whole engine map. One of the reasons to introduce such massive EGR rates is that the presence of EGR and the premixing of the mixture of air and fuel enlarge the ignition delay of the fuel blend (high reactivity fuel and low reactivity fuel). In this sense, the ignition delay improves combustion control that allows increasing the load and the engine speed.

Figure 2.13 presents below the boosting pressure and the EGR rate used in a medium-duty SCE operated under RCCI. Benajes et al. [53] operated this engine from low to full load under RCCI mode. In order to achieve the full load, the engine was boosted up to 3 bar for the whole engine speed points. In addition, in order to provide ultra-low NOx emissions and allow the control of the combustion, EGR rates up to 60% were required.

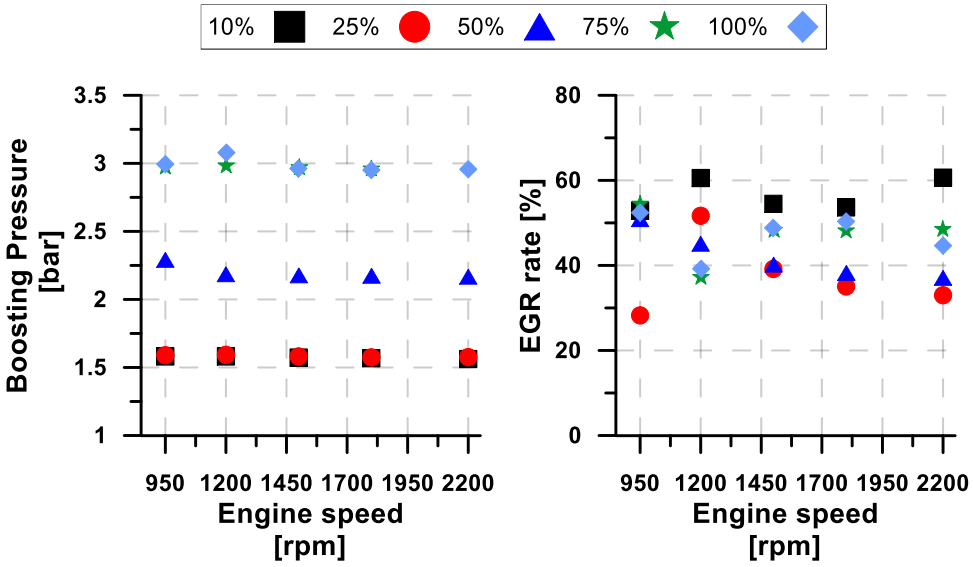

Figure 2.13. Boosting pressure and EGR rate used to operate a CI with a CR12.75:1 from low to full load under RCCI mode [53].

As it has been observed in Figure 2.13, the required air management conditions to operate a SCE under RCCI under a given mechanical and emissions constraints are depicted. The SCE requires a huge sort of subsystems in order to provide intake conditions required for every engine operation point. Hence, it is possible to adjust the boosting pressure, the intake temperature, the EGR rate and so on independently on the engine speed or the exhaust temperatures. Thus, during tests when using a SCE some settings might be difficult to achieve under real conditions without penalizing in excess in fuel consumption or limitations of the auxiliary elements such as the turbocharger.

In order to provide such as high boost pressures and considering the lack of thermal energy at the exhaust (reduced exhaust temperatures compared to CDC), a low pressure (LP) EGR system has been considered for the points presented in Figure 2.14. The figure presents the compressor flow and the compression ratio required to supply the engine and the compressor map from the stock engine configuration. It is worthy to note that the turbocharger design is optimized for the engine being operated under CDC. In this case, it has been considered the worst case for the compressor, LP-EGR system. The use of LP-EGR implies that the compressor has to compress the total amount of air mass (fresh air mass and EGR mass). Hence, the addition of the EGR mass instead the substitution of EGR mass flow by the fresh air mass flow is important in order to maintain the same air/fuel ratio that used when the SCE tests.

Regarding these considerations, the required total mass flow has been depicted over the stock compressor map in Figure 2.14. The engine used to carry the investigation was a Volvo D5K240. As it can be observed, the tested points are located outside the compressor map. That means, that the compressor should work in over speed with an extremely poor efficiency to provide such a high quantity of boosted intake air. As a result, another EGR loop should be used in a real engine or a redesigned turbocharger should be coupled to the engine in order to satisfy the RCCI requirements. A first approach seems to be a turbocharger with a bigger compressor that the stock turbocharger, but nothing is said about the turbine. Therefore, a dedicated study should be carried out to redesign the turbocharger.

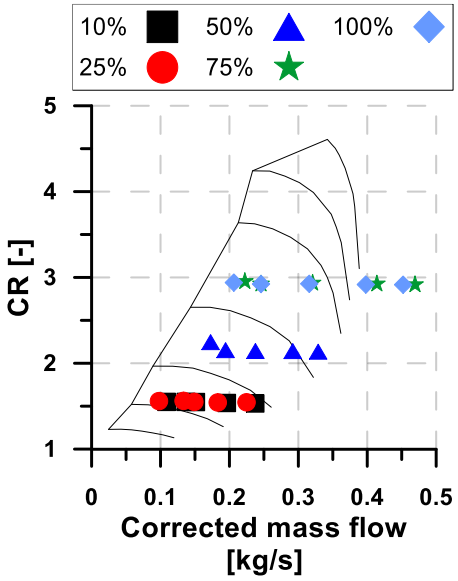

Figure 2.14. Approach of the SCE tested points over the stock compressor map (CR 12.75:1) [53].

From the EGR loop standpoint, numerous studies have been carried out in order to create models that allow operating hybrid solutions such as LP and HP EGR loops simultaneously. Anand studied different solutions to implement these air-handling systems in order to achieve high engine load operation while reducing the pumping work [54]. Anand also provide an air-handling study for the low load operation with the aim to improve CO and uHC emissions as well as the pumping penalty [54].

2.4.4 Particulates emitted by compression ignition engines

RCCI concept has been widely investigated measuring emissions in terms of performance and emissions such as NOx, smoke, CO and unburned HC. Despite the numerous studies, the smoke emissions only represent the opacity of the exhaust gases provided by the concept. Indeed, RCCI concept usually provides ultra-low values of smoke emissions but nothing is said about particle number emissions. Current standard emissions regulation (EURO

VI) also limits the number of particles (PN) and the particle size distribution (PSD) [55].

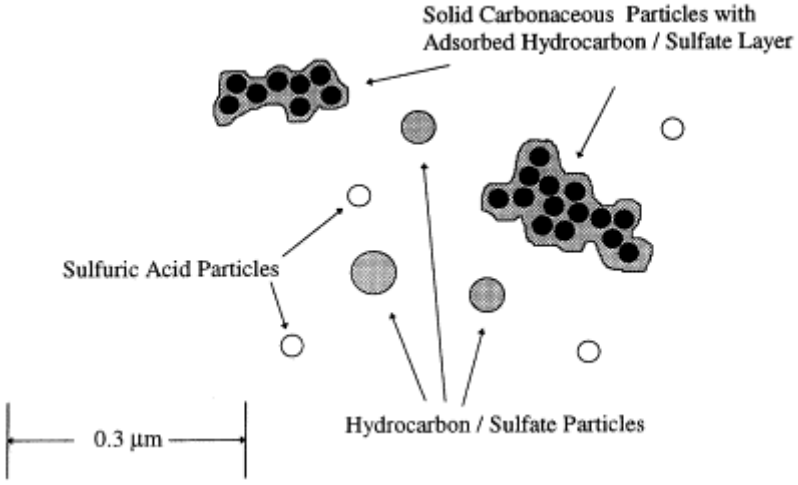

Figure 2.15. Composition and structure of exhaust gases promoted by a CI engine under CDC mode by Kittelson et al. [56].

Particles from CI engines operated under CDC strategy present a structure that it has been schematically depicted in Figure 2.15. Hence, the particles promoted by the CDC exhaust gases consist mainly of carbon, and volatile organic and sulfur compounds [56]. This carbonaceous nucleus is formed during the combustion process due to the local rich equivalence ratios reached while diesel is injected and burned (diffusive combustion). Most part of the soot formed is oxidized as the combustion process evolves, but some part of the soot is not oxidized and it is expulsed through the exhaust pipes. Hence, the residue exhausts with a solid agglomerates form. Volatile or soluble organic compounds (generally described as the soluble organic fraction, SOF) appear due to a tiny fraction of the fuel and the oil evaporated that escape from the oxidation process.

Particles measurement under CDC mode were usually mass-based. Thus, several studies have been performed to obtain the particle size distribution in order to improve the understanding of the particulate matter

(PM) emissions [56][57]. Kittelson et al. [56] described the particle size distribution (PSD) of CDC operation mode as it can be observed in Figure 2.16.

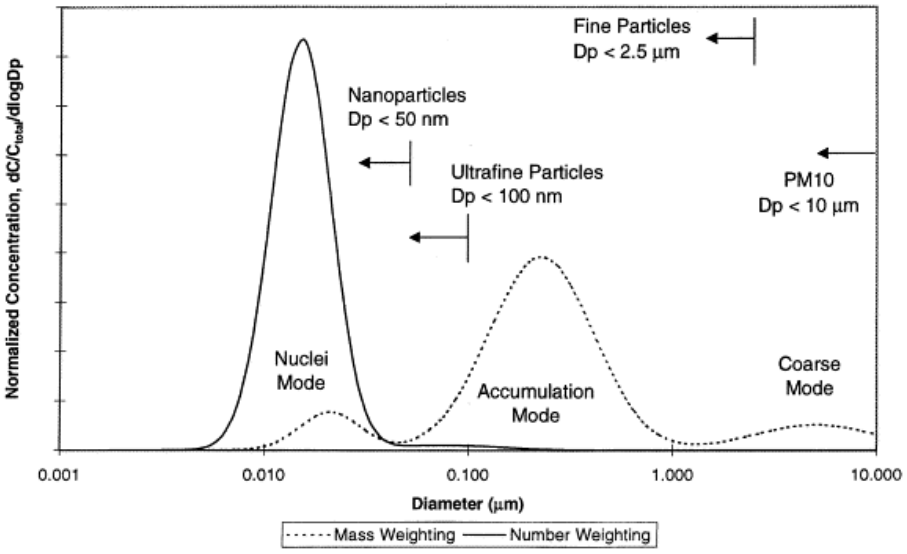

Figure 2.16. Particle size distribution in terms of number and mass provided by Kittelson et al. [56].

As it is depicted in the figure, the PSD curve is trimodal and lognormal in form. As it is observed, three types of particles have been considered under PM10 particles: nuclei mode, accumulation mode and coarse mode.

- **Accumulation mode:** The so-called accumulation mode particles refers to particles with a scanning mobility diameter range between 0.1-0.3µm. This range of particles represent most part of the particle mass due to the nature of the particle. In this case, the nature consists of carbonaceous agglomerates and associated adsorbed materials.
- **Nuclei mode:** The nuclei mode refers to particles with a scanning mobility diameter range that oscillates from 0.005 to 0.05µm. this mode is mainly formed by SOF and sulfur

compounds that are formed during the exhaust dilution and cooling. This mode may include solid carbon and metal components as well. The nuclei mode represents between 5 to 20% of the total particle mass and more than the 90% of total number of particles.

- **Coarse mode:** This mode is a combination of the two previous modes described. Hence, coarse mode particles are formed by accumulation mode particles that have been stopped at the cylinder and exhaust surfaces and later reentrained.

Additional studies on CI engines were focused on fuels by using ethanol-diesel and ethanol-biodiesel blends. Some of these investigations were carried out by Armas et al. [58][59] and were compared to diesel fueled only. Armas et al. stated that the use of oxygenated fuels provide a reduction in the number and size of the accumulation mode particles while the nuclei mode particles increased maintaining constant the peak diameter. Considering the total number of particles and the total mean diameter decreased when fuel blends were used.

In this sense, PSD analysis were performed on CI engines operated under LTC strategies [60]. Benajes et al. [60] compared the emissions on a CI under premixed LTC strategies from a heavy-duty engine and a light-duty engine and varying the SoI of the injection. Main conclusions of this work suggest that the highest smoke measurement were directly related with the number of large particles. In addition, it was observed that the number of smaller particles has an inverse trend with the larger particles.

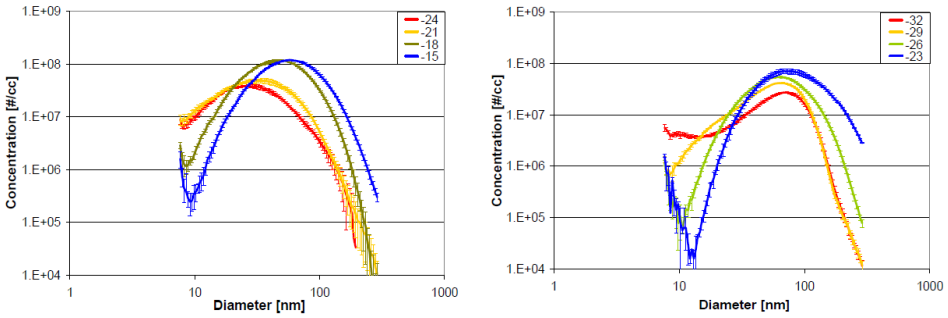

Figure 2.17. PSD measurements for multiple injection timings under LTC operation strategy. Left side results were obtained from a heavy-duty engine and right side results are provided by a light-duty engine [60].

Moving on to the RCCI strategy particles emissions, their speciation results indicate that the high boiling range of diesel hydrocarbons was likely responsible for the particulate matter mass captured on the filter media [59]. Prikhodko et al. [61] found that RCCI was highly dominated by nucleation mode particles. Several studies confirm that RCCI produces lower number of particles amongst other LTC strategies [62][63].

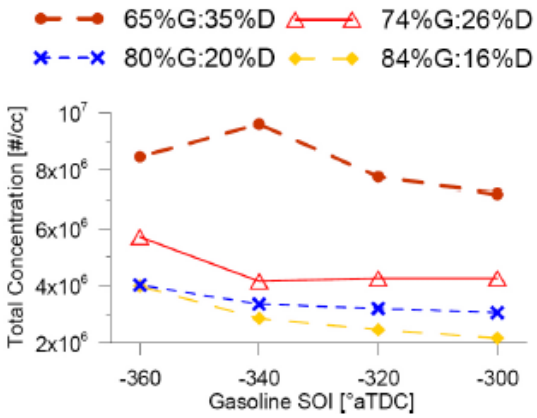

Figure 2.18. Effects of gasoline SoI on total particle number concentration [64].

Kolodziej et al. [64] also studied the effects of the diesel/gasoline proportion and the injection timings in the particle size while operating under RCCI. From the Figure 2.18 it is possible to observe that the particle concentration was not very sensitive to the SoI sweep. However, the PM was more sensitive to the SoI because of the inverse change between the number of nucleation mode and the accumulation mode particles. Respect to the gasoline proportion, it was observed that the number concentration of all particle size decreased when the gasoline proportion increased. Another interesting statement was the bi-modal curve shaped presented by the particle size distribution in a heavy-duty engine operated under RCCI strategy, which was coincident with the literature for light-duty engines. Following with these investigations, Zhang et al. [65] stated that LTC have very similar PSD shapes characterized by smaller sized particles.

Prikhodko et al. [61] also compared the results of FSN and PM filter mass measurements under RCCI operation mode, showing that RCCI PM is mostly organic carbon with almost no elemental carbon. Despite of having some correlations between FSN measurement and soot mass for premixed charged compression ignition (PCCI) operation [66], for RCCI is not possible to convert FSN in PM because most part of the PM comes from soluble organic fraction, which is not captured by the smokemeter [67].

2.5 Approach of the study

During the present chapter, a background of the investigation has been generated in order to justify the investigation carried out in this thesis document. Hence, the following subsections introduce the motivation, the general objective and the methodology of the work performed.

2.5.1 Motivation of the study

High thermal efficiency in reciprocating engines is one of the targets for the engine manufacturers. Compression ignition (CI) engines provide high

thermal efficiency as well as low fuel consumption. In particular, CI engines are usually fueled with diesel. By contrast, despite the CDC strategy benefits, several well-known challenges are still persistent due to the diffusive combustion as it has been afore explained in 2.2. The trade-off between nitrogen oxides (NOx) and soot impossibilities the reduction of both emission pollutants simultaneously. In order to meet current emissions regulations such as EURO VI, engine manufacturers have developed aftertreatment systems which drastically reduce theses emissions. These elements imply an increase in the engine cost and operational costs along the engine life. Indeed, the aftertreatment systems require late post injections of fuel to stimulate an active regeneration of the DPF, increasing the fuel consumption.

In order to solve the challenges of the diesel fueled engines, LTC strategies operated on CI engines reduce NOx and soot simultaneously while thermal efficiency is improved as it has been stated in 2.3.2. In 2.3.2.1, it has been mentioned that homogeneous charge compression ignition (HCCI) virtually avoids any NOx and soot formation. On the other hand, excessive pressure rise rate, due to the rapid heat release, limits the concept to the partial load range. In order to extend the range of application of the HCCI strategy, it was proposed to use different reactivity in function of the engine load. High engine load requires low cetane number and low load requires high cetane number. Hence, the use gasoline-like fuels (reduced cetane number) was extended in strategies such as Partially Premixed combustion (PPC), as it has been explained in 2.3.2.2. The PPC strategy results in a better method to control the heat release while promotes low levels of NOx and soot emissions. By contrast, it presents burning problems during low load operation when the gasoline presents a RON higher than 90. The excessive cycle-to-cycle variation at low load was deeply investigated in order to mitigate it. Thus, it was added a spark assistance what allow operating with high RON gasolines. However, the spark plug required local rich equivalence ratios at the start of the spark timing to promote the flame propagation, what increases fuel consumption. Another solution to improve the control of the PPC strategy was to use different ignitability fuels. Isooctane fuel was supplied by a PFI system and diesel fuel was injected by a DI system. Very

promising results were achieved by this structure, achieving up to 50% of gross indicated efficiency and promoting low values of NOx and smoke emissions. In this sense, the use of two fuels enabled the possibility to control the combustion facing by adjusting the reactivity of the fuel blend.

At this point, the strategy was named reactivity controlled compression ignition (RCCI) by Kokjohn et al. [29]. In 2.3.2.3, the RCCI concept has been introduced as the feasible solution to overcome the main challenges presented at the LTC strategies. Since the beginning, RCCI concept has been deeply investigated by the research community in order to explore the capabilities of the concept. Most part of these investigations were focused on the reactivity of the mixture with the aim to improve the understanding of the combustion control. Other studies were focused in heat transfer by optimizing the piston bowl design, exploring the best balanced compression ratio or injection pattern strategy in order to improve the reactivity stratification. RCCI concept demonstrated that it can be operated in a wide range of engine load and speed promoting ultra-low levels of NOx and smoke. Indeed, the ultra-low levels of NOx allow the engine-out emissions to meet the current EU VI limitation at steady state conditions without the need of the aftertreatment equipment. However, in real conditions, it is observed that the total remove of aftertreatment devices is not possible.

Nonetheless, RCCI also presents some challenges as it has been explained along the 2.4 subsection. The main challenges of the concept can be summarized as follows:

- In 2.4.1 it has been stated the excessive CO and uHC emissions provided by the concept. These emissions limit the operating range of the concept during low load operation. Even could limit the low engine speed operation. The combination of high emissions and low temperature at the exhaust difficult the catalytic activity conversion. Consequently, it is a challenge to provide reduced emissions at the tail pipe to meet the stringent standard limitations.

- In 2.4.2 the pressure rise rate appears as a limitation to increase the engine load. High PRR could exceed the mechanical constraints causing severe damage to the engine hardware. Thus, limiting or reducing the PRR contributes to increase the engine operating range towards the full load operation.
- In 2.4.3 it has been presented the challenge of the air handling. The RCCI requires massive EGR rates over the whole engine operation map. Hence, the EGR loop (LP, HP or hybrid between LP/HP), turbocharger, cooler need to be redesigned compared with the stock CDC hardware.

From the emissions standpoint, current standard emissions regulation has introduced a new limitation regarding particles emission. The subsection 2.4.4 has focused on the particles promoted by the compression ignition engines. Under CDC strategy, particles are mainly formed by carbon, and particle measurements are usually mass-based. In order to improve the understanding of the particulate matter (PM) emissions, several studies have been performed to obtain the PSD. Indeed, the PSD curve was described as a bimodal shape by Kittelson et al. [56]. Along this subsection, a deep background has been provided by explaining the nature of the particles provided by the CDC concept. In this sense, particles are divided in two modes, nucleation mode and accumulation mode. Nucleation mode particles represents less than the 20% of the PM mass emissions but may contain up to 90% of the total number of particles.

From the particle matter at RCCI mode standpoint, Prikhodko et al. [61] found that RCCI was highly dominated by nucleation mode particles. RCCI produces lower number of particles amongst other LTC strategies according to what the literature says. In this sense, some studies stated that LTC have very similar PSD shapes characterized by smaller sized particles. Other studies compared the results of FSN and PM filter mass measurements under RCCI operation mode, showing that RCCI PM is mostly organic carbon with almost no elemental carbon. Despite of having some correlations between FSN measurement and soot mass for premixed charged compression

ignition (PCCI) operation, under RCCI strategy these correlations are not useful due to most part of the PM comes from soluble organic fraction, which is not captured by the smokemeter. Despite the different studies performed, there is still a need to explore the particles emission over the whole engine map operation.

Taking in account these considerations, despite the benefits provided by the RCCI concept, there are still some drawbacks to be solved. Hence, the work carried out in this thesis focuses its effort in provide a dual-fuel strategy able to operate over the whole engine map promoting ultra-low levels of NOx and smoke. Additional work will be carried out to explore the PSD and the PN over the whole engine operation map.

2.5.2 Objectives of the study

According to the motivation previously stated, the general objective of the present work of investigation is *to overcome the challenges of the RCCI concept by developing a dual-fuel strategy capable to operate over the whole engine operation map promoting ultra-low NOx and smoke emissions* to be applied in a compression ignition engine derived from a EU VI commercial medium-duty stock engine developed for urban freight distribution purposes.

From the general objective, three partial objectives have been defined:

- *Operate a dual-fuel combustion strategy over the whole engine operation map promoting ultra-low NOx and smoke emissions.* This study aims to develop a dual-fuel strategy over the whole engine map promoting ultra-low NOx and smoke emissions below EU VI limitations under steady-state operating conditions.
- *Avoid excessive PRR at high engine load and reduce CO and uHC during low load operation.* For this purpose, the combustion phasing plays a key role in order to avoid excessive PRR at high engine load. In this sense, the injection pattern,

EGR rate and gasoline fraction adjustments will be managed for this purpose. In addition, not only the settings will be studied, the compression ratio also be modified in order to obtain the best balance possible between low load efficiency and high load operation.

- *Explore the particles emissions of the dual-fuel concept over the whole engine operation map.* This objective aims to explore the particle emissions of the dual-fuel combustion strategy over the whole engine map. The influence of the engine speed or the influence on the load as well as the particle mapping result interesting in order to meet current standard limitations such as EU VI.

2.5.3 General methodology and research development

Aimed to reach the objectives proposed in the previous subsection, a general methodology is followed by the combination of an experimental facility and theoretical tools.

The most important element at the test facility is the single cylinder medium-duty engine (SCE). The experiments are conducted in a SCE derived from a commercial EU VI stock medium-duty engine. Additional systems to handle the air in terms of fresh and exhaust recirculated air are coupled to replicate the air management conditions of the engine. In addition, the test facility also provides other mean values required by the theoretical tools to diagnose the combustion process and drive the analysis.

From the research development standpoint, the investigation performed consists of two different steps. Both steps are directly related and each of whom responds to a particular objective described previously. During this section only will be very briefly described the sequence followed during the research due to the specific methodology as well as the tools are deeply described along the next chapters.

Hence, chapter 4 will respond the first particular objective with the combustion strategy presented. In this sense, two different compression ratios have been tested and two raw calibrations demonstrate that it is possible to operate an engine from low to full load for all the engine speed range under dual-fuel combustion strategy. In addition, this chapter focuses on the PRR by adjusting the constraints and the diesel injection strategy to avoid excessive values and the CR aims to improve the burning during low load operation reducing the CO and uHC. Indeed, the exhaust temperatures are analyzed to verify which hardware improves the catalytic oxidation conversion.

Finally, chapter 5 responds to the last particular objective. Thus, this chapter contains a study on the particle emissions that provide a wide view of the particles emitted by the concept. Firstly, it was evaluated the particle emissions when the strategy operates under RCCI at different engine speeds. Then, a study was carried out with the aim to observe possible trends with the engine load when the combustion strategy switches from fully premixed to dual-fuel diffusion. Finally, the whole engine operation map was used obtaining particle emissions maps. All the studies were performed obtaining the particle size distribution analysis and the total number of particles emitted. In addition, the particle emissions were compared with the CDC strategy to improve the understanding of the concept.

2.6 Bibliography

[1] Dec J. E. "A conceptual model of DI diesel combustion based on laser-sheet imaging". SAE Paper 970873, 1997.

[2] García J. M. Aportaciones al estudio del proceso de combustión turbulenta de chorros en motores Diésel de inyección directa. Tesis doctoral, Universidad Politécnica de Valencia, Departamento de Máquinas y Motores Térmicos, 2004.

[3] Musculus Mark P.B., Miles Paul C. and Pickett Lyle M. "Conceptual models for partially premixed low-temperature diesel combustion". Progress in Energy and Combustion Science, Vol. 39 no 2-3, pp. 246-283, 2013.

[4] Taylor C. F. The internal Combustion Engine in Theory and Practice Vol 2, 2 Ed. Revisada. The MIT Press, 1985.

[5] Payri González Francisco and Desantes José María. Motores de combustión interna alternativos. Editorial Reverté, España, 2011.

[6] Heywood J. B. Internal combustion engine fundamentals. McGraw-Hill Publishing, 1988.

[7] Espey C., Dec J. E., Litzinger T. A. and Santavicca D. A. "Planar laser rayleigh scattering for quantitative vapor-fuel imaging in a diesel jet". Combustion and Flame, Vol. 109 no 1-2, pp. 65-78, 1997.

[8] Kosaka H., Drewes V. H., Catalfamo L., Aradi A. A., Iida N. and Kamimoto T. "Twodimensional imaging of formaldehyde formed during the ignition process of a diesel fuel spray". SAE Paper 2000-01-0236, 2000.

[9] Bruneaux G. "Study of the correlation between mixing and auto-ignition processes in high-pressure Diesel jets". SAE Paper 2007-01-0650, 2007.

[10] Glassman I. and Yetter R. Combustion, 4 Ed. Academic Press, 2008.

[11] Dec J. E. and Tree D. R. "Diffusion-flame/wall interactions in a heavy-duty DI diesel engine". SAE Paper 2001-01-1295, 2001.

[12] Dec J. E. y Canaan R. E. "PLIF imaging of NO formation in a DI diesel engine". SAE Paper 980147, 1998.

[13] Dec J. E. y Kelly-Zion P. L. "The effects of injection timing and diluent addition on late-combustion soot burnout in a DI diesel engine based on simultaneous 2-D imaging of OH and soot". SAE Paper 2000-01-0238, 2000.

[14] Li T. and Ogawa H. "Analysis of the Trade-off between Soot and Nitrogen Oxides in Diesel-Like Combustion by Chemical Kinetic Calculation". SAE Int. J. Engines, Vol. 5, pp. 94-101, 2011.

[15] Neely G.D., Sasaki S., Huang Y., Leet J.A. and Stewart D.W. "New Diesel Emission Control Strategy to Meet US Tier 2 Emissions Regulations". SAE Technical Paper, no 2005-01-1091, 2005.

[16] Kamimoto T. and Bae M. "High Combustion Temperature for the Reduction of Particulate in Diesel Engines". SAE Technical Paper, no 880423, 1988.

[17] Y. Lee, K. Huh. "Analysis of different modes of low temperature combustion by ultra-high EGR and modulated kinetics in a heavy duty diesel engine". Appl. Therm. Eng. 70, 776–787, 2014.

[18] Y. Qian, Q. Zhou, X. Wang, L. Zhu, X. Lu. "Enabling dual fuel sequential combustion using port fuel injection of high reactivity fuel combined with direct injection of low reactivity fuels". Appl. Therm. Eng. 103 399–410, 2016.

[19] Hiroyasu, H., Hiroyasu, T., Miki, M., Jamiura, J., & Watanabe, S. (2003). "Genetic Algoritms Optimization of Diesel Engine Emissions and Fuel Efficiency with Air Swirl, EGR, Injection Timing and Multiple Injections". SAE Paper 2003-01-1853, 2003.

[20] García, A. Estudio de los efectos de la post inyección sobe el proceso de combustión y la formación de hollín en motores Diésel. Barcelona: Editorial Reverté S.A., 2011.

[21] Pickett L. M. and Siebers D. L. "An investigation of diesel soot formation processes using micro-orifices". Proceedings of the Combustion Institute, Vol. 29 no 1, pp. 655-662, 2002.

[22] Siebers D. L. and Pickett L. M. "Injection pressure and orifice diameter effects on soot in DI Diesel fuel jets". Proceedings of THIESEL conference, pp. 199-213, 2002.

[23] Pickett L. M. and Siebers D. L. "Non-Sooting, Low Flame Temperature Mixing-Controlled DI Diesel Combustion". SAE Paper 2004-01-1399, 2004.

[24] Huestis E., Erickson P. A. and Musculus M. P. B. "In-cylinder and exhaust soot in low temperature combustion using a wide-range of EGR in a heavy-duty Diesel engine". SAE Paper 2007-01-4017, 2007.

[25] Benajes J., Molina S., Novella R. and Belarte E. "Evaluation of massive exhaust gas recirculation and Miller cycle strategies for mixing-controlled low temperature combustion in a heavy duty diesel engine". Energy, Vol. 71, 355-366, 2014.

[26] Benajes J., Molina S., Martin J. y Novella R. "Effect of advancing the closing angle of the intake valves on diffusion-controlled combustion in a HD diesel engine". Applied Thermal Engineering, Vol. 29, 1947-1954, 2009.

[27] Belarte E. Estudio del proceso de combustión premezclada controlada por la reactividad del combustible en un motor de encendido por compresión. 2015.

[28] Splitter Derek A. and Reitz Rolf D. "Fuel reactivity effects on the efficiency and operational window of dual-fuel compression ignition engines". Fuel, Vol. 118 no 0, pp. 163-175, 2014.

[29] Kokjohn S. L., Hanson R. M., Splitter D. A. and Reitz R. D. "Fuel reactivity controlled compression ignition (RCCI): a pathway to controlled high-efficiency clean combustion". International Journal of Engine Research, Vol. 12, 3, 209-226, 2011.

[30] Manente V., Johansson B., Tunestal P. and Cannella W. "Effects of Different Type of Gasoline Fuels on Heavy Duty Partially Premixed Combustion". SAE International Journal of Engines, 2, 71-88, 2010.

[31] Benajes J., García A., Monsalve-Serrano J., Boronat V. "Dual-Fuel Combustion for Future Clean and Efficient Compression Ignition Engines". Applied Sciences 7(1):36, 2017.

[32] Benajes J., Molina S., García A., Monsalve-Serrano J. and Durrett R. "Performance and engine-out emissions evaluation of the double injection strategy applied to the gasoline partially premixed compression ignition spark assisted combustion concept". Applied Energy, 134, 90-101, 2014.

[33] Benajes J., Molina S., García A., Monsalve-Serrano J. and Durrett R. "Conceptual model description of the double injection strategy applied to the gasoline partially premixed compression ignition combustion concept with spark assistance". Applied Energy, 129, 1-9, 2014.

[34] Alperstein M., Swim W.B. and Schweitzer P.H. "Fumigation kills smoke-improves diesel performance". SAE Technical Paper, no 580058, 1958.

[35] Najafabadi MI, Aziz NA. "Homogeneous charge compression ignition combustion: challenges and proposed solutions," J. Combustion, 2013-783, 2013.

[36] Lu X., Han D. and Huang Z. "Fuel design and management for the control of advanced compression-ignition combustion modes". Prog Energy Combust Sci 2011-37-741, 2011.

[37] Bessonette PW, Schleyer CH, Duffy KP, Hardy WL and Liechty MP. "Effects of fuel property changes on heavy-duty HCCI combustion". SAE paper 2007-01-0191; 2007.

[38] Manente V, Tunestal P, Johansson B et al. "Effects of Ethanol and Different Type of Gasoline Fuels on Partially Premixed Combustion from Low to High Load". SAE Technical Paper 2010-01-0871, 2010.

[39] Singh AP, Agarwal AK. "Combustion characteristics of diesel HCCI engine: an experimental investigation using external mixture formation technique". Appl Energy 2012-25-99:116, 2012.

[40] Bessonette P, Schleyer C, Duffy K, Hardy W., Liechty M. "Effects of Fuel Property Changes on Heavy-Duty HCCI Combustion". SAE Technical Paper 2007-01-0191, 2007.

[41] Peng Zhijun, Zhao Hua and Ladommatos Nicos. "Effects of Air/Fuel Ratios and EGR Rates on HCCI Combustion of n-heptane, a Diesel Type Fuel". SAE Technical Paper, Vol. 2003-01-0747, 2003.

[42] Park H, Youn IM, Lim Y and Lee CS. "Influence of the mixture of gasoline and diesel fuels on droplet atomization, combustion and exhaust emission characteristics in compression ignition engine". Fuel Processing Technology 2013-106-392, 2013.

[43] Inagaki K, Fuyuto T, Nishikawa K, Nakakita K and Sakata I. "Dual-Fuel PCI Combustion Controlled by In-Cylinder Stratification of Ignitability". SAE Technical Paper 2006-01-0028, 2006.

[44] Kokjohn SL, Hanson M, Splitter D, Reitz RD. "Experimental Moodeling of Dual-Fuel HCCI and PCCI Combustion Using In-Cylinder Fuel Blending", SAE Technical Paper 2009-01-2647, 2009.

[45] Benajes J, Molina S, García A and Monsalve-Serrano J. "Effects of Direct injection timing and Blending Ratio on RCCI combustion with different Low Reactivity Fuels". Energy Conversion and Management, 99, 193-209, 2015.

[46] Benajes J, Molina S, García A and Monsalve-Serrano J. "Effects of low reactivity fuel characteristics and blending ratio on low load RCCI (reactivity controlled compression ignition) performance and emissions in a heavy-duty diesel engine". Energy, 90, 1261-1271, 2015.

[47] Benajes J, García A, Pastor J.M and Monsalve-Serrano J. "Effects of piston bowl geometry on Reactivity Controlled Compression Ignition heat

transfer and combustion losses at different engine loads". Energy, 98, 64-77, 2016.

[48] Benajes J, Pastor José V, García A and Monsalve-Serrano J. "An experimental investigation on the Influence of piston bowl geometry on RCCI performance and emissions in a heavy-duty engine". Energy Conversion and Management, 103, 1019-1030, 2015.

[49] Desantes JM, Benajes J, García A and Monsalve-Serrano J. "The role of the in-cylinder gas temperature and oxygen concentration over low load reactivity controlled compression ignition combustion efficiency". Energy, 78, 854–868, 2014.

[50] Splitter Derek A., Kokjohn Sage L., Rein Keith, Hanson Reed M., Sanders Scott and Reitz Rolf D. "An Optical Investigation of Ignition Processes in Fuel Reactivity Controlled PCCI Combustion". SAE Technical Paper 2010-01-0345, 04 2010.

[51] Monsalve-Serrano J. Dual-Fuel compression ignition: Towards clean, highly efficient combustion. 2016.

[52] Prikhodko V., Curran S., Parks J. and Wagner R. "Effectiveness of Diesel Oxidation Catalyst in Reducing HC and CO Emissions from Reactivity Controlled Compression Ignition". SAE Int. J. Fuels Lubr. 6(2):2013, doi: 10.4271/2013-01-0515.

[53] Benajes J, García A Monsalve-Serrano J. and Boronat V. "A RCCI operational limits assessment in a medium duty compression ignition engine using an adapted compression ratio", Energy Convrsion and Management, 126, 497-508, 2016.

[54] Anand Nageswaran Bharat. "Optimization of the air handling system of a multi-cylinder light-duty engine running on reactivity controlled compression ignition- a simulation study, 2016.

[55] European Union official bulletin diary: CEPE number 83 regulation, 07 series. [2015/1038].

[56] Kittelson D. "Engine and Nanoparticles: a Review," Journal of Aerosol Science, 1998-29-575, 1998.

[57] Shi J, Harrison R, Brear F. "Particle size distribution from a modern heavy duty diesel engine," The Science of the Total Environment, 1999-235-305, 1999.

[58] Armas O., Gómez A., Mata C., Ramos A. "Particle size distributions from a city bus fuelled with ethanol–biodiesel–diesel fuel blends". Fuel 111, 393– 400, 2013.

[59] J. Storey, S. Curran, S. Lewis, T. Barone, T. Dempsey, M. Moses-DeBusk, M. Hanson, V. Prikhodko, W. Northrop, Evolution and current understanding of physicochemical characterization of particulate matter from reactivity controlled compression ignition combustion on a multi cylinder light-duty engine, Int. J. Engine Res. (2016).

[60] Benajes, J., Novella, R., Arthozoul, S., Kolodziej, C., "Injection Timing Effects on Premixed Low Temperature Combustion Particle Emissions from Light and Heavy Duty Diesel Engines," 14th ETH-Conference on Combustion Generated Nanoparticles, ETH-Zurich, Switzerland, August 1-4, 2010.

[61] Prikhodko V., Curran S., Barone T., Lewis S. "Emission characteristics of a diesel engine operating with in-cylinder gasoline and diesel fuel blending". SAE Int. J. Fuels Lubr., 946–955, 2010.

[62] Lucachick G., Curran S., Storey J., Prikhodko V., Northrop William F. "Volatility characterization of nanoparticles from single and dual-fuel low temperature combustion in compression ignition engines". Aerosol Sci. Technol. 50, 436–447, 2016.

[63] Northrop William F., Madathil Praveen V., Bohac Stanislav V., Assanis Dennis N. "Condensational growth of particulate matter from partially premixed low temperature combustion of biodiesel in a compression ignition engine". Aerosol Sci. Technol. 45, 26–36, 2011.

[64] Kolodziej C., Wissink M., Splitter D., Hanson R. et al. "Particle size and number emissions from RCCI with direct injections of two fuels". SAE Technical Paper, 2013.

[65] Zhang Y., Ghandhi J., Rothamer D. "Comparison of particulate size distributions from advanced and conventional combustion – part I: CDC, HCCI, and RCCI". SAE Int. J. Engines, 2014.

[66] Northrop W., Bohac S., Chin J., Assanis D. "Comparison of filter smoke number and elemental carbon mass from partially premixed low temperature combustion in a direct-injection diesel engine". J. Eng. Gas Turbines Power 133, 102804, 2011.

[67] Curran S., Prikhodko V., Cho K., Sluder S., Parks J., Wagner R.et al. "In-cylinder fuel blending of gasoline/diesel for improved efficiency and lowest possible emissions on a multi-cylinder light-duty diesel engine". SAE technical paper 2010-01-2206, 2010.

Chapter 3

Tools and methodology

Content

3.1 Introduction

Regarding the main objectives of the investigation provided in chapter 2, the present investigation requires a considerable experimentalist work as well as a detailed post-process. Hence, the work will need dedicated experimental and theoretical tools to perform test campaigns and the combustion analysis.

This chapter is divided in two sections. The first section focuses on the experimental tools such as single cylinder engine (SCE), test cell, instrumentation, fueling system and so on. The second section is dedicated to the theoretical 0-D tool to analyze the combustion process.

3.2 Experimental facilities

As it has been observed during the previous chapter, the current investigation requires a high number of experimental work. Particularly, the section regarding the approach of the study, bases the investigation on a SCE test campaign, which information will play a key role at this investigation. Hence, the present subsection is mandatory in order to provide a background of the experimental tools used. Not only the tools are described in this chapter but also the error of the instrumentation and all the required data is provided.

In this sense, the SCE is deeply described firstly in this section. Next subsections will describe the hybrid DI/PFI fuel injection system and the different fuels used. As the SCE has been operated from a test cell, a description of the test cell follows the engine description 3.2.2. the test cell agglomerates different subsystems in order to operate the engine and obtain the information for the theoretical tools. Hence, the instrumentation and the data acquisition devices are also described along this section.

Further information of the equipment used and the characteristics of the test facilities and testing activities can be found at [1][2][3].

3.2.1 Single cylinder engine

The single cylinder engine (SCE) represents the most representative tool of the current investigation. All the experiments have been performed in this SCE and its hardware has been adapted to the different studies conditions. In addition, some limitations or constraints imposed during the test campaigns come from the mechanical limitations of the SCE.

On the other hand, a hybrid fuel injection system has been installed to operate the SCE under RCCI concept and, in general, to be operated under dual-fuel strategies. Hence, during this subsection, the two fuel systems are described as well as the different fuels used.

3.2.1.1 Engine description

The experiments presented in this work are conducted in a single cylinder engine (SCE). By contrast, the engine is not a conventional SCE research engine, it is a hybrid solution between a multi cylinder engine (MCE) and a SCE. Indeed, this solution allows the use of a SCE but with a more cost-effective way to implement this type of engines. The SCE used derives from a commercial medium-duty engine. The stock engine is a VOLVO D5K with 4 in-line cylinders developed for urban freight distribution purposes. Main specifications of the engine are shown in Table 3.1. As it can be observed at the table, the stock engine calibration is prepared to meet the EU-VI standard emissions limitation with the complete aftertreatment elements installed. Thus, a dedicated work has been carried out in order to split the engine in two parts. The main objective is to isolate the first cylinder operation from the rest of the engine. Hence, the stock hardware configuration has been modified in order to operate the first cylinder as a single-cylinder diesel engine and the other 3 cylinders with the stock configuration.

Table 3.1. Main characteristics of the base engine.

Style	4 stroke, DI diesel engine
Manufacturer/Model	Volvo/D5K240
OEM EVO calibration	EURO VI
Piston bowl geometry	Re-entrant
Maximum power	177 kW @ 2200 rpm
Maximum brake torque	900 Nm@1200-1600 rpm
Maximum in-cylinder pressure	190 bar
Maximum injection pressure/N° injections	2000 bar/3
Bore x Stroke	110 mm x 135mm
Connecting rod length	212.5 mm
Crank length	67.5 mm
Total displaced volume	5100 cm^3
Number of cylinders	4
Compression ratio	17.5:1

From the engine operation standpoint, both engines are operated at the same time. The SCE is operated under dual-fuel strategies and the other 3 cylinders are operated under CDC. In this sense, the three remaining cylinders are driven by the original equipment of the manufacturer (OEM), engine control unit (ECU) with the aim to balance the cylinder-to-cylinder maximum pressure and load. With this method of engine operation it is expected to preserve the engine integrity avoiding excessive internal stress at the crankshaft that could break it. An outline of the SCE configuration can be observed in Figure 3.1.

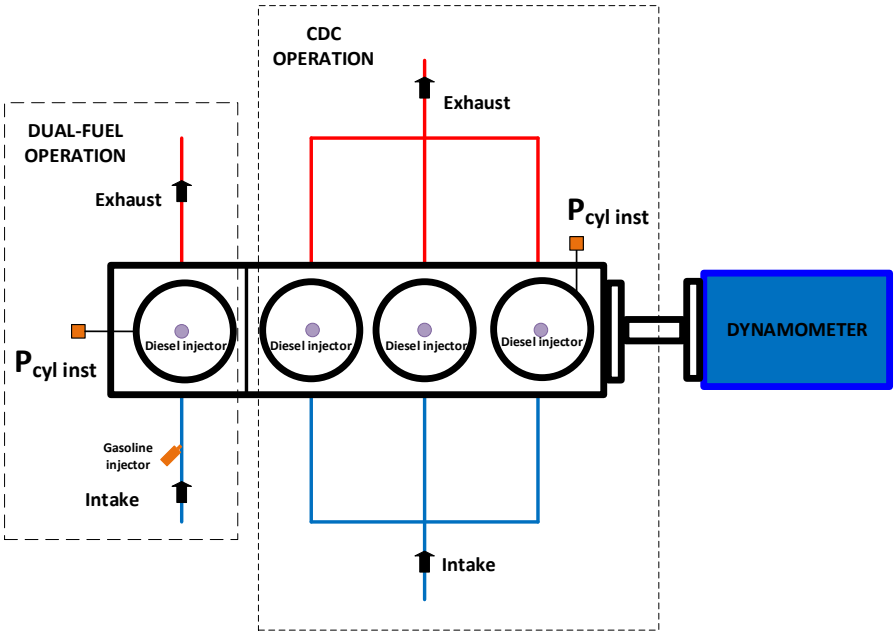

Figure 3.1. Outline of the SCE configuration.

In addition, the after-treatment elements have been removed. Next subsections will describe the different elements used to provide the fresh air mass flow as well as the EGR mass flow. Indeed, the stock engine operates without EGR flow due to it is not enabled aimed to increase the simplicity of the overall engine operation. Similar engine configurations are found in [4][5][6].

The main advantage of using a SCE instead of a MCE regards in the control of the combustion. Managing a unique cylinder provides a precise control over the combustion process because of the avoidance of the typical dispersion cycle-to-cycle at the MCE. Hence, the measurements performed during the engine operations can be directly correlated to the combustion process.

3.2.1.2 Fuel injection systems

The main objective presented in chapter 2 implies the use of two fuel at the same time. Figure 2.6 presents the fuel injection scheme proposed by Inagaki [7]. This scheme requires a mixed injection system for the diesel direct injection (DI) and the gasoline port fuel injection (PFI). Hence, the engine has been equipped with a mixed injection system in order to allow dual-fuel operation. Dual-fuel strategies require both fuels gasoline/diesel injection during the same cylinder cycle. Therefore, the mixed system allows varying the in-cylinder fuel blending ratio and fuel mixture properties for each engine operating condition. The engine control is done by a real time National Instruments powertrain control system with two controllers, combining a field-programmable gate array (FPGA) based synchronization of the injection, and a peripheral component interconnect (PCI) extensions for instrumentation (PXI) system is used for the in-cylinder pressure acquisition and processing. The control software was developed in-house and allows performing transitions between different injection conditions, and a closed loop control of the combustion characteristics. This control allows operating at the same engine point while the fuel blend is modified in function of the air management variations.

From the injector standpoint, diesel injector is the original of the engine. Main properties of the diesel injector are presented in Table 3.2.

Table 3.2. Diesel direct injector characteristics.

Actuation type	Solenoid
Steady flow rate @ 100 bar [cm^3/min]	1300
Number of holes	7
Hole diameter [µm]	177
Included spray angle [°]	150

Regarding the port fuel injector (PFI) system, the main properties of the injector are detailed in Table 3.3.

Table 3.3. PFI main characteristics.

Injector style	Saturated
Steady flow rate @ 3 bar [cm^3/min]	980
Included spray angle [°]	30
Injector pressure [bar]	5.5
Injection strategy	Single
Start of Injection timing	340 CAD aTDC

3.2.1.3 Fuels used during experiments

The fuels used during the experiments were obtained directly from the regular petrol stations. Hence, the high reactivity fuel used was diesel (EN590) and the low reactivity fuel used was gasoline 95 research octane number (RON) (EN 228). Main physicochemical properties are presented in

Table 3.4. Physical and chemical properties of the different fuels used.

	Diesel	Gasoline
Density [kg/m^3] (T=15°C)	820	720
Viscosity [cm^2/s] (T=40°C)	2.8	-
RON [-]	-	95.0
MON[-]	-	85.0
Cetane number [-]	>51	-
Lower heating value [MJ/kg]	42.97	42.4

3.2.2 Test cell characteristics

The test cell is one of the most important and complex elements of the experimental setup. It contains the engine and all the elements and devices that allow monitoring the engine in real time as well as operating the engine.

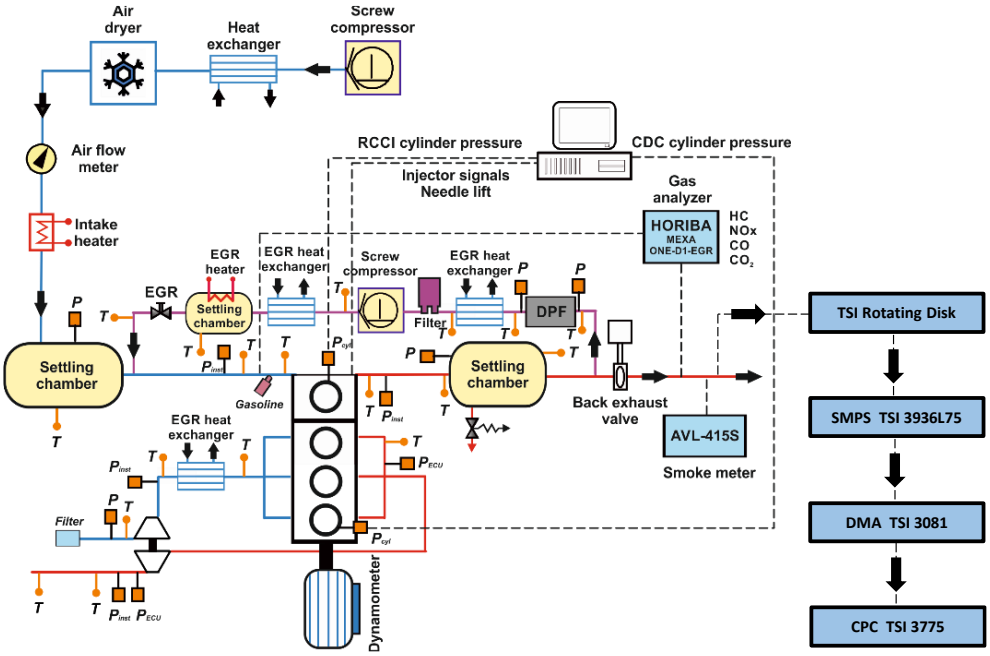

Figure 3.2. Scheme of the test bench.

Figure 3.2 presents the scheme of the test bench and all the equipment required to carry out the test campaign. Along this section, the different subsystems are described regarding the engine operation (temperature control, air management and fuel supply) and data acquisition. Next subsection describes the instrumentation and measuring devices such as instantaneous pressure sensors, mean values, emissions analyzers and so on.

3.2.2.1 Engine speed and torque regulation system

The tests have been performed under stable and steady conditions. The engine speed and the engine torque are controlled to maintain always the engine speed constant without noticeable engine speed fluctuations despite the load conditions. The constraints in terms of engine speed and engine torque are imposed by the user according the tested point desired.

In this sense, the element in charge of keeping stable the engine operation and preserve the rest of elements of the test cell in case of emergency is the dynamometer. The dynamometer consists of a robust asynchronous foot-mounted machine for speed- and torque-controlled operation. During combustion operation, the dynamometer produces electricity and, during motored conditions, the dynamometer uses electricity to drive the engine. The control of the dynamometer is based in the frequency variations adjustments, what gives an excellent accuracy and a fast response allowing to test steady state conditions as well as some simple dynamic tests runs. The main characteristics of the dynamometer are presented in Table 3.5.

Table 3.5. Main characteristics of the dynamometer.

Manufacturer	AVL-ELIN
Model	INDY 44/4z
Type	Asynchronous
Power [kW]	440/300
Voltage [V3~]	500
Current [A3~]	591
Frequency [Hz]	140
Power factor	0.87
Speed range [rpm]	0-4200

3.2.2.2 Air supply and exhaust system

Regarding the air handling of the engine, Figure 3.2 shows the different elements that are required to manage the air renovation at the engine. As it is observed, the SCE is not using the stock turbocharger system or the stock short route HP-EGR. Thus, a fresh air loop and an EGR loop has been coupled to provide the desired air management conditions at the engine.

The intake required fresh air is provided by a screw compressor that provides compressed air from 1 to 3.7 bar. The air is conditioned by cooling it after the compression stage in a water cooler and it flows through an air dryer. The air dryer removes the humidity by means of a cooling process. The specific humidity of the air is determined by the dew temperature and the pressure of the cooler, which is 3°C. After securing that compressed air is free of water droplets, the fresh air is measured by using a volumetric air mass flowmeter. Then, the temperature of the intake fresh air is adjusted using a heater. At this point, the intake fresh air is adjusted in terms of pressure, temperature and humidity. Finally, the air mass flow is directed to the settling chamber with the aim to mitigate the pressure waves generated due to the SCE pulsating nature. The settling chamber (500 liters) has been sized according the criteria proposed by Kastner´s and SAE J244 methods [8][9].

Concerning the exhaust manifold, the exhaust line is equipped with a backpressure valve that generates the exhaust pressure desired by the engine operation point. Between the valve and the exhaust pipes it is located a settling chamber in order to mitigate the pressure valves generated by the SCE. The size of the settling chamber is the same as the settling chamber placed at the intake line. The back pressure valve contributes to the EGR loop as well.

Regarding the EGR loop, it can also provide low or high pressure EGR, but not simultaneously. The EGR system is similar, at least in concepts, as the intake line. It contains a DPF to remove the soot particles from the exhaust gases, a cooler to reduce the exhaust temperature and a water decanter to remove the condensates. A filter is also installed to remove the water droplets and ensure that the air is free of water content. This step is mandatory to preserve the mechanical durability of the screw compressor in charge of increase the EGR flow pressure over the intake manifold pressure. This pressure difference allows to provide EGR flow to the intake. After the screw compressor there is a heater. The EGR flow goes directly to the EGR settling chamber (100 liters) in order to mitigate the possible pressure waves

provided by the compressor. Finally, the EGR system provides an EGR flow according the desired pressure, temperature and humidity desired conditions. Both EGR and fresh air flows are sent to the mixer prior to the intake manifold. Hence, the air mixture between EGR and fresh air is homogeneous at the intake manifold.

Both systems and the backpressure valve are controlled by physical PID. During the engine operation, the temperature and the pressure desired are set and these systems are adjusted automatically to reach the targets. In addition, the EGR rate is also set, adjusting the rate by increasing or reducing the pressure of the EGR conditioning system.

3.2.2.3 Lubrication and cooling system

Typical research SCE engine require external cooling and external lubrication system. In this particular case, the lubrication system used is the same as the stock engine uses. Hence, the oil pump used is the one fitted in the engine as well as the oil cooler, which is cooled by the engine water cooling system.

The water cooling system requires a double circuit. The engine conserves its water cooling circuit and the heat is exchanged in an external cooler with the cooling system provided by the test cell. Thus, a big water-to-water cooler is placed in the test cell to provide enough cooling capacity to the engine. The water used by the test cell is cooled by a cooling tower located at the CMT-Motores Térmicos facilities, which is shared with other test facilities.

Additionally, with the aim to monitor all the parameters of the engine, the temperature and the pressure of the coolant and the oil is recorded by the OEM ECU and by the instrumentation provided to the engine during the tests.

3.2.2.4 Fuel conditioning system

Dual-fuel strategies require a double injection system. Particularly in this investigation, the injection scheme uses a hybrid solution with a DI for the diesel fuel and a PFI for the gasoline fuel. The properties of the injectors and fuels have been described previously in 3.2.1.2 and 3.2.1.3. The scheme of the injection system used at the test bench can be observed in Figure 3.3.

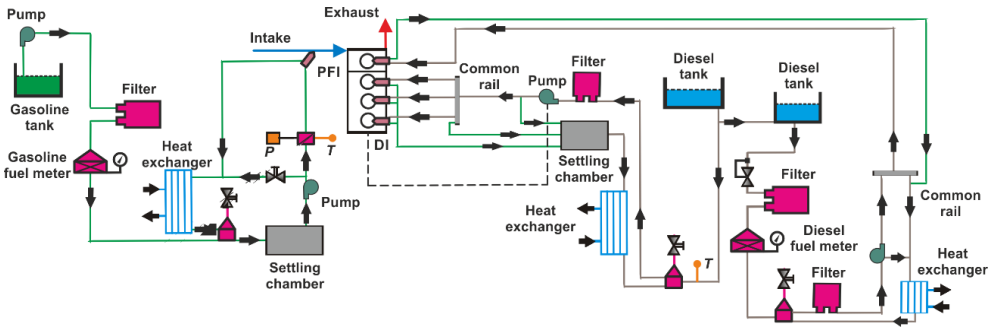

Figure 3.3. Mixed fuel injection scheme.

As it can be observed in the figure, the hybrid solution contains similar elements regarding the fuel supply. From the diesel fuel supply, the diesel system is presented on the left side of the figure. The diesel fuel supply starts with a reservoir of 200 liters that refuels the 1-liter tank of the fuel balance every time the fuel balance is empty. The fuel balance is an AVL 733S and gives the measurement directly in kg/s. The fuel is conducted to a mixer where is mixed with the returned fuel from the common rail and driven to the fuel pump. The common rail is a typical common rail that can be found in every engine but with only one line available for one single injection, the pressure sensor and the return line to the mixer. The fuel pump was an in-house fuel pump driven with an electric motor that was controlled by the pressure sensor actuating over the motor speed. The speed of the motor is varied by means of frequency variation device. In this sense, a physical PID was in charge of the injection pressure. On the other hand, the diesel fuel return line is usually filled with fuel heated due to the compression process. It has been demonstrated that the temperature provokes error at the fuel

measurements [10][11]. Thus, a cooler is installed for the correct control of the temperature of the fuel. The cooler uses the water provided by the cooling system of the test cell.

Gasoline fuel supply system follows the same scheme. Main differences are observed at the pump and at the absence of a common rail. Fuel balance is the same that for diesel fuel and it contains also a mixer and a cooler.

3.2.2.5 Data acquisition systems

The data acquisition system is the system in charge of the measurements recording. Hence, it is needed to feed the 0-D theoretical tool to analyze the combustion event. The acquisition system must work with different nature sensors that operate with different signals, frequencies and so on. Hence, the acquisition system allows the independent configuration depending on the nature of the sensor.

The system used in the test cell is the AVL-PUMA 5 Compact. This system allows to acquire instantaneous variables that are recorded at high frequency such as pressure at the intake manifold. Low frequency variables such as temperatures, fuel flow, air mass flow, emissions and etcetera are also recorded by the AVL-PUMA system.

Regarding the high frequency signals from the in-cylinder pressure and the injection settings, they are recorded combining a field-programmable gate array (FPGA) based synchronization of the injection, and a peripheral component interconnect (PCI) extensions for instrumentation (PXI) system. These systems are provided by National Instruments.

3.2.3 Instrumentation and measuring equipment

Previous subsections, 3.2.1 and 3.2.2, have described the SCE and the test bench used for the experimental component of the present investigation.

The last subsection of the present chapter focuses on the instrumentation used to measure the different parameters considered for the post-process required for the investigation. Hence, some additional information such as accuracy is also provided.

3.2.3.1 Torque and engine speed measurements

Regarding the torque measurement, a load cell is installed at the torque shaft between the engine flywheel and the dynamometer brake. The load cell nominal torque is 2000 Nm. The nominal torque exceeds by far the current capabilities of the SCE, and doubles the maximum torque achievable by the stock engine configurations. The precision of the transducer is 1%.

The crank angle degree (CAD) is measured with an AVL 364 optical angle encoder installed at the front side of the crankshaft. The angle encoder provides a resolution of 0.2 CAD.

3.2.3.2 Mean pressure and temperature measurement

Mean variables such as pressure and temperature are measured for the correct engine control during the tests and the combustion analysis. From the engine control standpoint, mean variables provide information regarding the engine operation point and the boundary conditions. The 0-D theoretical tool used for the diagnose of the combustion requires mean variables for the correct analysis. Most of these mean variables come from the intake and exhaust gases, cooling and lubricating system and the fuel supply elements. Table 3.6 shows general information about instrumentation used to obtain mean variables.

Table 3.6. Instrumentation used for mean variables measurements.

Device	Manufacturer and model	Variable measured	Accuracy	Range
Piezoresistive transducer	PMA (P40)	Intake and exhaust pressure	±25mbar	0-10 [bar]
Thermocouple	TC direct K type	Temperature	±2.5 ^{0}C	0-1100 [°C]
Thermoresistance	Pt100	Temperature	±0.3 ^{0}C	-200-850 [°C]

3.2.3.3 Instantaneous pressure transducers

The instantaneous pressure is measured at the cylinder and at the intake and exhaust manifolds. The in-cylinder pressure is basic for the combustion analysis due to the 0-D tool basis the calculations on the instantaneous pressure signal. Both pressure sensors are coupled to amplifiers in order to filter the signal and adequate it before the high frequency resolution acquisition system record. The in-cylinder pressure sensor uses a Kistler 5011B10 and the intake and exhaust pressure sensor uses a Kistler 4045A10 amplifier. General characteristics of the instantaneous instrumentation are shown in Table 3.7.

Table 3.7. In-cylinder pressure sensor.

Device	Manufacturer and model	Variable measured	Linearity	Range
Piezoelectric transducer	Kistler 6125C	In-cylinder pressure	<±0.5%	0-250[bar]
Piezoresistive transducer	Kistler 4045A10	Intake and exhaust pressure	<±0.3%	0-10 [bar]

3.2.3.4 Mass flow measurement

With the aim of controlling the different elements that are supplied to the engine during combustion tests, the flow mass of the air and fuel are extremely important. Both measurements play a key role regarding the emissions and fuel consumption. Hence, it was measured the air mass flow and the gasoline and diesel fuel mass flow. The general description of the flowmeters used are described in Table 3.8. As it can be observed in the table, the units of the air mass flow are in [m^3/h]. Those units are transferred to [kg/h] by measuring the intake pressure and temperature.

Table 3.8. Mass flow meters used at the test facility.

Device	Manufacturer and model	Variable measured	Precision	Range
Air flow meter	Elster RVG G100	Fresh air mass flow	±0.1%	0.05-160 [m^3/h]
Fuel balance	AVL 733S	Fuel mass flow	±0.2%	0-160 [kg/h]

3.2.3.5 Horiba gas analyzer

The current emissions standard limitations are getting more and more stringent. Thus, the measurement of the emissions requires a reliable equipment in order to provide good accuracy and a wide range of emissions components. The equipment selected is a Horiba-MEXA-ONE-D1-EGR analyzer. The five-gas Horiba analyzer accounts the molar fraction of NO, NO_2, CO, unburned HC, CO_2 and O_2. This equipment can be observed in Figure 3.2 downstream the backpressure valve. The sample acquired by the equipment flows towards the analyzer through a heated line (≈190°C) in order to avoid condensation of the HC species. Every specie of the exhaust gases is analyzed by a specific device. Full description of the different measuring principles are provided in [12][13][14]. The most relevant characteristics of the different measurement techniques are described as follows:

- NO_x emissions are determined by means of chemiluminescence. This technique consists of reducing the NO_x to NO. Then, the NO is mixed with ozone (O_3). This mixture provokes a reaction that activates the NO → NO_2^*, which luminescence broadband visible to infrared light when reverting to its lower energy state (NO_2). Hence, the light is detected by the measurement device and it is converted to NO_x concentration.
- O_2 emissions are measured considering oxygen´s paramagnetic properties.
- CO and CO_2 emissions are measured by using the non dispersive infrared detector (NDIR). The technique used is based on wavelength of infrared light absorption. Both emissions absorb a known wavelength that is converted into concentration values.
- Unburned HC emissions are measured by using the flame ionization principle. This technique consists on burning a sample of exhaust gas in presence of a mixture of hydrogen helium and synthetic air. As a consequence of the burning, ions are produced in presence of an electrical field generating a proportional to the carbon quantity ionization current. Finally, this current is converted into uHC concentration.

Table 3.9 presents the ranges and the precision that provides the five gas Horiba Analyzer for the different emissions species measured.

Table 3.9. General information of the emissions measured by the five gas Horiba analyzer.

Emission	Range	Precision
NO_x	0-5000ppm	±4%
O_2	0-25%	±4%
CO/CO_2	0-10% (CO)	±4%
	0-20% (CO_2)	
uHC	0-10000ppm	±4%

The EGR rate is obtained taking in account the CO_2 at the intake and at the exhaust and the ambient content of CO_2. Hence, the EGR rate is calculated according to equation (3.1, where $CO_2 ambient$ is equal to 400ppm. CO_2 concentration at the intake air at the exhaust are introduced in ppm.

$$EGR[\%] = \frac{CO_2 intake_{dry} - CO_2 ambient}{CO_2 exhaust_{dry} - CO_2 ambient} \times 100 \qquad (3.1)$$

It is worthy to note that the gas analyzer equipment is calibrated every testing session. The calibration procedure is performed automatically by the device, but it has to be executed manually by the user. The calibration process uses different calibrated gases as a reference in order to compare the concentrations obtained with the target concentrations provided by the air gases supplier.

Indeed, the emissions concentrations are corrected into g/h in order to consider the humidity (HC are not corrected due to they are not previously dried) according to the European Directive 2007/46/EC [15].

Finally, the ratio between air and fuel (A/F) and lambda are also calculated by the Horiba analyzer. Measurements are addressed according to the exhaust gas composition [16].

3.2.3.6 AVL smoke meter

An AVL 415S Smoke Meter was used to measure smoke emissions. The AVL 415S device is a filter-type smoke meter. The procedure to measure the soot content of the exhaust gases starts with an extraction of a certain quantity of exhaust gas. This portion of exhaust gas passes through a clean filter made of paper. The soot is adhered to the paper after the portion of gas has passed blackening the paper. The blackening of the paper is measured by an optical reflectometer and provides a measurement in FSN (Filter Smoke Numbers) units. The range of FSN goes from 0 to 10 FSN. FSN indicates

that the paper is totally clean and 10FSN indicates that the paper is totally black (completely full of soot). Main characteristics of the AVL smokemeter are shown in Table 3.10.

Table 3.10. General properties of the AVL 415S smokemeter.

Device	Emission	Range	Lower limit	Resolution
AVL 415S	Smoke (Soot content)	±4%	0.002 FSN	0.001FSN

In particular, measurements were averaged between three samples of a 1 L volume each with paper-saving mode off, providing results directly in FSN (Filter Smoke Number) units. In order to transform the FSN units to soot concentration (mg/m^3), it has been used the correlation proposed by Christian et al. [17]. The equation considered is (3.2). Finally, the soot mass is calculated considering a density of 1.65 kg/m^3.

$$Soot[\frac{mg}{m^3}] = \frac{1}{0.405} \times 4.95 \times FSN \times e^{(0.38 \times FSN)} \quad (3.2)$$

The soot correlation provided in equation (3.2) is only valid for the CDC mode. As it has explained in chapter 2, the results of FSN and PM mass measurements under RCCI strategy shown that is not possible to convert the FSN into PM [18]. What makes not possible to use the FSN correlations under RCCI or Dual-Fuel strategies is that most part of the PM comes from soluble organic fraction [19].

3.2.3.7 Particle size distribution equipment

The particles measurement device is used to perform the particle size distribution (PSD) analysis and measure the total number of particles promoted by the engine. The particle size distribution equipment was located

downstream the backpressure valve, as it is depicted in Figure 3.2. As it can be observed at the scheme of the PSD equipment presented in Figure 3.4, the measurement device consists of a diluter and a scanning mobility particle sizer (SMPS). The diluter is a thermodiluter TSI Rotating Disk. The equipment dilutes the sample using the rotating disk method. Each unit is supplied with two disks and, each disk contains different number of cavities. Then, a raw portion of the exhaust flow is captured by the cavities and is driven through the mixer with particle-free air. This method provides high precision and excellent stability. The air must be heated to avoid nanodroplets formation due to the condensates from the volatile elements. These nanodroplets are detected as particles and can interfere on the measure. Dilution of the exhaust gases is required to adapt the particulate inlet concentration for the SMPS. In the present investigation, the dilution ratio selected was 90:1, and the diluted sample was heated up to 150°C in order to avoid volatiles condensation.

The SMPS (TSI model 3936L75) system consists of two main devices, the Differential Mobility Analyzer (DMA, TSI model 3081) and the Condensation Particle Counter (CPC, TSI model 3775). DMA equipment method is based on the physical principle that the ability of a particle to cross an electric field is directly related to particle size. Once the particle sample is sized by the DMA, it is measured using a condensation particle counter (CPC, TSI model 3775). The system has been configured to count particles between 5 and 250 nm. The Aerosol Instrument Manager (AIM, TSI) software acquires high resolution data and process the particulate size distribution (PSD) data.

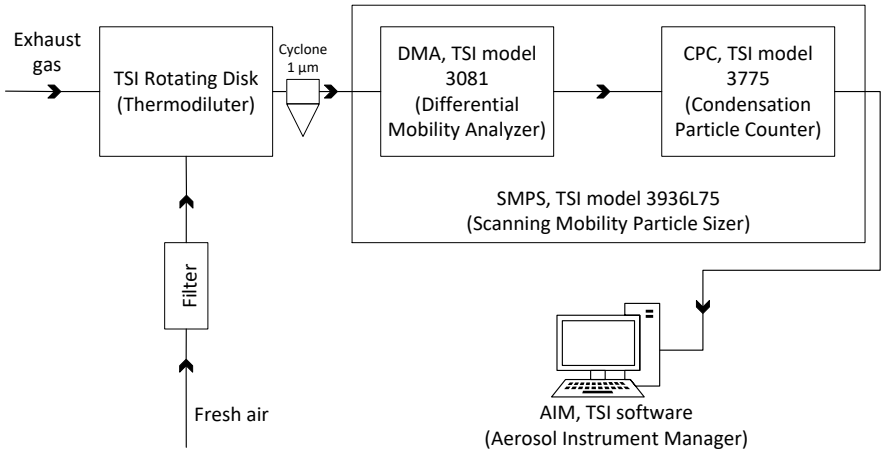

Figure 3.4. Particulates size distribution measurement equipment.

3.2.3.8 Experimental procedure

The operation of a SCE is a complex process when every engine parameter needs to be under control. Indeed, every process such as cooling or lubrication system are usually critical in this kind of test facilities. In particular, the non-research origin of the SCE used in the current investigation implies an extra at the complexity of the tests execution. In order to enhance the quality of the testing procedure by detecting possible errors during the tests, the present investigation applies a similar methodology that was defined by Monsalve-Serrano[20]. In addition, the fundamentals of this methodology are described in [21]. In Figure 3.5 can be observed a scheme of the methodology followed along the present work of investigation.

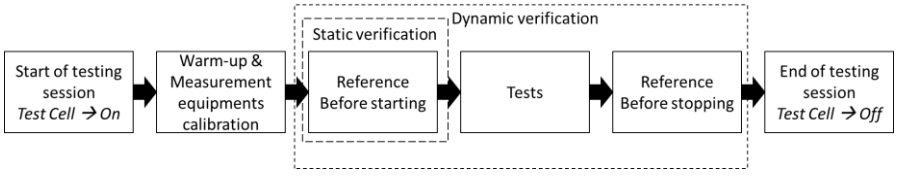

Figure 3.5. Experimental procedure methodology. Adapted from Novella [3].

As it is observed, the methodology provides two steps of verification. First step consists of a static verification and the second one consists of a dynamic verification.

- Static verification: This step starts with a selection of a reference engine operation point. This engine point will allow checking the correct operation of the engine and all the subsystems that are required for the engine operation. The reference point is usually repeated at the beginning of every test session. While running this engine point, the measurement equipments such as emissions, mean variables acquisition systems, fuel supply and the fuel injection system are checked. Variables are compared with the previous reference point in order to observe possible dispersion or anomalies at the measurements. This process is produced immediately after the warm-up process of the test facility under steady state conditions.
- Dynamic verification: During the execution of the tests, the equipments can suffer a failure or can require a new calibration. Thus, in order to avoid this kind of dispersion or lack of reliability, the second step of verification is needed. This step will focus on the air management of the engine (fresh air mass flow, EGR rate, ...). Hence, the reference point will be set again and the main parameters will be compared. Other errors such as mean variables measured, emissions are also checked. If the dispersion observed is inside the control limits, the tests are considered as correct.

After these two steps of verification, it is possible to proceed with the process of the data recorded during the test session. Otherwise, some protocols have to be followed to detect and solve the possible failures of the equipment [21].

3.3 Theoretical tools

In order to process the experimental data obtained from the experimental setup, a theoretical tool is used. This tool diagnoses the combustion process. According to the desired results from this tool, the variables required for the correct analysis will vary.

3.3.1 Combustion diagnosis: 0-D model

The theoretical 0-D tool used to perform the combustion analysis is based on the in-cylinder pressure signal to obtain a wide variety of combustion parameters such as rate of heat release (RoHR) or heat release law (HRL). The theoretical principles of the 0-D models are usually based on the first law of the thermodynamic applied to a control volume during the closed cycle.

The 0-D model used during the present investigation was in-house developed at CMT-Motores Térmicos. It was named CALMEC and it is completely described in [22]. The general hypotheses have been detailed below:

- A uniform pressure is assumed in the combustion chamber. As the flame propagation and fluid velocity are lower than the speed of sound, this hypothesis is generally accepted.
- The considered fluid inside the combustion chamber is a mixture of air, fuel and burned products.
- The evolution of the fluid mixture in the combustion chamber is considered with an ideal gas behavior. This assumption might present some issues regarding the gaseous fuel. Lapuerta [23] investigated the results obtained by the combustion model by using different state equations for the gaseous fuel without observing relevant differences at the mean temperature and HRL. Hence, the hypothesis can be accepted.

According to these hypotheses, the first law of thermodynamics is proposed by CALMEC to solve open systems considering the fuel injection and blow-by flow. In this sense, the raised equation (3.3) solves the first law of thermodynamics using the resolution that provides the in-cylinder pressure measurement (0.2 CAD in the present investigation).

$$\Delta HRL = m_{cyl} \times \Delta u_{cyl} + \Delta Q_{\omega} + p \times \Delta V - \left(\bar{h}_{f,inj} - u_{f,g}\right) \times \Delta m_{f,evap} + R_{cyl} \times T_{cyl} \times \Delta m_{bb} \quad (3.3)$$

The following list of parameters explain the different terms of the equation:

- ΔHRL: This term refers to the thermal energy released during the combustion process due to the fuel injected.
- $m_{cyl} \times \Delta u_{cyl}$: This term accounts the energy variation due to the trapped mass in the control volume.
- ΔQ_{ω}: This term corresponds to the heat transfer to the cylinder liner and cylinder head from the trapped gas. It is worthy to note that the model is not considering the fuel that might be at the walls of the cylinder liner due to the jet impacts. Heat transfer coefficients are based on Woschni [24] with some enhanced adjustments performed by Payri et al. [25]. From the wall temperatures calculation standpoint, a nodal model has been implemented [26][27].
- $p \times \Delta V$: This term takes in account the total work made by the gas trapped in the control volume. When the instantaneous calculation of the volume contained at the combustion chamber is calculated, it is considered a model of the mechanical deformations taking in account the pressure exerted by the gas and the inertial forces of the moving masses.
- $\left(\bar{h}_{f,inj} - u_{f,g}\right) \times \Delta m_{f,evap}$: This terms present the energetic considerations because of the fuel injection process [28].

- $R_{cyl} \times T_{cyl} \times \Delta m_{bb}$: The last term of the equation considers the lost energy due to the blow-by through the piston rings.

The main parameters used in the present investigation provided by the combustion analysis tool are the combustion phasing (CA50), indicated mean effective pressure (IMEP), in-cylinder temperatures during the combustion process, trapped mass at the intake valve closing (IVC), in-cylinder peak pressure, pressure rise rate and combustion noise.

3.4 Summary and conclusions

The present chapter presents the different experimental and theoretical tools used to carry out the present investigations. First part of the chapter introduces the SCE and its particularities. A second subsection is dedicated to describe the test facility. In this subsection the lay out of the test cell has been provided as well as the main components description that formed the test cell. In order to acquire the most important parameters during the tests, a dedicated subsection is focused on the instrumentation used. Indeed, it has been introduced the experimental procedure of the investigation. Finally, the last subsection addresses the description of the 0-D tool used to perform the combustion analysis.

3.5 Bibliography

[1] García A. " Estudio de los efectos de la post inyección sobre el proceso de combustión y la formación de hollín en motores diésel". Doctoral Thesis, Universitat Politècnica de València, CMT-Motores Térmicos, 2009.

[2] Molina S. A. "Influencia de los parámetros de inyección y la recirculación de gases de escape sobre el proceso de combustión en un motor Diésel". Tesis doctoral, Universitat Politècnica de València, CMT-Motores Térmicos, 2003.

[3] Novella R. "Estudio de la influencia de los ciclos Atkinson y Miller sobre el proceso de combustión y la formación de emisiones contaminantes en un motor Diésel". Tesis doctoral, Universidad Politécnica de Valencia, CMT-Motores Térmicos, 2009.

[4] Benajes J., Pastor J.V., García A., Boronat V., "A RCCI operational limits assessment in a medium duty compression ignition engine using an adapted compression ratio". Energy Convers. Manage, 126, 497–508, 2016.

[5] Kakaee A.-H., Nasiri-Toosi A., Partovi B., Paykani A. "Effects of piston bowl geometry on combustion and emissions characteristics of a natural gas/diesel RCCI engine". Appl. Therm. Eng., 102, 1462–1472, 2016.

[6] Benajes J., Pastor J. V., García A., Monsalve-Serrano J. "An experimental investigation on the Influence of piston bowl geometry on RCCI performance and emissions in a heavy-duty engine". Energy Convers. Manage., 103, 1019–1030, 2015.

[7] Inagaki K, Fuyuto T, Nishikawa K, Nakakita K and Sakata I. "Dual-Fuel PCI Combustion Controlled by In-Cylinder Stratification of Ignitability". SAE Technical Paper 2006-01-0028, 2006.

[8] Kastner L.J. "An investigation of the airbox method of measuring the air consumption of internal combustion engines". Proceedings of the Institution of Mechanical Engineers, Vol. 157 no 1, pp. 387-404, 1947.

[9] “Measurement of intake air or exhaust gas flow of Diesel engines". SAE Standards J244, 1992.

[10] de Rudder K. “An approach to low-temperature combustion in a small HSDI diesel engine”. Doctoral Thesis, Universitat Politècnica de València, Departamento de Máquinas y Motores Térmicos, 2007.

[11] Novella R. “Estudio de la influencia de los ciclos Atkinson y Miller sobre el proceso de combustión y la formación de emisiones contaminantes en un motor Diésel. Doctoral Thesis, Universitat Politècnica de València, Departamento de Máquinas y Motores Térmicos, 2009.

[12] Sherman M.T., Chase R., Mauti A., Rauker Z. and Silvis W. “Evaluation of Horiba MEXA 7000 Bag Bench Analyzers for Single Range Operation”. SAE Technical Paper, 1999-01-0147, 1999.

[13] Sherman M.T., Mauti A., Rauker Z. and Dageforde A. “Evaluation of Mass Flow Controller Gas Divider For Linearizing Emission Analytical Equipment”. SAE Technical Paper, 999-01-0148, 1999.

[14] Degobert P. Automobiles and pollution. SAE International, 1995.

[15] “Regulation (EC) No 595/2009 of the European Parliament and of the Council of 18 June 2009 on type-approval of motor vehicles and engines with respect to emissions 100 3. Tools and methodology from heavy duty vehicles (Euro VI) and on access to vehicle repair and maintenance information and amending Regulation (EC) No 715/2007 and Directive 2007/46/EC and repealing Directives 80/1269/EEC, 2005/55/EC and 2005/78/EC. Official Journal of the European Union, Vol. 52 no L275, pp. 1-14, 2009”. http://eur-lex.europa.eu.

[16] Silvis W.M. “An Algorithm for Calculating the Air/Fuel Ratio from Exhaust Emissions”. SAE Technical Paper, no 2016-04-05, 1997.

[17] Christian R., Knopf F., Jasmek A. and Schindler W. “A new method for the filter smoke number measurement with improved sensitivity”. MTZ Motortechnische Zeitschift, 54, 16-22, 1993.

[18] Prikhodko V., Curran S., Barone T., Lewis S. "Emission characteristics of a diesel engine operating with in-cylinder gasoline and diesel fuel blending". SAE Int. J. Fuels Lubr., 946–955, 2010.

[19] Curran S., Prikhodko V., Cho K., Sluder S., Parks J., Wagner R.et al. "In-cylinder fuel blending of gasoline/diesel for improved efficiency and lowest possible emissions on a multi-cylinder light-duty diesel engine". SAE technical paper 2010-01-2206, 2010.

[20] Monsalve-Serrano J. Dual-Fuel compression ignition: Towards clean, highly efficient combustion. 2016.

[21] Benajes J., López J.J. and R. Novella A. García. "Advanced methodology for improving testing efficiency in a single-cylinder research diesel engine". Experimental Techniques, 32, 41-47, 2008.

[22] Payri F, Olmeda P, Martín J, García A. "A complete 0D thermodynamic predictive model for direct injection diesel engines". Appl Energy, 2011. http://dx.doi.org/10.1016/j.apenergy.2011.06.00.

[23] Lapuerta M., Ballesteros R. and Agudelo J.R. "Effect of the gas state equation on the thermodynamic diagnostic of diesel combustion". Applied Thermal Engineering, 26, 1492-1499, 2006.

[24] Woschni G. "A Universally Applicable Equation for the Instantaneous Heat Transfer Coefficient in the Internal Combustion Engine". SAE Technical Paper, no 670931, 1967.

[25] Payri F., Margot X., Gil A. and Martn J. "Computational Study of Heat Transfer to the Walls of a DI Diesel Engine". SAE Technical Paper, no 2005-01-0210, 2005.

[26] Degraeuwe B. "Contribution to the thermal management of DI Diesel engines". Doctoral Thesis, Universitat Politècnica de València, Departamento de Máquinas y Motores Térmicos, 2007.

[27] Torregrosa A., Olmeda P. and Degraeuwe B. and Reyes M. "A concise wall temperature model for DI Diesel engines". Applied Thermal Engineering, 26, 1320-1327, 2006.

[28] Martín J. “Aportación al diagnóstico de la combustión en motores Diésel de inyección directa”. Doctoral Thesis, Universitat Politècnica de València, Departamento de Máquinas y Motores Térmicos, 2007.

Chapter 4

Dual-Mode Dual-Fuel operating under a dual-fuel diesel/gasoline combustion strategy from low to full load

Content

4.1 Introduction

As it has been mentioned at the second chapter, the RCCI concept presents high potential in simultaneous reduction of NOx and smoke emissions while the benefits in terms of performance and fuel consumption are maintained or improved respect the CDC. Indeed, due to the possibility of adjusting the reactivity of the fuel blend on demand in order to operate at low loads and also in high load, this concept becomes a real choice for the future of the compression ignition engines. However, there are some challenges which limit the range of application such as excessive fuel consumption at low load and excessive pressure rise rate at high engine load. Dual-Fuel Dual-Mode (DMDF) concept has been proposed in order to enhance the range of operation of the engine. Hence, DMDF is based on dual fuel premixed combustion strategies such as RCCI concept.

Regarding these considerations, the first objective of this chapter is to introduce the Dual-Mode Dual-Fuel concept as well as the experimental methodology followed. In order to explore the concept, a SCE developed from a compression ignition engine will be used to explore this concept over the whole engine map. The second objective of this chapter is to explore this concept by using two different hardware configurations. Two dedicated piston designs have been used to reduce the geometrical compression ratio up to 12.75:1 and 15.3:1. The use of these compressions ratios is aimed to reach the full load over the whole engine speed range while the emissions in terms of NOx and smoke are lower than EU VI limitations.

A third objective will be accomplished at the last part of the present chapter comparing the results obtained by the DMDF concept with the CDC mode. This comparison will be performed in terms of gross indicated efficiency (GIE), fuel consumption and also in terms of NOx and smoke reduction respect the CDC mode.

4.2 Conceptual description

The DMDF concept proposed is aimed to operate a dual-fuel combustion over the whole engine map while the mechanical and emissions constraints are not exceeded. The combustion strategy of the concept is modified as the engine load is increased. Hence, during the low load operation the concept uses a fully premixed (reactivity controlled combustion ignition type) strategy. From medium load, the concept switches to highly premixed and Dual-Fuel diffusive strategy up to full load operation. The exactly engine load where the concept switches from fully premixed to highly premixed will be dependent of the compression ratio used. The lower compression ratio, the higher the engine load boundary.

The following sections of the present chapter will detail the different combustion strategies used by the concept and the behavior in terms of performance and emissions.

4.2.1 Low load operation: Fully Premixed strategy

DMDF uses a fully premixed strategy when it is operating at low load. The strategy is based in the RCCI concept. Therefore, the load limit in order to switch to other strategy will mainly vary in function of the compression ratio used. The present study has tested two different compression ratios and the limit of this combustion process moves from 40 to 60% engine load.

The combustion strategy is achieved using a double injection pulse for the HRF with highly advanced injection timings. The LRF is injected at the intake manifold by using a PFI at 340 CAD (bTDC). The injection pattern and a typical RoHR curve can be observed at the Figure 4.1.

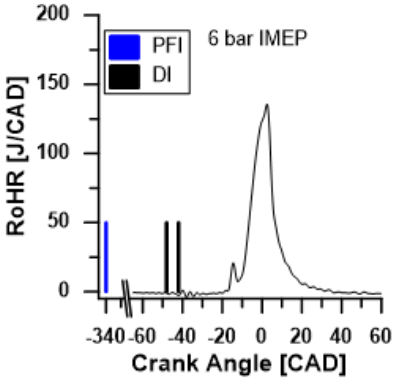

Figure 4.1. RoHR and injection pattern for fully premixed operation.

The high mixing time available prior to the start of the combustion allow reaching ultra-low NOx and smoke emissions. Indeed, the HRF injection timing has not a direct influence on the combustion phasing due to it is governed by the fuel blend reactivity. As a result, this fully premixed combustion strategy is characterized by providing a Gaussian-shaped heat release as it can be observed in Figure 4.1. This RoHR curve is characterized by having a short duration and a rapid expansion period. Consequently, the fully premixed strategy will show the highest efficiency of the DMDF concept.

4.2.2 Combustion process description (Dual-Fuel strategy) for medium and high load operation

Medium and high load operation varies the strategy from highly premixed to dual-fuel diffusive combustion. Hence, the strategy will be adjusted on the fly in order to limit the pressure rise rate below 15 bar/CAD and the in-cylinder pressure below 190 bar.

4.2.2.1 Highly premixed strategy

This combustion strategy uses also two injection pulses of the HRF. Highly premixed strategy presents its main difference from fully premixed at

the second pulse timing. The second injection pulse is placed at the vicinities of the TDC. The strategy is aimed to increase the reactivity at the crevices zone [1] with the first injection pulse and ignite the combustion process with the second injection pulse. The injection pattern can be observed in Figure 4.2.

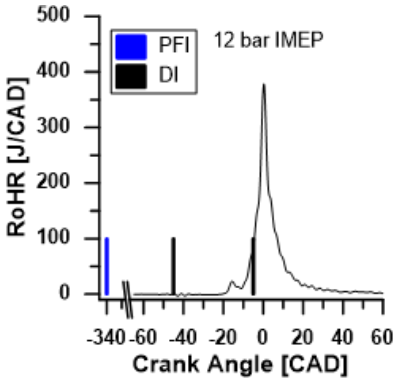

Figure 4.2. RoHR and injection pattern for highly premixed operation.

The injection pattern used at the highly premixed strategy reduces drastically the premixing time of the fuel blend due to the second injection pulse near the TDC. Thus, higher smoke emissions are achieved due to higher local fuel equivalence ratios obtained while it is possible to maintain ultra-low levels of NOx emissions.

Highly premixed strategy provides a higher degree of combustion control due to the partial diffusion burning as it is observed at the rate of heat release presented in Figure 4.2. As a consequence, the combustion phasing is really sensitive to the second injection pulse.

4.2.2.2 Dual Fuel diffusive strategy

In order to achieve the full load operation, the highly premixed strategy evolves to a more diffusive strategy. Hence, Dual-Fuel diffusive is achieved using a single injection pulse of the HRF with a delayed injection timing.

HRF single injection pulse allows to introduce the required amount of fuel to reach the desired load without exceeding the mechanical constraints (pressure rise rate and maximum in-cylinder pressure). Figure 4.3 shows the injection pattern used in this strategy. It is observed that the PFI timing is set at the same CAD for every strategy used along the DMDF concept.

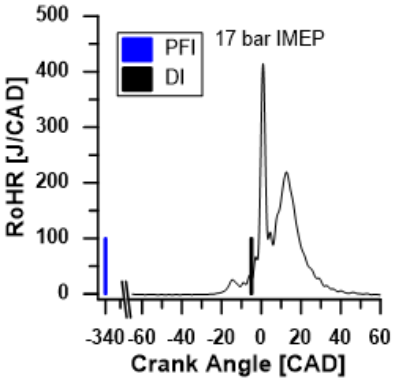

Figure 4.3. RoHR and injection pattern for Dual-Fuel diffusive operation.

From the rate of heat release standpoint, the combustion starts with a high RoHR peak due to the LRF burning during the first HRF reactions. Immediately after this, the HRF is burned being characterized by a long diesel-like tail during the expansion event. This phenomena is observed in Figure 4.3.

This diffusive nature observed at the RoHR provokes high levels of smoke and NOx emissions compared with the previous strategies, but reduces the NOx emissions comparing with the CDC strategy.

4.3 Experimental methodology

In order to apply the DMDF concept, a dedicated methodology has been developed. The experimental procedure has been summarized in three consecutive steps shown in Figure 4.4. The first objective shown in the figure is to find the potential engine settings in order to obtain stable engine

operation at the desired engine load while the self-imposed mechanical constraints (PRR and P_{max}) and coefficient of variation of the IMEP are fulfilled.

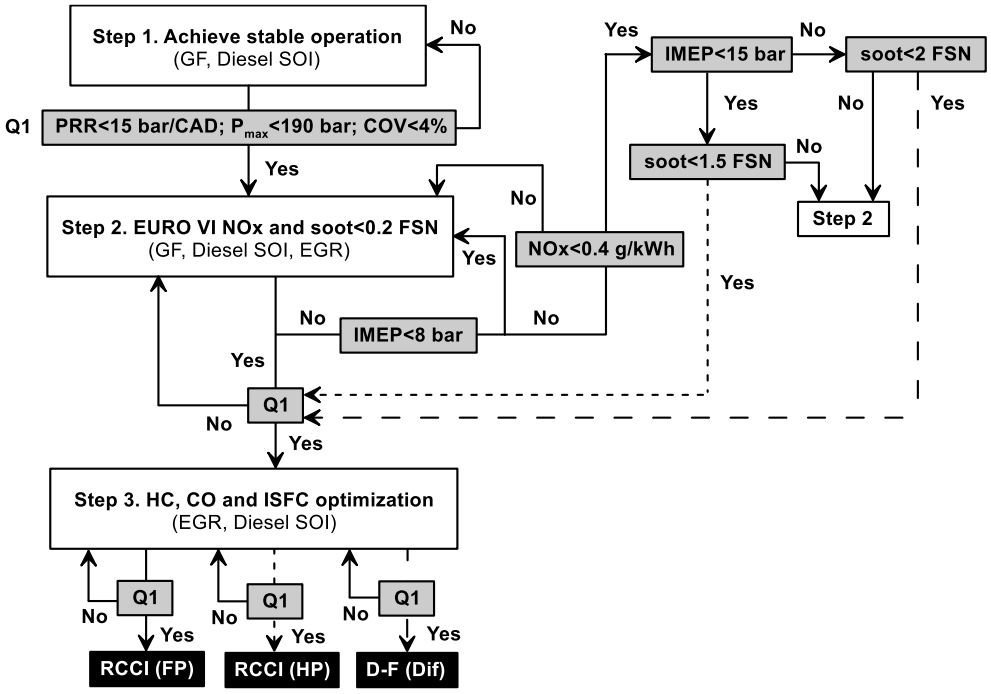

Figure 4.4. Experimental procedure followed to apply the DMDF concept into a SCE.

As literature demonstrates [2], HRF injection timing and the fraction of LRF are the most effective parameters in order to control the RCCI concept. DMDF also shares these particularities. Thus, for a given conditions in terms of air management characteristics, the adjustment of these parameters will modulate the combustion process allowing to reach stable operation. The LRF fraction will allow adjusting the reactivity of the fuel blend, providing a good control of the combustion and, therefore a proper combustion phasing. The HRF injection pulse timing would affect directly to the premixing. The mixing time will vary depending on the engine speed and the injection timing. Consequently, the premixing has a direct impact on the

NOx and smoke emissions. Both parameters are limited in range due to the constraints aforementioned. The LRF fraction will be limited by the COV_{IMEP} (COV_{IMEP}<4%) and the HRF timing will be limited by the PRR (PRR < 15 bar/CAD).

The second step proposes a procedure to reach the operation conditions required to meet the EURO VI NOx limitations and ultra-low smoke emissions. Once a stable operation point has been reached, the EGR is adjusted in order to reduce the NOx emissions below the EU VI limitation. EGR reduces the temperatures reached during the combustion process, avoiding NOx formation. Small adjustments should be done in order to maintain the same combustion conditions by modifying the injection pulse timing and the LRF fraction. Thus, the COV_{IMEP} is maintained below 4% as well as the mechanical constraints imposed (PRR and P_{max}). Resulting of this second step performed, the engine operation point should be stable and meet EU VI NOx limits while ultra-low smoke emissions are achieved at this point. However, there has not been any action in order to control CO and unburned HC emissions. An additional step is required.

Finally, the third step is aimed to reduce the CO and unburned HC emissions while improving the indicated specific fuel consumption (ISFC). This step can be considered as a rough tuning of the combustion settings. In order to ensure that the NOx emissions and mechanical constraints are not over exceeded, HRF injection pulse timing and the EGR rate are adjusted.

The second step contains a particularity. Some of the emissions constraints vary in function of the load achieved. This load is affected by the compression ratio. Thus, in Figure 4.4 it has been depicted several conditions in terms of IMEP which provide different emissions restrictions while the mechanical constraints are fixed for every engine load condition.

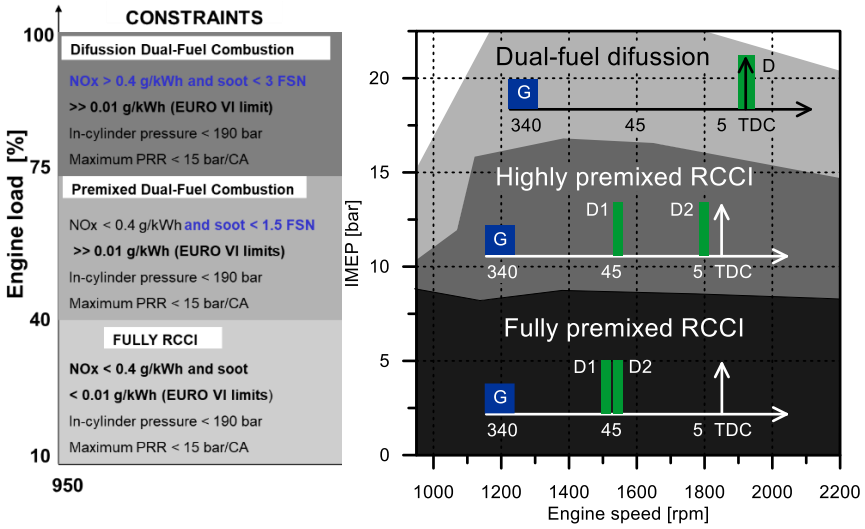

Figure 4.5. Constraints and strategies scheme of the DMDF concept.

Figure 4.5 shows an approach of the DMDF concept in terms of self-imposed constraints and range of load operation. On the right side of the figure, there is a summary of the injection pattern for every strategy.

DMDF combustion concept has been applied to a SCE. The SCE used to carry out this study differs from a regular research SCE. The SCE derives from a commercial multi cylinder engine, representing a hybrid solution between a stock multi cylinder engine and a research SCE [3]. This solution was taken in order to use a more cost-effective SCE. Indeed, it had the advantage to extend the scope of the investigation. However, this hybrid solution did not allow to obtain torque-based results for the SCE due to the whole number of cylinder are operating under combustion. Hence, the results have to be in indicated parameters.

Both engines (SCE and MCE resultant) were fully instrumented during the operation. In-cylinder pressure sensors were installed at the first and the fourth cylinders in order to monitor the pressure in real time. The in-cylinder pressure signal for both cylinders was measured with Kistler 6125C pressure transducers and their respectives amplifiers Kistler 5011B10.

The injection systems for the SCE was in-house developed, as it has been afore explained at the previous chapter. The injection system consists of a DI for the HRF and a PFI for the LRF. Both injectors are conducted with an in-house ECU developed that sets the injection timing, number of injections and the duration.

Regarding the air management of the engine, the SCE was provided with a fresh compressed air supply which guarantee stable operation over the whole engine operating points. This system was able to condition the air in terms of humidity and temperature. The EGR rate supply was also in charge of the test cell. There was a dedicated system which cleaned the exhaust gases of particles and water, cooled the flow mass and compressed again to reintroduce it to the intake of the SCE.

The emissions NOx, O_2, unburned HC and CO experimentally measured were obtained with a five gas Horiba MEXA-ONE-D1-EGR analyzer. From the smoke emissions standpoint, the experimental measurements were performed by an AVL 415 Smoke Meter. Smoke Meter provides the results directly in FSN.

In order to perform the combustion analysis, it was used an in-house developed one-zone model named CALMEC. This combustion diagnosis tool is fully described in [4] and uses the in-cylinder pressure signal and other mean variables, such as engine speed, temperatures and so on, obtained during the experiments.

4.4 Hardware effects on Dual-Mode Dual-Fuel operational limits

4.4.1 Different compression ratios evaluated

Internal combustion engines typical outgoing energy paths are the exhaust enthalpy, the output work and the heat transfer (HT). Focusing on

the heat transfer, the most important amount of heat transferred is produced during the combustion and expansion events [5]. Therefore, most interesting research areas to increase the whole engine efficiency are engine heat transfer and the exhaust losses (representing around two thirds of the total energy).

From the heat transfer standpoint, around half part of the heat transfer losses within the engine come from in-cylinder heat transfer losses. Hence, heat transfer can be reduced by working on the piston design or increasing the exhaust gas enthalpies in a bottoming cycle [6]. Several solutions in order to improve fuel efficiency by reducing heat transfer losses such as low heat rejection engines (LHR) [7]. Focusing in RCCI concept, Kokjohn et al. [8] compared the concepts RCCI and CDC by increasing the efficiency when the heat transfer losses were reduced. Thus, the study operated an engine at 9 bar of IMEP while the operation was considered adiabatic for both concepts. The most important results from that study showed that the apparent rate of heat release (ARR) increased significantly for the RCCI case. This phenomena brought a rapid end of combustion as well as the suppression of cool regions at the cylinder liner. By contrast, the CDC concept was not really sensitive to the HT elimination. Thus, it was possible to increase the GIE for the RCCI while for the CDC case was close to the 44%.

Hence, HT reduction provides a great potential in order to increase the overall efficiency of the RCCI mode. Monsalve-Serrano [9] compared the heat transfer breakdown and the total heat transfer energy between low, medium and high engine load. The main results of this study are shown in Figure 4.6.

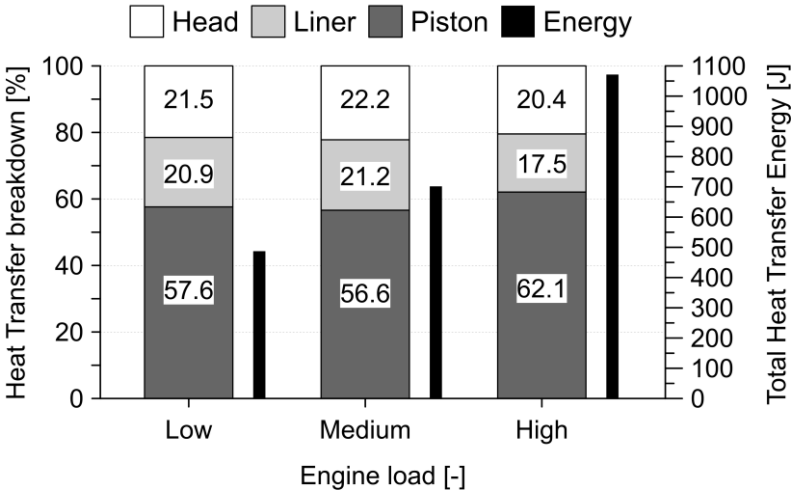

Figure 4.6. Comparison of the heat transfer breakdown and the total heat transfer energy through different engine loads operation [9].

The study carried out in [9] used two different geometries applied in two different compression ratios (CR). An effective CR of 14.4:1 was used for low and medium engine load operation and an effective CR of 11:1 was used for high engine load operation. The effective compression ratio was achieved by using a Miller cycle. Indeed, the SCE was fitted with a variable distribution system which allow to obtain such a wide range of effective compression ratios.

The CR was reduced at high engine load operation in order to avoid exceeding the mechanical limitations of the engine. These studies reached up to 25 bar/CAD (excessively high for a commercial engine). For low and medium load operation a higher CR was used in order to reach a good efficiency. The geometries selected were the stock, a tapered and a bathtub. The tapered and the bathtub geometries were designed by using CFD simulations in order to provide a raw optimization of the piston (heat transfer, surface, volume of the piston bowl). The main characteristics are presented in the Table 4.1 below:

Table 4.1. Main characteristics of the three combustion chambers studied in [9].

Piston	Stock	Tapered	Bathtub
Area [mm^2]	15895	14977(-5.7%)	13383(-15.8%)
Volume [mm^2]	110705	110705	110705
Area/Volume [mm^{-1}]	0.143	0.135	0.121
Squish cavity shape [-]	flat	tapered	rounded
Min. squish height [mm]	13.1	13.1	13.1

Concluding with the study of the effects of the piston bowl geometry on RCCI combustion performed at [9], the main objectives were to reduce the surface-to-volume ratio and to promote more quiescent combustion chamber. As a result, at low load all the geometries presented ultra-low levels of NOx and smoke while very similar values of CO and unburned HC emissions were obtained. However, the stock piston bowl geometry presented an enhanced mixing process due to the more pronounced geometry resulting in an earlier SOC than the other two geometries. At medium load, bathtub geometry promoted higher combustion temperature peaks due to a lower surface-to-volume ratio contributing to reduce combustion losses and fuel consumption. Finally, high engine load operation showed that the best results were provided by the tapered geometry. The main conclusions of this study were that the two new geometries provide better efficiency to the RCCI concept than the stock geometry. It is worthy to remember that the compression ratio was 14.4:1 for low and medium load and 11:1 for high engine load.

Monsalve-Serrano [9] also concluded with the thesis work suggesting to operate the engine under a Dual-Mode combustion strategy. This Dual-Mode consisted of combining the RCCI and CDC concept. The CR used was 17.5:1 and the operation range of RCCI mode was limited from 25% to 35% [10]. The rest of the engine operation was done under CDC mode.

Hence, the DMDF concept proposes to operate under a dual-fuel combustion strategy from low to full load. The piston design is a key point as well as the CR selected. It has been proposed two compression ratios with different piston bowl geometries design. The compression ratios selected have been CR12.75:1 and 15.3:1. According to [9], CR12.75 could provide good performance at high load operation. However, the lower compression ratio could promote excessive CO and unburned HC at low engine load operation. The excessive CO and uHC levels at low load operation would worsen the fuel consumption. By contrast, the CR 15.3:1 is expected to provide better performance at low load operation but the pressure rise rate and in-cylinder pressure peak could be increased, limiting the high engine load operation. In this case, the main problem is that the fully premixed strategy operational zone would be shortened.

From the geometry standpoint, the bathtub and non-reentrant geometry have been selected for the CR12.75:1 and CR15.3:1 respectively. According to the Monsalve-Serrano´s study, this design of piston bowl shows good results at low load operation. This design allows increasing the reactivity at the crevices volume. The stock piston profile corresponds to a re-entrant design. The different piston profiles configurations are depicted in Figure 4.7. The black line shows the stock piston, the grey line shows the CR12.75:1 piston profile and the dashed line presents the CR 15.3:1 piston profile.

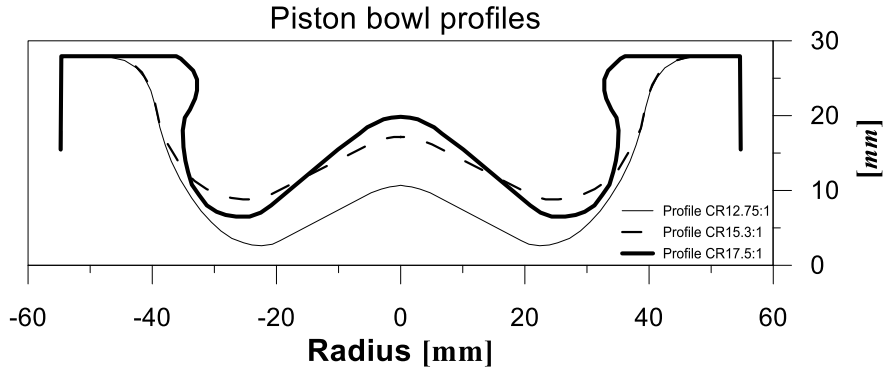

Figure 4.7. Stock piston bowl design and adapted compression ratios profiles (CR12.75:1 and CR15.3:1).

The design performed at the pistons has not been optimized. This design is aimed to reach three different targets:

- To reach the desired geometrical compression ratio (around 13:1 and around 15:1)
- Respecting a minimum wall thickness to avoid mechanical damage during their operation.
- Avoiding re-entrant design in order to improve the low load operation.

The main properties of the piston bowls are presented in Table 4.2. There are compared the two different piston bowls tested with the stock bowl.

Table 4.2. Main characteristics of the piston bowls tested

Production bowl (CR 17.5:1)	**Bathtub bowl (CR 12.75:1):**	**Non re-entrant bowl (CR 15.3:1):**
Area/volume: 8.18 cm^2/ 63.51 cm^3= 0.128	Area/volume: 9.78 cm^2/ 97.86 cm^3= 0.1	Area/volume: 9.05 cm^2/ 77.8 cm^3= 0.116
Depth: 20.8 mm	Depth: 24.35 mm	Depth: 20.8 mm
Min. distance to oil gallery: 5.7 mm	Min. distances to oil gallery: 4.5 mm > 3.9 mm (used in bathtub design)	Min. distances to oil gallery: 5.35 mm > 3.9 mm (used in bathtub design)
Min. distance in center: 19.3 mm	Min. distance in center: 10.37 mm	Min. distance in center: 16.79 mm

4.4.2 Bathtub geometry. Compression ratio of 12.75:1

This subsection investigates the capabilities of the DMDF concept applied in a SCE with a CR 12.75:1. This work has focused on the development and evaluation of an engine map with the aim to achieve full load without exceeding the self-imposed mechanical and emissions constraints. The 4.4.2 subsection is structured in performance and gaseous emissions of the DMDF concept.

4.4.2.1 Performance

The present section is dedicated to the performance of the concept obtained with the CR12.75. Thus, the indicated specific fuel consumption

(ISFC), the in-cylinder maximum pressure, indicated mean effective pressure (IMEP) and the pressure rise rate (PRR) are presented in Figure 4.8.

From this figure is possible to observe the different levels of IMEP achieved for all the engine speeds tested. Thus, from low to full load has been progressed systematically in order to obtain a proper engine map for the DMDF. In this sense, the in-cylinder pressure observed follows the same trend. The higher the IMEP, the higher the maximum pressure. For all the cases tested the in-cylinder pressure has been kept under the self-imposed constraints, in this case a limit of 190 bar. Indeed, the maximum pressure achieved corresponds to the medium engine speed zone, where the maximum torque is achieved. The Figure 4.8 shows the different levels of IMEP achieved and the legend indicates different load steps up to 100%. However, the maximum engine load achieved only for the 950 rpm and 2200 rpm cases. The center points of the engine speed (1200, 1500 and 1800 rpm) were limited up to 90% engine load due to the excessive PRR. In this sense, the engine would lose a 10% of the engine maximum torque but the maximum output power is maintained.

From the fuel consumption standpoint, logically the fuel consumption decreases as the engine load increases. This fact is due to the better gross indicated efficiency as it can be observed in Figure 4.9. This improvement at the efficiency is due to two main reasons. The first reason is that the efficiency of the combustion increases due to the reduction of the CO and uHC emissions by means of higher combustion temperature. The second reason is related with the heat transfer. A proper combustion phasing and the increase of the engine load reduces relatively the heat transfer across the cylinder walls and the piston. Additionally, the friction effect also explains the general trend observed in reciprocating engines. Friction losses are not directly related to the engine load, what causes that the friction losses reduce proportionally as the engine load increases.

By contrast, a delayed combustion phasing at high engine load operation worsens the efficiency keeping the fuel consumption in similar or

higher values than at 75% engine load. Consequently, the burning process happens during the expansion stroke, losing part of the pressure available to generate more work.

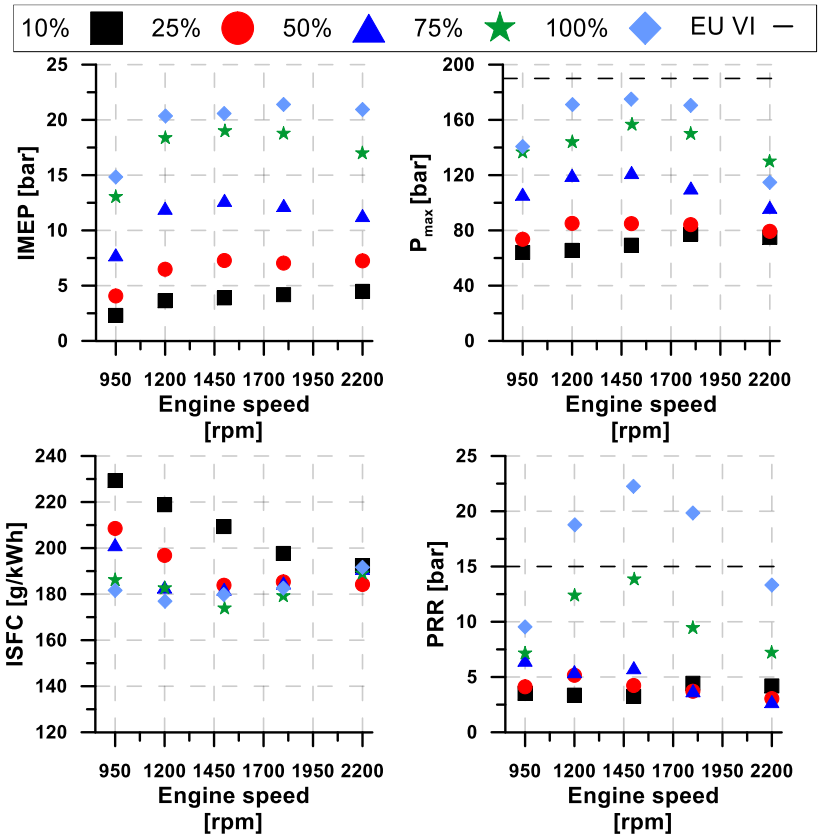

Figure 4.8. Indicated mean effective pressure (IMEP), in-cylinder maximum pressure (P_{max}), indicated fuel specific fuel consumption (ISFC) and pressure rise rate (PRR).

Despite of having a delayed CA50, the PRR observed at full load exceeds the self-imposed constraint. The PRR provokes high RoHR peaks which increase the temperature of the combustion chamber promoting a better oxidation of the CO and improving the burning of the HC. As a result,

both pollutants result drastically reduced at full load compared with the low load operation.

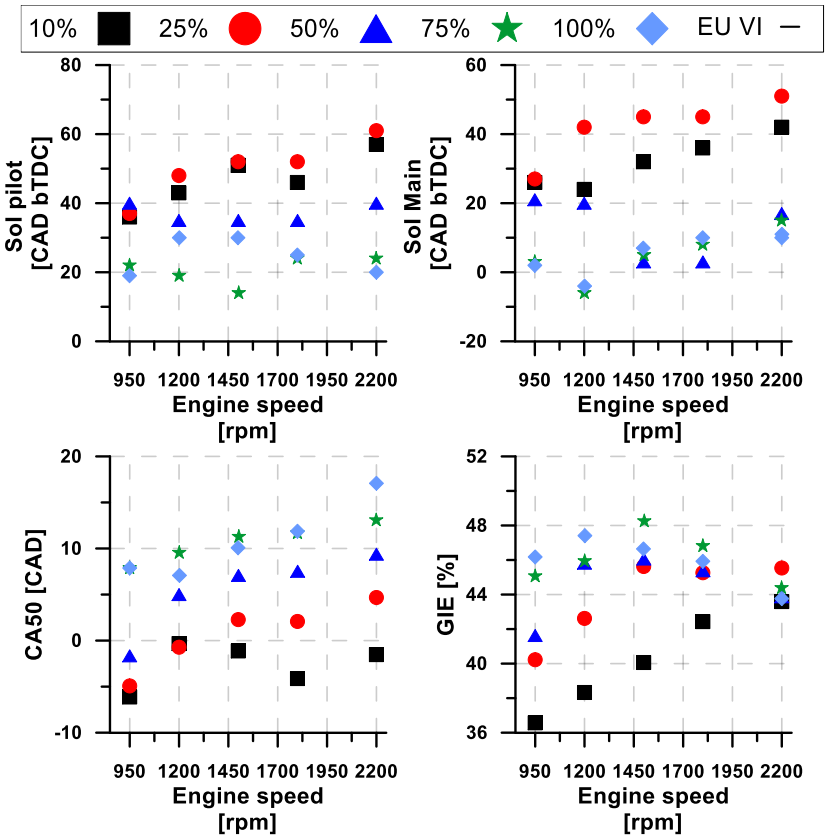

Figure 4.9. Pilot and main start of injection (SoI), combustion phasing (CA50) and gross indicated efficiency (GIE) for the whole engine points tested.

By contrast, the benefits observed of such an extremely high PRR peaks, provide a lower GIE. This trend might be explained by the combustion phasing. In order to reduce the PRR, the combustion phasing needs to be delayed and provoke the combustion process during the expansion stroke. Hence, the combustion duration increases causing to increase the heat transfer, which reduces the GIE at full load.

4.4.2.2 Emissions

The present subsection is focused on the emissions promoted by the DMDF concept when using the adapted compression ratio o f 12.75:1. Figure 4.10 shows the NOx, smoke, CO and unburned HC emissions provided by using the lowest CR of the present work. The loads depicted at the figure start at 10% and go up to full load. Different engine loads are presented with different colors as the legend shows.

A first approach to the results is that NOx emissions fulfill EU VI for all the engine operation points (below 0.4g/kWh). Smoke emissions also present ultra-low values, showing a maximum of 0.28 FSN at 1800 rpm and full load. Regarding the CO and uHC emissions, both are exceeding the limitation imposed by the EU VI standard emissions. Note that the dashed line depicted at the figures represent the EU VI limitation, just draw as a reference to be compared with the results obtained.

Considering NOx emissions, the low values obtained (below EU VI limitation) are possible mainly due to a proper air/fuel mixing and reduced in-cylinder temperatures reached during combustion process. Figure 4.11 shows the EGR rate, mixing time, gasoline fraction, the Air-Fuel effective ratio, intake pressure and the global equivalence ratio (GER). From the Figure 4.11, it is observed that mixing time is positive for almost every engine operating point tested. In order to complete the combustion process information, Figure 4.12 shows the maximum bulk gas peak temperature of the concept applied to the CR 12.75:1.

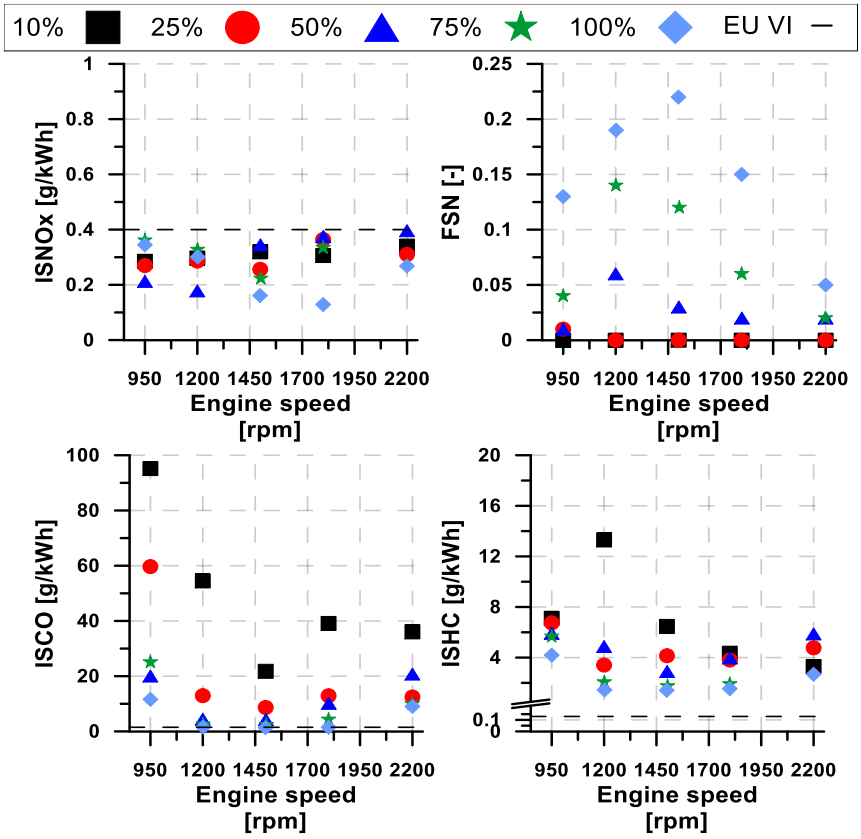

Figure 4.10. Engine-out emissions for the DMDF concept by using a CR12.75:1 in a SCE.

In order to provide a proper explanation, it is interesting to differ low load operation (10 and 25% engine load) from medium and high (from 50 to 100% engine load) engine load. In general, the low NOx emissions provided by the concept are related to the premixing of the fuel blend, which reduces the areas with rich equivalence ratios. However, different combination of settings at lower or higher loads will determine the ultra-low levels obtained.

Hence, low load operation has a very lean mixture which provokes the reduction of the mean bulk gas temperatures peak during combustion and, therefore the NOx formation is avoided. This phenomena also explains the

ultra-low levels of smoke achieved by the concept. The reduced areas with rich equivalence ratios avoid smoke formation.

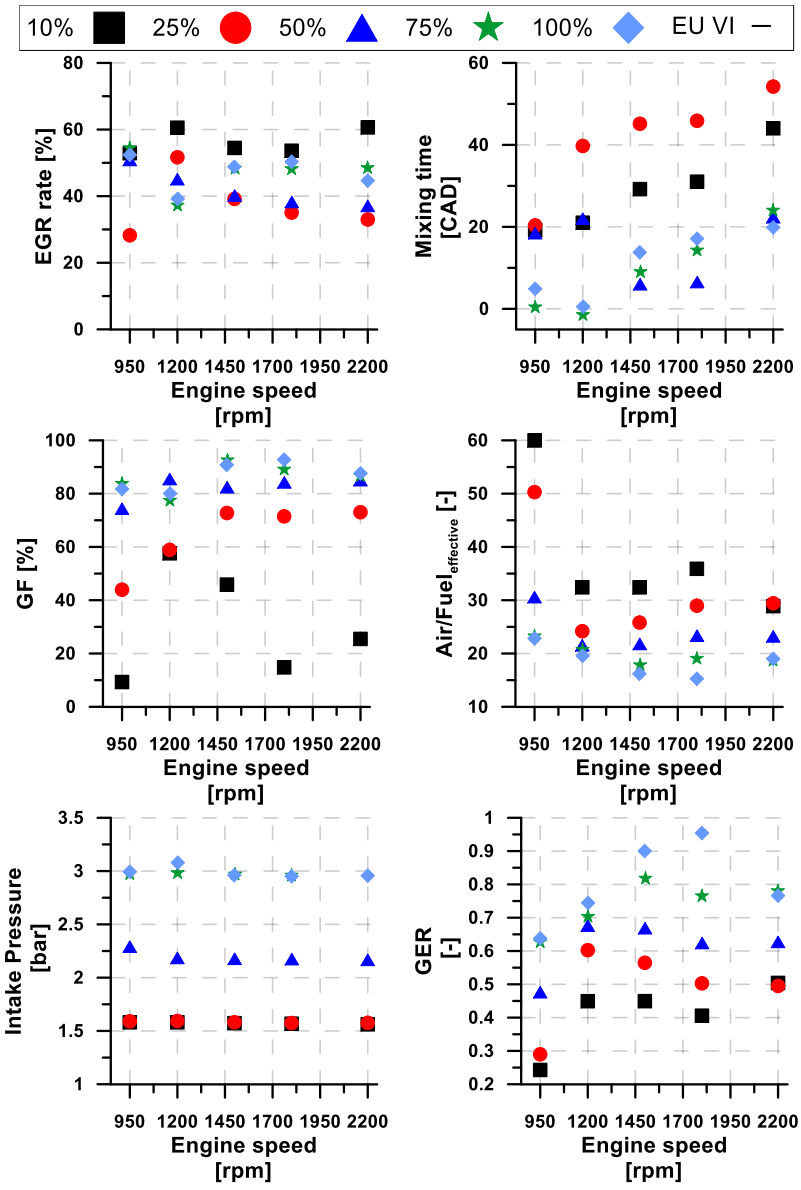

Figure 4.11. EGR rate, mixing time (EoI-CA10), gasoline fraction (GF), Air-Fuel effective ratio, intake pressure and GER.

From the high load operation standpoint, mixing time has been a key point in order to avoid NOx formation [11]. Thus, the mixing time is possible due to a proper reactivity of the fuel blend, allowing to inject very advanced from the TDC and allows to set the combustion phasing properly, having an excellent control over the onset of the combustion process. This reactivity has been reached by using huge amounts of EGR (up to 60%) and gasoline fraction (up to 90%). In addition, the premixing allows these rates of EGR and GF without affecting the smoke emissions as it can be observed in Figure 4.10. Concluding with the NOx and smoke emissions, it is stated that the concept is able to break also the existing trade-off in CDC of NOx and smoke emissions.

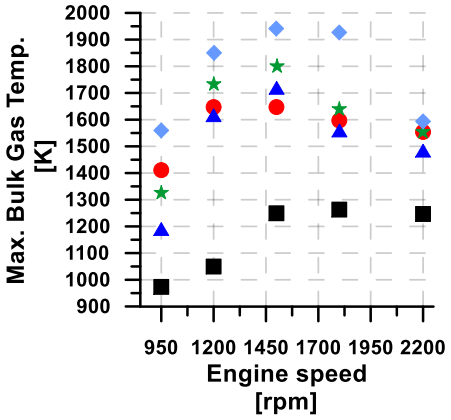

Figure 4.12. Maximum bulk gas temperature for the DMDF concept under CR12.75:1

Regarding smoke emissions, it has been showed in Figure 4.10 that the values of smoke obtained are below 0.25 FSN. Those values mean that smoke emissions values are ultra-low for the whole engine operation map. During low load operation, the mixing time observed in Figure 4.11 provides a fully premixed fuel blend which avoids richer local equivalence ratios. For medium and high engine loads, higher EGR rates are used and the diesel injection is delayed compared with the low load operation. Despite of the reduction of the mixing time, the premixing level of the fuel blend continues being very

high due to the gasoline fraction has been increased. Hence, from low to full load operation the richer local equivalence ratios are avoided. Consequently, smoke formation is also avoided.

Carbon monoxide (CO) and unburned hydrocarbons (uHC) are presented in Figure 4.10. In general the values provided by the DMDF concept are exceeding the EU VI limitations for every engine operation point tested. Low load operation presents unacceptable levels of CO due to the bulk gas temperature. The in-cylinder mean bulk gas temperature peak reached is lower than 1200K for 950 and 1200 rpm cases and, therefore the CO emissions are extremely high because of the CO oxidation process is not promoted. The rest of low load cases with high CO and uHC emissions are explain due to the fuel burning capabilities. In this sense, the combustion chamber has not enough high thermodynamic conditions to ensure the totally burning of the gasoline. Indeed, the GF used in every operation point correlates with the trend observed at the uHC, as it can be observed in Figure 4.10 and Figure 4.11. Summarizing the uHC emissions, the higher the reactivity and the higher energy released during the combustion, the lower the uHC emissions. As it has been commented previously, medium and high engine load operation is far from EU VI limitations in terms of CO and uHC emissions. As the mean bulk gas temperature peaks observed are over 1200K, the CO emissions have been reduced significatively comparing with the low load operation. By contrast, the uHC levels observed are very similar to the values observed at low load operation. Hence, despite the icreaso observed at the mean peak bulk gas temperature, the amount of uHC is not reducing as the CO emissions. Observing the Figure 4.11, the GF plot shows that the fraction of gasoline also increases when the engine load is increased. The gasoline is injected by using PFI during the intake stroke aimed to generate the maxium premixing of the gasoline prior to the combustion process. Part of this premixed gasoline might be located at the crevices volume causing this amount of uHC. Hence, the results obtained are aligned with the literature [12], stating that the higher the GF, the higher the uHC.

4.4.3 Non re-entrant geometry. Compression ratio of 15.3:1

Following to the capabilities of the DMDF concept applied in a SCE with a CR 12.75:1 observed at the previous subsection, the current subsection uses a CR15.3:1. This work has focused on the development and evaluation of an engine map with the aim to achieve full load without exceeding the self-imposed mechanical and emissions constraints. The 4.4.3 subsection is structured in gaseous emissions and performance of the DMDF concept.

4.4.3.1 Performance

The present section is dedicated to the performance of the concept obtained with the CR15.3:1. Thus, the indicated specific fuel consumption (ISFC), the in-cylinder maximum pressure, indicated mean effective pressure (IMEP) and the pressure rise rate (PRR) are presented in Figure 4.13.

Figure 4.13 shows the IMEP from low to full load for every engine speed tested. Compared to the previous piston geometry tested, it is possible to find more number of points tested due to the combustion switches to Dual-Fuel diffusive strategy at high engine load operation. More number of engine points tested ensures that more than one point is tested in every combustion strategy. As it can be observed in the figure, the engine map has been obtained without exceeding the self-imposed mechanical constraints (PRR<15 bar/CAD and P_{max}<190bar). This results obtained from the combustions are possible due to a combination of factors which provide a proper combustion process. Figure 4.14 presents the SoI of the two injections of the diesel fuel, the combustion phasing and the GIE.

As it is depicted in the figure, the combustion phasing is more delayed as the engine load is increased. The SoI of both diesel injections evolves from a very advance injection timing to a more delayed diesel injection at medium and high engine load. In particular, from 75% to full load engine load there is only one diesel injection, as it is possible to observe at the figure. Therefore,

the diffusive nature of the combustion at high engine load provides a slow combustion process which provides a delayed combustion phasing. Consequently, this combustion phasing during the expansion stroke avoids excessive values of PRR and maximum in-cylinder pressure, allowing the operation of the concept up to full engine load.

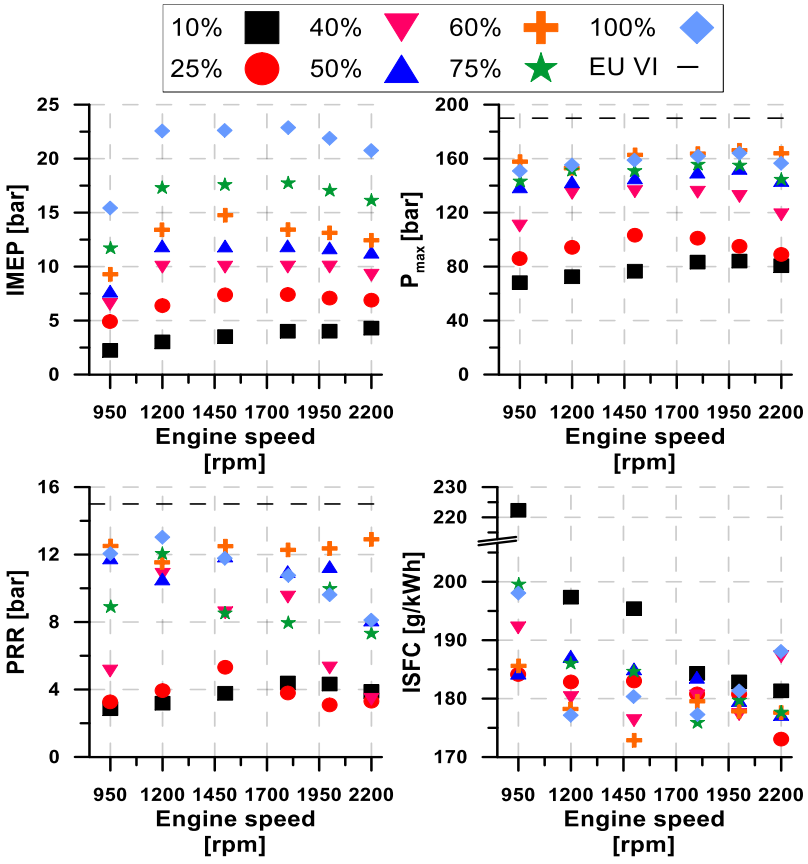

Figure 4.13. Indicated mean effective pressure (IMEP), in-cylinder maximum pressure (P_{max}), indicated fuel specific fuel consumption (ISFC) and pressure rise rate (PRR).

Despite of having the combustion phasing delayed at high engine load, the GIE of the concept remains with good values for the whole engine map operation. There is only one point at 950 rpm with the lowest GIE result due to the excessive values of CO and unburned HC obtained as a consequence of a poor combustion process.

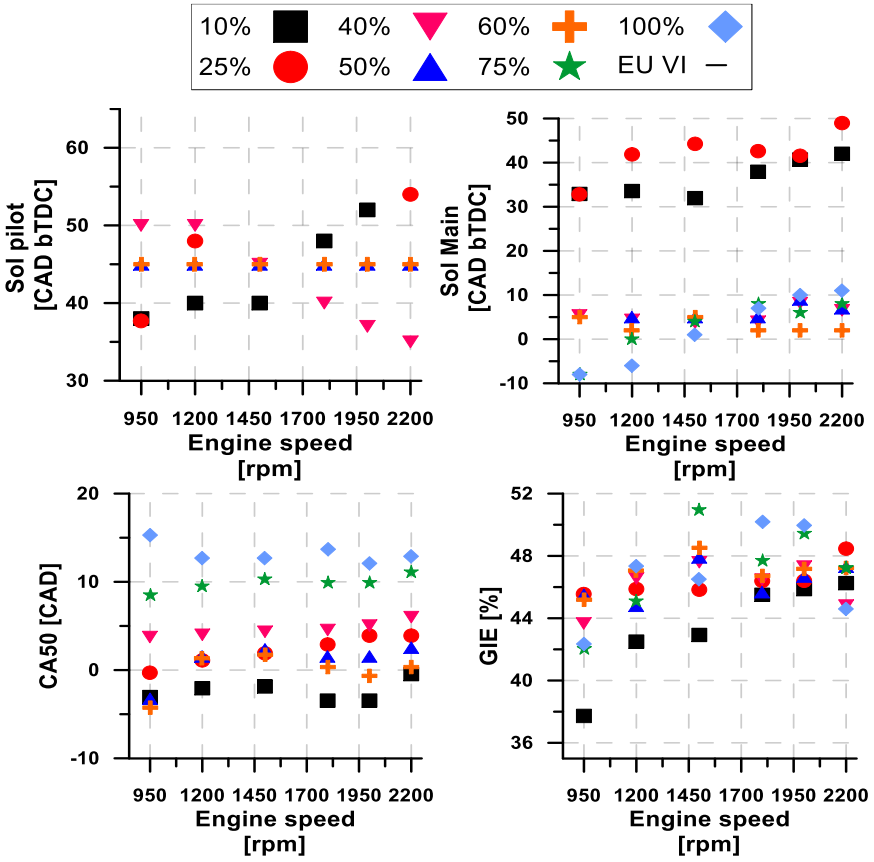

Figure 4.14. Pilot and main start of injection (SoI), combustion phasing (CA50) and gross indicated efficiency (GIE) for the whole engine points tested.

Hence, the combination of a proper combustion phasing and a fast combustion process with low heat transfer results in an excellent GIE, which provides an excellent ISFC, as it is depicted in Figure 4.13.

4.4.3.2 Emissions

The present subsection focuses on the engine-out emissions in terms of NOx, smoke, CO and unburned HC. Each pollutant is represented in an independent graph for every engine operation point tested.

It is worthy to note that, as it was presented in 4.4.2 subsection, the points depicted at the graphs form several emissions maps for the DMDF concept operating under steady state conditions.

Focusing on the NOx emissions, from the Figure 4.15 it is possible to observe that the values promoted by the concept are below the EU VI limits (0.4 g/kWh) up to 75% load for all the engine speeds tested. The region formed from idle up to 75% engine load is operated under fully and highly premixed combustion strategy. The trend observed at the NOx emissions is well related to the maps of GF and EGR depicted in Figure 4.16. Hence, the points of higher NOx values correspond with those points with lower GF and EGR rates. In this sense, increasing the direct injection fraction of diesel fuel causes locally higher equivalence ratios and higher temperatures which increase the NOx emissions. From 75% to full load the combustion strategy switches to Dual-Fuel diffusive increasing NOx and smoke emissions. Thus, this part of the NOx map emissions is mainly fulfilled with NOx values between 0.6 and 0.8 g/kWh reaching some points of 1.2 and 1.4 g/kWh. Despite of being over the EU VI limits (0.4 g/kWh), these values imply a drastic reduction in NOx emissions compared to a regular CDC operated CI engine, which reaches up to 10 g/kWh due to the stock calibration uses SCR aftertreatment system.

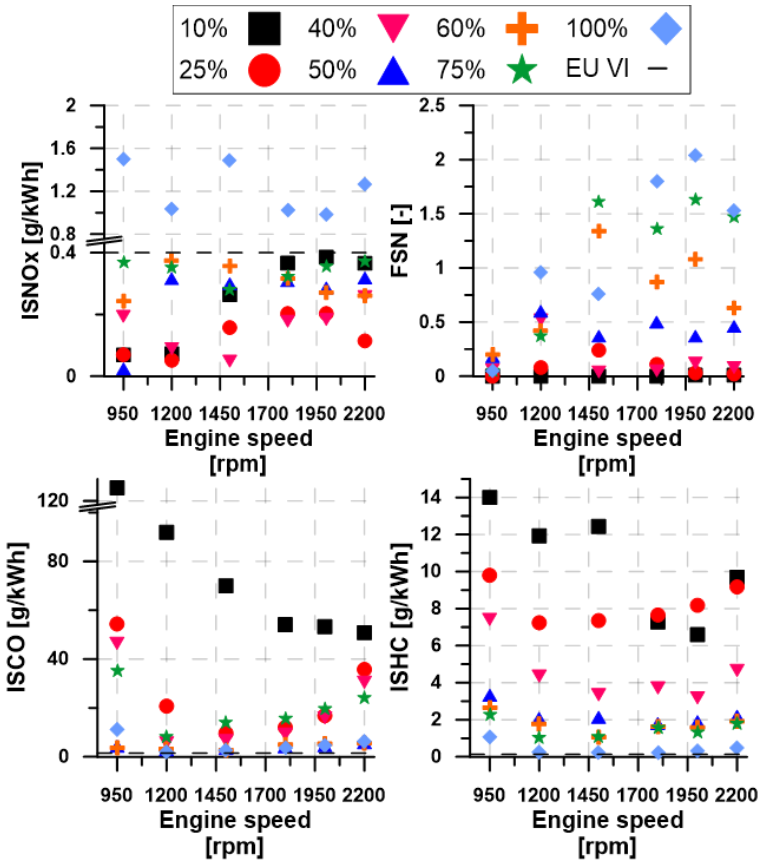

Figure 4.15. Engine-out emissions for the DMDF concept by using a CR15.3:1 in a SCE.

The smoke emissions presented in Figure 4.15 show that the smoke increases with the engine load. Indeed, the smoke increases over 0.5 FSN for 60% engine load. Hence, the smoke emissions responds directly to the combustion strategy, starting to increase the smoke values when the strategy switches to a highly premixed and being maximum when the Dual-Fuel diffusive mode is operated. Up to 40% engine load, the low smoke emissions (below 0.2FSN) are consequence of the wide mixing time and the low EGR rate used in these engine points. From 40% to 60% the smoke emissions average are around 0.6 FSN with some local peaks of around 1.2 FSN. The

smoke has been increased in this region due to the switch to a less premixed strategy for the diesel fuel and the increase of the EGR rate used. In addition, the effective Air/Fuel ratio presented in Figure 4.16 shows that decreases as the engine load increases. Also the EGR rate graph shows the variation of the EGR rate from low to medium load, where the EGR rate passes from 20% to 50%. Finally, from 60% to full load, the smoke emissions of these operating points are over 0.75 FSN reaching up to 2 FSN for some particular points with high engine speed.

The GF was typically set to the highest ratio achievable with the highest combustion stability and lowest unburned HC emissions. As shown in Figure 4.16, the lowest GF values were obtained during low load and low engine speed operation. The GF values achieved in these points were around 20% in order to avoid excessive unburned products and combustion instabilities. However, the GF was increased up to 80-90% in the mid region of the engine operation map. At high load, the GF was reduced again below 60% in order to avoid excessive PRR. Figure 4.16 also present the EGR rate, showing that the highest values are obtained for the medium load cases (around 50%). Low load operation was covered with a 20% of EGR rate due to the use of the fully premixed strategy. Fully premixed strategy allows to use lower EGR rates because is possible to reach ultra-low NOx and smoke emissions inherently. When the medium load is operated, the EGR rate increases up to 50% in order to extend the premixing time and minimize the diffusion burning of the diesel fuel provided by the second injection pulse. Finally, the high engine load operation was performed by using a 30% of EGR rate to avoid excessive smoke emissions provoked by the Dual-Fuel diffusive strategy.

Focusing on the CO and unburned HC emissions, Figure 4.15 shows that both pollutants follow similar trends. Hence, the emission levels decrease when the engine load and speed increase.

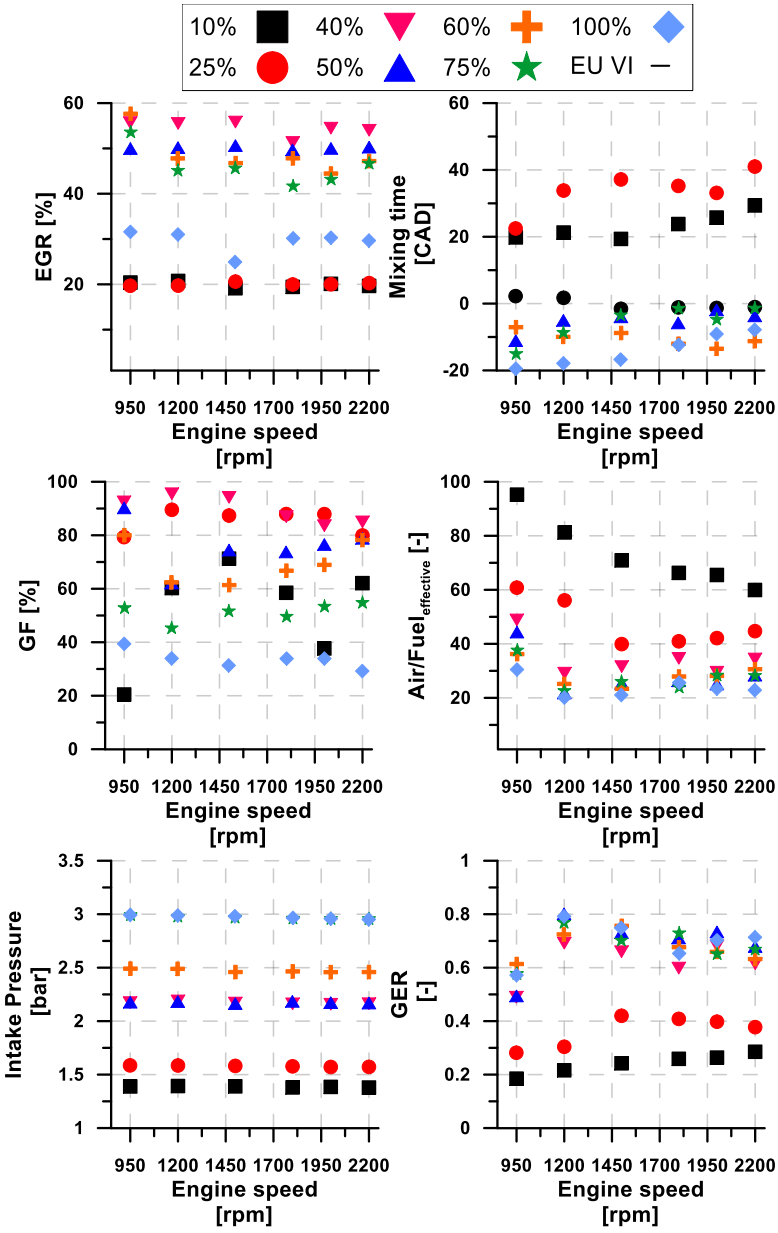

Figure 4.16. EGR rate, mixing time (EoI-CA10), gasoline fraction (GF), maximum bulk gas temperature, boosting pressure and GER.

The worst CO and uHC emissions levels are reached at low load and low engine speed conditions. In particular, 950 and 1200 rpm at 10% engine load present excessive CO and uHC emissions. The high amount of CO emissions found at low load operation can be explained with the maximum bulk gas temperature peak shown in Figure 4.17. In this figure, it is clear that the regions of lowest temperature correspond with the regions with highest values of CO.

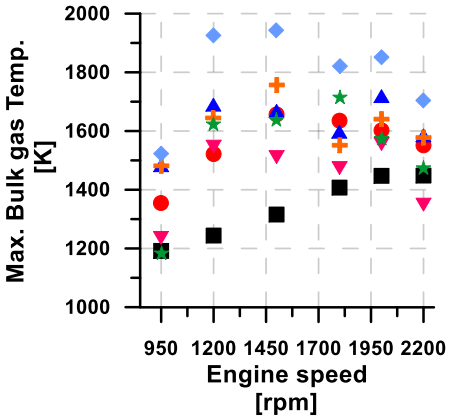

Figure 4.17. Maximum bulk gas temperature for the DMDF concept under CR15.3:1.

In particular, during low load operation, the global equivalence ratio is very low and, therefore it is possible to state that the incomplete combustion of over-lean fuel/air mixture is the dominant mechanism responsible of the CO oxidation. Thus, the combination of low bulk gas temperature (around 1200K) and the over-lean fuel/air mixture promotes such a high CO levels. In this sense, the optimal combustion strategy will result in bulk gas temperatures in the range of 1500-1700 K, where the lower temperatures limit ensures complete oxidation of CO and upper temperature limit promotes minimal NOx formation.

From the unburned HC standpoint, the trends observed are very similar to the CO emissions. Higher peaks of around 14g/kWh are observed

at low load and low engine speed operation. Considering the equivalence ratio and the bulk gas temperature at this region, it is thought that the main precursor of HC emissions is the flame quenching due to the slowing down of the chemical reaction rates. Above the 40-50% engine load, the DMDF concept provides low values of unburned HC emissions, where bulk gas temperatures are over 1600K.

4.4.4 Compression ratio comparison

The present subsection is specifically dedicated to a comparison in terms of emissions and fuel consumption of both compression ratios used. In order to perform this comparison between CR15.3:1 and CR12.75:1, several interpolated maps have been performed. For every emission and parameter shown in this subsection, an interpolated map has been obtained by using the engine tested points used at the previous sections. Then, the different pictures used at the present subsection have been obtained subtracting the CR12.75:1 maps from CR15.3:1 maps and plotting the results.

In order to select the better option for the CR that best suits with the DMDF concept, the criteria followed by the author combines emissions and fuel consumption mainly. As it has been stated along this chapter, the target in NOx emissions was 0.4 g/kWh and ultra-low NOx emissions with the aim to meet the stringent EU VI standard limitation. Above this targets, this concept is aimed to preserve the benefits in terms of efficiency through the whole engine map operation. Hence, fuel consumption will be compared along this subsection also.

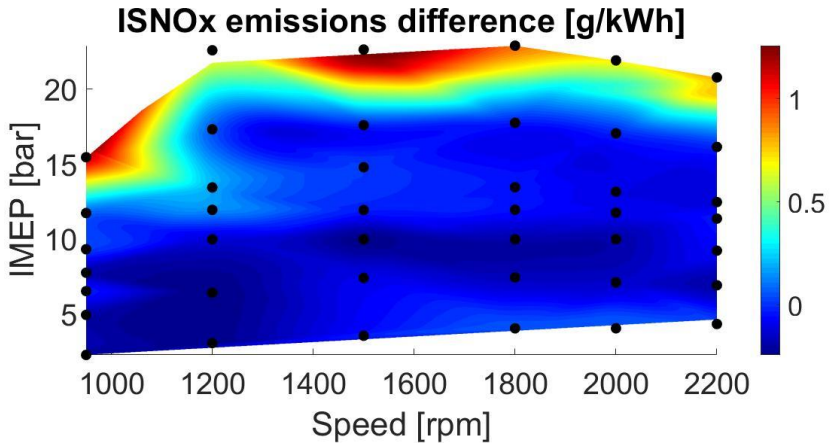

Figure 4.18. ISNOx emissions difference map.

Regarding the subtract between the interpolate maps obtained, the negative values mean that CR15.3:1 < CR12.75:1 and positive values mean the opposite. This criteria has been followed in every map presented in this subsection.

In this sense, Figure 4.18 shows the differences for both CR used in terms of NOx emissions. As it can be observed, the most part of the map there is not any major difference. NOx emissions remain below 0.4g/kWh, as it has been at the previous subsection, and both CR provide similar emissions. By contrast, at high engine load operation it is possible to observe up to 1.5 g/kWh of NOx emissions. These differences occur because the combustion strategy switches to Dual-Fuel diffusive combustion promoting levels of NOx above the EU VI limit. Hence, below 75% engine load NOx emissions are quite close between both CR configurations.

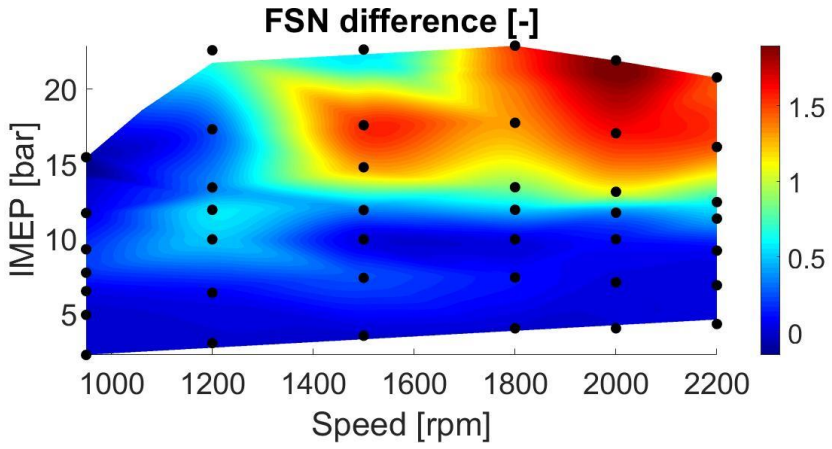

Figure 4.19. Smoke emissions difference map.

Figure 4.19 shows the differences obtained in terms of smoke emissions. Ultra-low smoke emissions are achieved by both concepts up to 50% of engine load approximately. At higher loads and high engine speed it appears a difference up to 1.5 FSN of smoke region. This results are provoked when the strategy switches to highly-premixed and Dual-Fuel diffusive strategies. The second mode of the DMDF contains a diffusive nature combustion which grade increases with the load. The same trend is observed with the NOx and the smoke emissions. The diffusive nature avoids breaking completely the trade-off between NOx and smoke emissions observed typically at CDC mode.

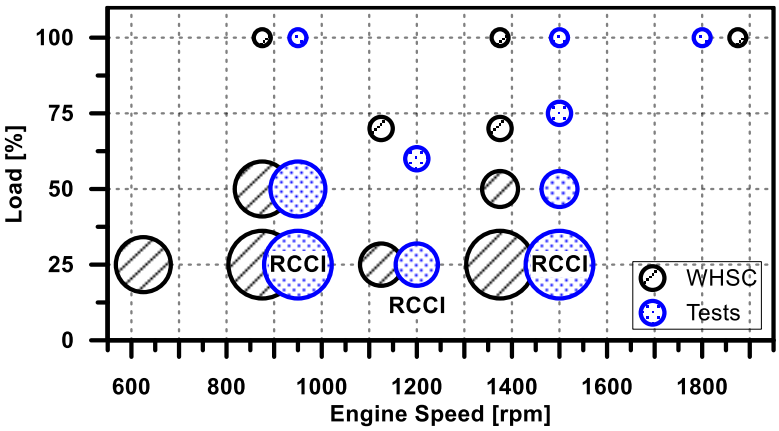

Figure 4.20. WSHC 13 modes points map for nominal and tested points[9].

In order to foresee the better option in terms of NOx and smoke emissions, it has been approached a 13 modes WSHC. Figure 4.20 shows the nominal points of the test in black and the blue colored points show the tested points, highlighting those that are operated in fully premixed Dual-Fuel strategy (RCCI mode). The size of the circles represent the specific weight respect the total cycle. The bigger, the more specific weight. As this approach may contain a leak of accuracy due to the differences observed at the points tested, the aim of this approach is to obtain a raw comparison between both CR tested against a standard cycle. The main results are summarized in Table 4.3, showing that both concepts meet hypothetically the EU VI limitation in terms of NOx emissions. From the smoke standpoint, it is not possible to verify the soot of the concept because the nature of the particles. Hence, the existing correlations to transform the FSN values to soot are not possible to be applied without carrying an error. However, the ultra-low smoke emissions achieved during the tests may suggest that the values of soot should be really low. By contrast, the transient operation has not been developed during these tests, but it will probably need a Diesel Particulate Filter (DPF) in order to mitigate the smoke emissions. Therefore, the smoke emissions are not a key point because the DPF would not disappear in any case. Indeed, the ultra-low smoke emissions would result in

a smaller DPF requirements improving the overall efficiency of the engine due to a reduction of the air management losses.

Table 4.3. Main results of the NOx emissions provided by the WSHC for both CR.

Emissions	EU VI Limits	WHSC [CR 15.3:1]	WHSC [CR 12.75:1]
NOx	0.4	0.223	0.138
Soot	0.01	0.016	$7.4x10^{-4}$

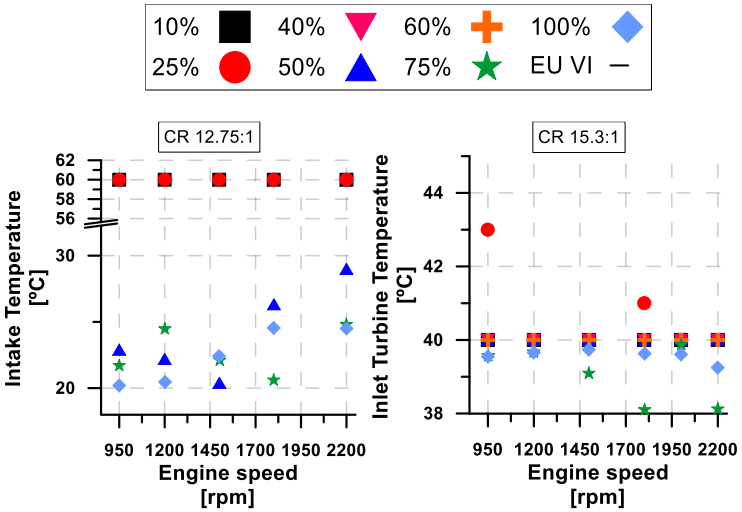

Figure 4.21. Intake air temperatures set during the tests.

Considering the CO and unburned HC emissions, Figure 4.22 and Figure 4.23 show the difference obtained between both CR. Figure 4.21 shows the intake air temperature set during the tests. Most remarkable results are that CR15.3 provides higher CO and HC at low load and low engine speed operation (up to 30g/kWh). This difference is huge and probably will be reflected at the combustion efficiency. These differences might be explained

with the intake air temperature. During the CR 12.75:1 case, the intake temperature was raised up to 60 Celsius degrees whereas when using the CR15.3:1, the temperature was only of 40 Celsius degrees. The reason of this change was to try to avoid big steps between the engine operating settings (and more realistic as well). Hence, the study performed with the CR 15.3:1 was softened compared with the CR12.75:1. But the rest of the map the differences are really low being in general higher for CR15.3. DMDF concept, as happens with the RCCI mode, promotes higher quantity of CO and unburned HC even operating at high engine load as it has been explained at the previous sections. Hence, exhaust temperature acquires a certain relevance at this point since the light-off of the diesel oxidation catalyst is around 300ºC.

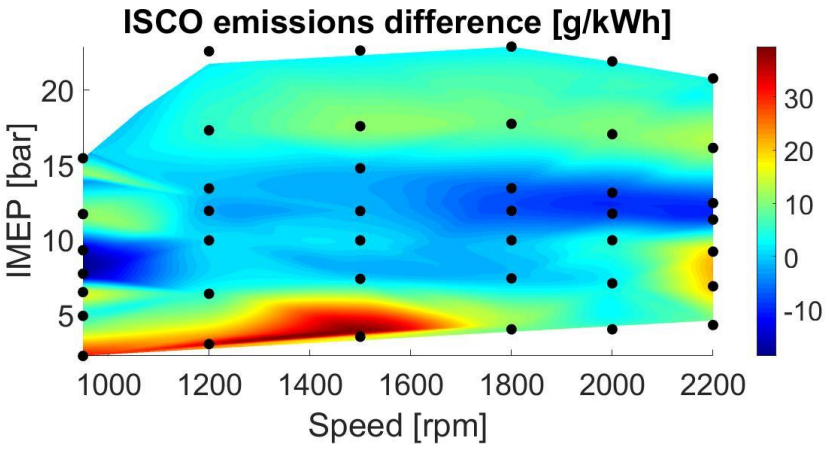

Figure 4.22. ISCO difference emissions map.

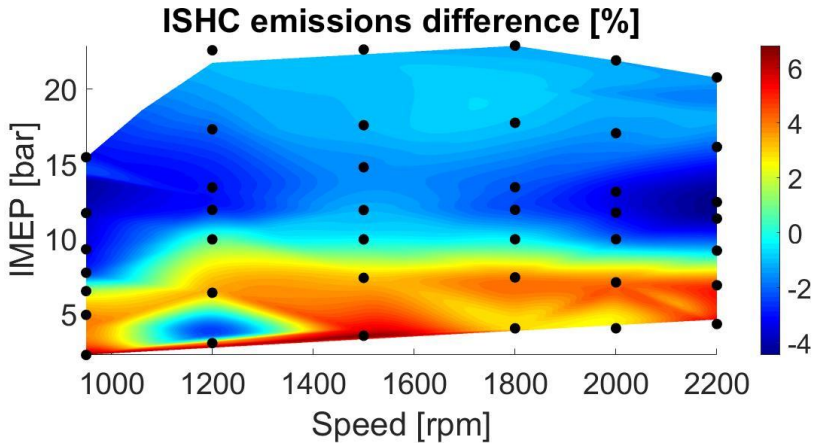

Figure 4.23. ISHC difference emissions map.

Figure 4.24 shows the differences observed at the exhaust temperature. Despite of the increase at the compression ratio from 12.75 to 15.3, the temperatures at low load remain in similar values for both cases. However, from 10 to 50% of engine load map portion presents some areas with lower temperature from the 15.3 case than the 12.75 case. Nevertheless, from 50% of the engine load the temperatures obtained with the 15.3 compression ratio step up considerably. In this sense, from 20% of engine load both cases present exhaust temperatures around 300ºC, which are enough to reach the typical DOC light-off temperature. Indeed, these temperatures have been achieved in a SCE and thereby, they are expected to be higher in a MCE. Thus, it can be considered that below the DOC light-off temperature it is only operated up to 20% engine load where both cases present similar temperatures. Thus, both cases would present similar efficiency at the DOC at low load. From 20 to 50% the CR12.75:1 case would be more efficient in some areas and from 50% to full load the CR15.5:1 case would be more efficient.

Concluding with the exhaust temperatures and CO and uHC emissions, both compression ratios studied would be equally interesting at this point.

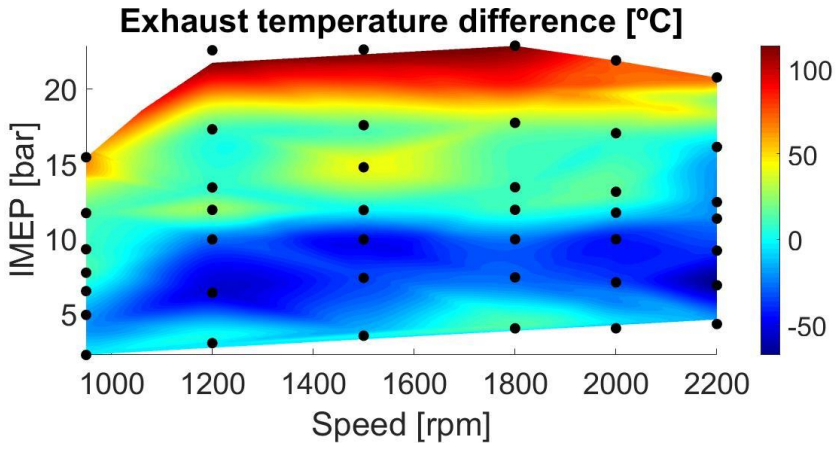

Figure 4.24. Exhaust temperature difference map.

Following with the comparison of both compression ratios used, the difference of ISFC is shown in Figure 4.27. Figure 4.25 shows the differences observed at the combustion efficiency and Figure 4.26 presents the differential values of the GIE.

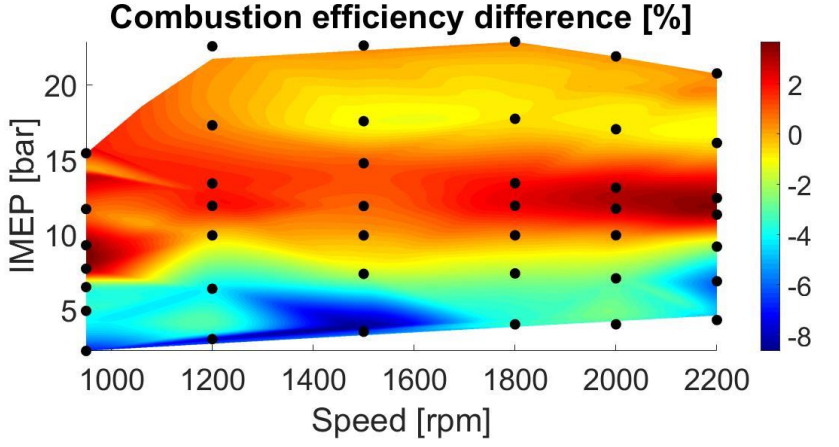

Figure 4.25. Combustion efficiency difference map.

As it has been observed in the previous Figure 4.22 and Figure 4.23, CO and unburned HC emissions where higher at low load for the CR 15.3:1

case. As it can be observed in Figure 4.25, the combustion efficiency is higher for the CR12.75:1 case than the CR15.3:1. Indeed, the portion of the map with negative values represents a 25% of the map shown. In this sense, the other 75% of the map is around 0% of difference between both CR tested and the med area of the map presents up to 2% of improvement for the CR15.3:1 case.

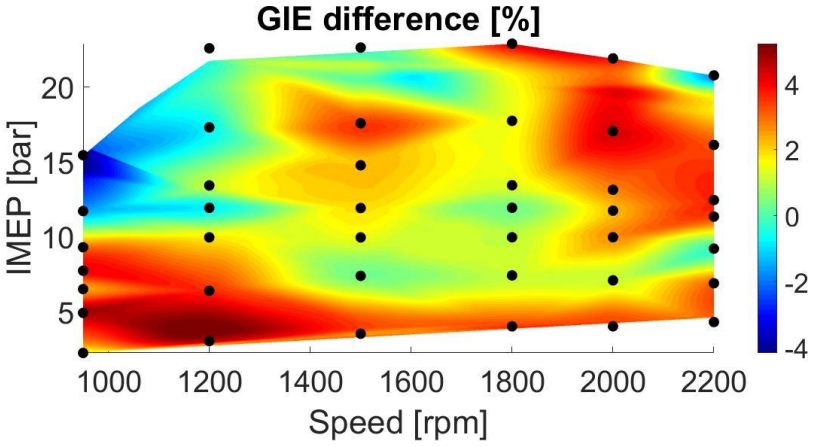

Figure 4.26. GIE difference map.

Despite the CO and uHC emissions and the combustion efficiency difference map, the differences observed at the GIE state that the DMDF concept by using a CR15.3:1 results in a better efficiency for most of the engine map operation. As it has been aforementioned, this improvement at the efficiency is caused due to a lower thermal losses provoked by a better combustion phasing. The GIE difference map shows a couple of points at 950 rpm with a lower GIE for the 15.3 case (up to 4% lower efficiency) and another point at 2200 rpm with a difference of around 1% poorer than with the CR12.75:1 hardware.

Considering the GIE, the last difference map provided shows the ISFC variations between both hardware. Figure 4.27 is presented below with the ISFC differences obtained.

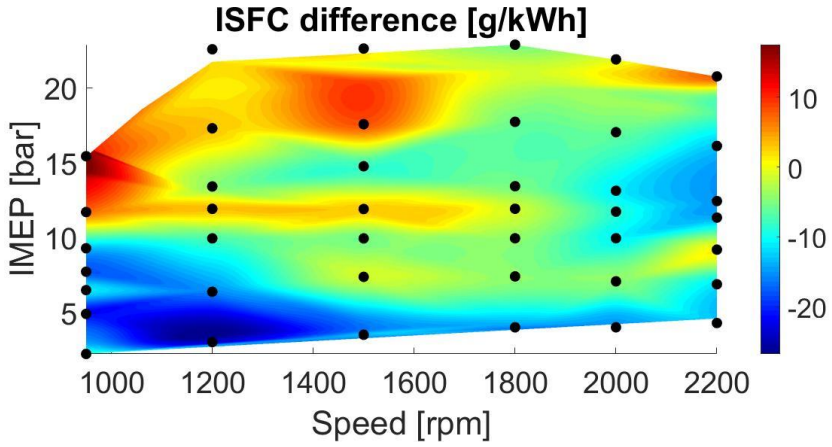

Figure 4.27. ISFC difference map.

From the figure is possible to state that most portion of the map presents negative values. Indeed, a big dark blue-colored zone is located at low load and low engine speed (up to 1500 rpm) which represent a drastic improvement (up to 20%) in fuel consumption compared with the 12.75:1 hardware. The same points that present lower GIE in Figure 4.26 show a high fuel consumption and it appears a small zone with an improvement of the fuel consumption of around 5% at 1500 rpm and high load operation.

Considering all the parameters exposed along the present subsection, in terms of NOx and smoke emissions as well as in terms of performance and fuel consumption, it is clear that the best hardware combination for the DMDF concept is the non-reentrant piston bowl geometry with a compression ratio of 15.3:1.

4.5 Bibliography

[1] Nazemi M, Shahbakhti M. “Modeling and analysis of fuel injection parameters for combustion and performance of an RCCI engine”. *Appl Energy* 2016;165:135–50.

[2] Splitter D., Hanson R., Kokjohn S., Wissink M. and Reitz R.D. “Injection Effects in Low Load RCCI Dual-Fuel Combustion". *SAE Technical Paper*, no 2011-24-0047, 2011.

[3] Yu S, Zheng M. Ethanol–diesel premixed charge compression ignition to achieve clean combustion under high loads. Proc Inst Mech Eng, Part D: *J Autom Eng* 2015.

[4] Payri F, Olmeda P, Martín J, García A. A complete 0D thermodynamic predictive model for direct injection diesel engines. *Appl Energy* 2011;88(12):4632–41.

[5] Payri F. and Desantes J.M. *Motores de combustion interna alternativos.* Editorial Reverté, 2011.

[6] Giakoumis E.G. “Cylinder wall insulation effects on the first- and second-law balances of a turbocharged diesel engine operating under transient load conditions”. Energy Conversion and Management, Vol. 48 no 11, pp. 2925-2933, 2007.

[7] Shabir M.F., Authars S., Ganesan S., Karthik R. and Kumar Madhan S. “Low Heat Rejection Engines – Review”. SAE Technical Paper, no 2010-01-1510, 2010.

[8] Kokjohn S., Hanson R., Splitter D. and Reitz R.D. “Fuel reactivity controlled compression ignition (RCCI): a pathway to controlled high-effciency clean combustion”.International Journal of Engine Research, Vol. 12 nº 3, pp. 209-226, 2011.

[9] Monsalve-Serrano J. Dual-Fuel compression ignition: Towards clean, highly efficient combustion. 2016.

[10] Benajes J., García A., Monsalve-Serrano J., Balloul I., Pradel G. "An assessment of the dual-mode reactivity controlled compression ignition/conventional diesel combustion capabilities in a EURO VI medium-duty diesel engine fueled with an intermediate ethanol-gasoline blend and biodiesel". Energy Conversion and Management, Vol. 123, Pages 381-391, 2016.

[11] Benajes J., Molina S., García A., Belarte E., Vanvolsem M. An investigation on RCCI combustion in a heavy duty diesel engine using in-cylinder blending of diesel and gasoline fuels. Applied Thermal Engineering, Vol. 63, Pages 66-76, 2014.

[12] Yifeng Wang, Mingfa Yaoc, Tie Lia, Weijing Zhanga, Zunqing Zhengc. A parametric study for enabling reactivity controlled compression ignition (RCCI) operation in diesel engines at various engine loads. Applied Energy, Vol. 175, Pages 389–402, 2016.

Chapter 5

Particle size distribution assessment

Content

5.1 Introduction

Previous chapter showed the potential of the DMDF concept in terms of emissions and performance by using two different compression ratios. From the emission standpoint, NOx, smoke, CO and unburned HC emissions were considered. Smoke emissions were expressed in FSN units instead the traditional AVL conversion to specific soot.

Hence, this chapter is aimed to perform an analysis of the particle size distribution of a diesel-gasoline combustion concept. Indeed, the present chapter consists of two parts. The first part is focused on the particles emitted by the RCCI concept in order to improve the understanding on the particle emission in a known combustion concept. The second part of the study is dedicated to the DMDF concept.

5.2 Experimental procedure and methodology

This section presents the methodology followed to perform the particle size distribution (PSD) and particle number (PN) analysis carried out for the RCCI and DMDF concepts.

In Figure 3.2 is presented a scheme of the test bench and the PSD equipment location. All the elements used for the PM data acquisition such as the thermodiluter, the scanning mobility diameter and the condensation particle counter, are presented in Figure 5.1.

As depicted in Figure 3.2, the PSD measurement equipment was placed downstream the backpressure valve, which is located after the settling exhaust chamber. The equipment used to measure the particulate matter consist of a diluter, a scanning mobility particle sizer (SMPS) and a condensation particle counter (CPC). The diluter is a thermodiluter TSI

Rotating Disk. The equipment dilutes the sample using the rotating disk method [1].

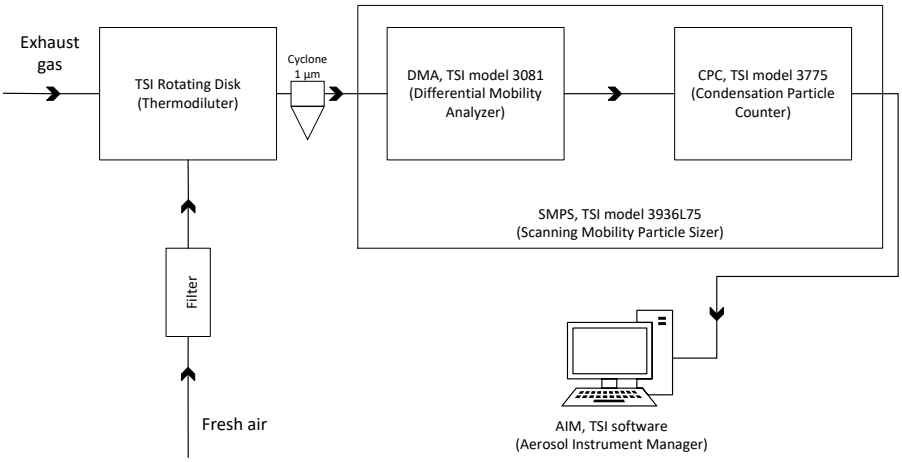

Figure 5.1. Scheme of the PSD analyzer equipment.

Each unit is supplied with two disks which are prepared with different number of cavities per disk. Then, a raw portion of the exhaust flow is captured by the cavities and is conducted through the mixer with particle-free air. This method provides high precision and great stability. In order to avoid measuring the condensates from the volatile elements, the air must be heated avoiding thereby nanodroplets formation, which are detected as particles too. Dilution of the exhaust gases is required to adapt the particulate inlet concentration for the SMPS. In the present study, the dilution ratio selected was 90:1, and in order to avoid volatiles condensation, the diluted sample was heated up to 150 °C [2][3].

The SMPS (TSI model 3936L75) system is formed mainly by the Differential Mobility Analyzer (DMA, TSI model 3081) and the Condensation Particle Counter (CPC, TSI model 3775). DMA equipment method is based on the physical principle that the ability of a particle to cross an electric field is directly related to particle size. Once the particle sample is sized by the DMA, it is measured using a condensation particle counter (CPC, TSI model

3775). The system operating range only counts particles between 5 to 250 nm. The Aerosol Instrument Manager (AIM, TSI) software acquires high-resolution data and process the particulate size distribution (PSD) data.

5.3 Particle size distribution analysis

The PSD analysis has been performed for RCCI and the DMDF concepts operated under a CR15.3:1.

5.3.1 Results under RCCI mode. Comparison with the CDC mode.

This section is dedicated to the study of the PSD promoted by the RCCI and CDC concept. Thus, the emissions from both concepts have been compared. In order to perform this study, the engine has been run at 25% engine load where the combustion strategy is RCCI, as it can be observed at the previous chapter. The main results in terms of emissions and performance have been already presented in chapter 4. Table 5.1 presents the engine operation point in terms of engine speed and engine IMEP as well as the main emissions promoted such as ISNOx, ISCO, unburned ISHC and smoke.

Table 5.1. Engine-out emissions and EGR rate for RCCI operation.

Speed	IMEP	EGR	ISNOx	ISCO	ISHC	Smoke
rpm	bar	%	g/kWh	g/kWh	g/kWh	FSN
950	4.9	20	0.069	54.4	9.8	0
1200	6.3		0.051	20.7	7.2	0.08
1500	7.3		0.157	9.7	7.3	0.12
1800	7.4		0.203	12.0	7.6	0.11
2000	7.1		0.203	16.9	8.2	0.03
2200	6.8		0.114	35.7	9.2	0.02

The strategy followed to perform the CDC operating points was based on replicating the stock combustion settings. It is worthy to note that these points were performed under CR of 15.3:1 while the stock CR is 17.5:1. Small differences were observed at the intake air conditions due to the low pressure (LP) EGR loop respect to the high pressure EGR loop. Table 5.2 presents the engine operation point in terms of engine speed and engine IMEP as well as the main emissions promoted such as ISNOx, ISCO, unburned ISHC and smoke.

Table 5.2. Engine-out emissions and EGR rate for CDC mode.

Speed	IMEP	EGR	ISNOx	ISCO	ISHC	Smoke
rpm	bar	%	g/kWh	g/kWh	g/kWh	FSN
950	4.5	20.0	3.5	0.8	0.3	0.07
1200	6.3	18.2	3.8	0.6	0.2	0.1
1500	6.9	24.1	3.0	0.4	0.2	0.1
1800	7.0	23.8	3.1	0.6	0.2	0.14
2000	7.0	25.2	2.6	0.7	0.2	0.17
2200	7.1	13.3	3.4	0.7	0.2	0.2

Table 5.1 and Table 5.2 have been provided in order to facilitate the comparison between the results obtained from both combustion strategies. Thus, the trends observed at the PSD analysis have a reference in terms of performance and emissions. More information regarding the operation points can be observed in [4].

The main injection settings, mixing time, combustion duration and the intake pressure are depicted in Figure 5.2. This picture provides additional information regarding the engine operation conditions in order to increase the understanding of the particle emissions.

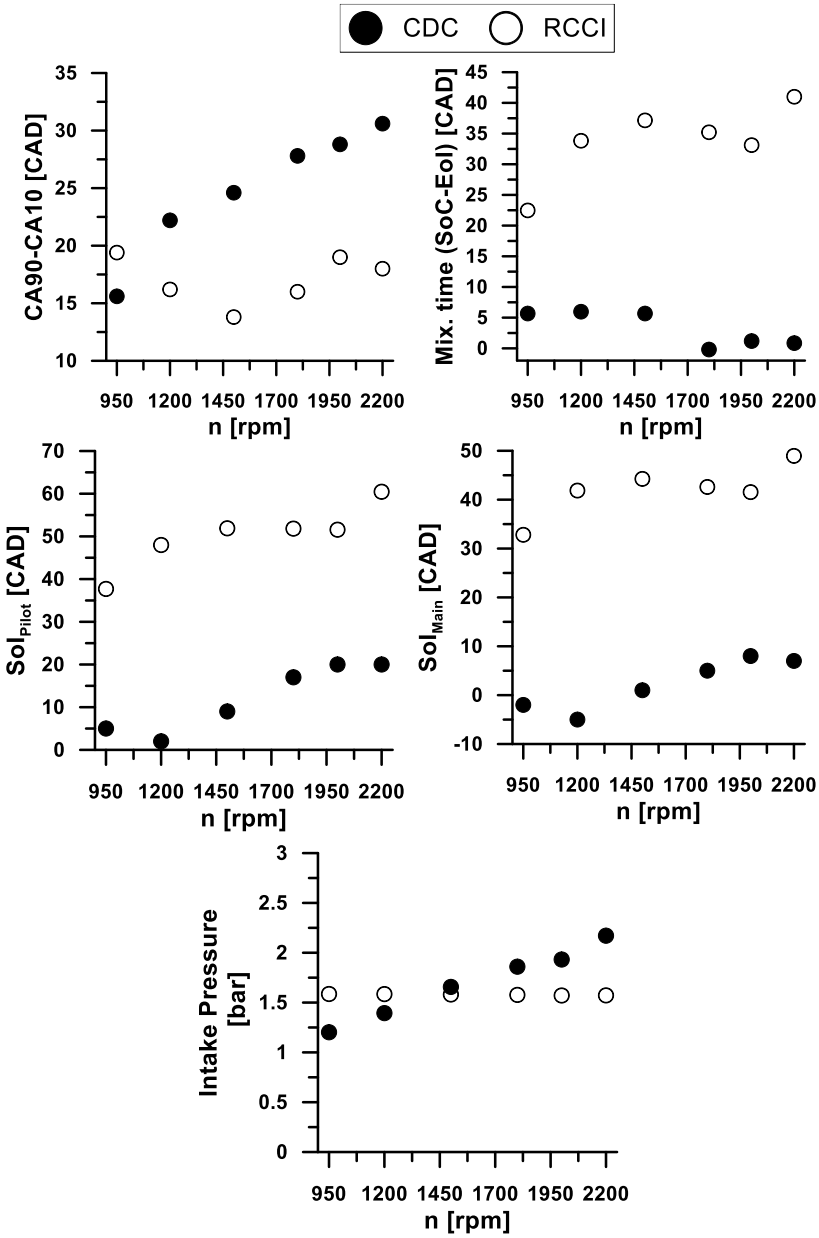

Figure 5.2. Combustion duration (CA90-CA10), mixing time, injection timings and intake pressure for the tested points.

The PSD measurements are depicted in Figure 5.4, Figure 5.5 and Figure 5.6. Figure 5.3 shows the total number of particles emitted by the combustion strategy of a size between 5-250 nm. As it is seen, the particles number increases with the engine speed for both combustion modes, which was also observed in the smoke emissions trend up to 1800 rpm (Table 5.1 and Table 5.2). As it can be observed at the Figure 5.3, both concepts present similar number of particles. This result differs from previous works [5][6][7], in which it has been seen that CDC operation mode produces higher number of particles than RCCI. The different behavior found in the current investigation can be explained considering the stock calibration and hardware of the diesel engines used for comparison. In this sense, the majority of engines used in literature are calibrated to accomplish the EU IV type approval, while in the case of the present research the engine used is a currently under production EU VI heavy-duty engine. Thus, the stock diesel calibration relies on producing high levels of NOx, reduced later by means of a twin parallel SCR system, and low levels of smoke.

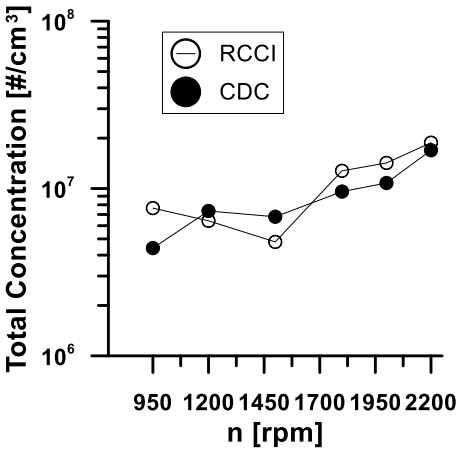

Figure 5.3. Total number of particles for RCCI and CDC modes.

Figure 5.4, Figure 5.5 and Figure 5.6 present the PSD at each engine speed for both operating modes. Tests have been performed at the same engine load (25%), while the engine speed has been divided in six steps from

950 to 2200 rpm. Thus, six graphs compare the PSD of the RCCI mode versus the CDC mode. At first sight, RCCI curves at 950 and 2000 rpm seem to be noisy for larger particles, probably due to the low particle concentrations in the diluted exhaust. Something similar occurs at the CDC curve operated at 1500 rpm, where some noise affects the smoothness of the depicted curve.

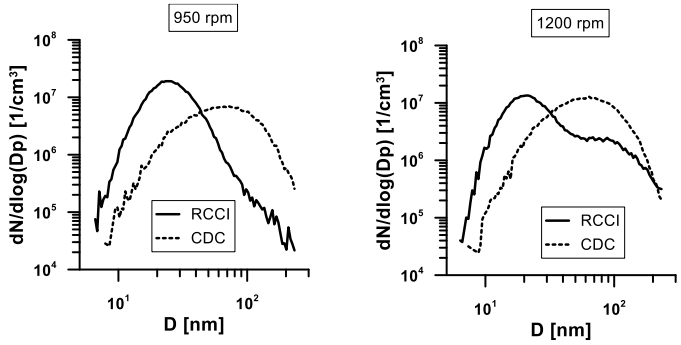

Figure 5.4. PSD at 950 rpm and 1200 rpm.

Figure 5.4 shows the PSD obtained at the lowest engine speed tested, 950 rpm and 1200 rpm. CDC shows lower particle concentrations at low mobility diameters (<30 nm), being the difference higher at 950 rpm. On the other hand, CDC shows higher particle concentrations at high mobility diameter (>30 nm). In any case, the differences in particles number are lower, suggesting that the total number of particles would be at the same order of magnitude. At 1200 rpm, the PSD curve presents a bimodal shape. There is one main peak at 20 nm of diameter and a second peak at 80 nm. This second peak presents lower number of particles that the particles measured at CDC mode. Moreover, CDC case presents a peak at 60 nm of mobility diameter, lower than for RCCI mode.

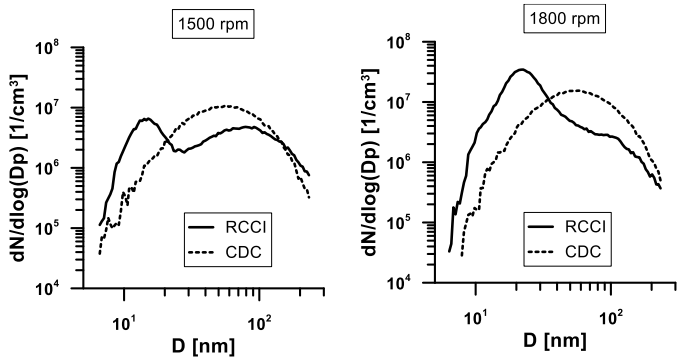

Figure 5.5. PSD at 1500rpm and 1800rpm.

Figure 5.5 presents PSD curves for 1500 and 1800 rpm. The trend followed is very similar to the shapes presented in Figure 5.3. Main differences are found at RCCI mode, with a bimodal shaped curve at 1500 rpm. Operating under RCCI, the first peak observed at the PSD curve stands at 18 nm, while the second peak is located at 90 nm of mobility diameter. These two peaks observed at the curve could be explained by the coagulation phenomenon. Particle coagulation is defined as a combination of growth by coalescence and agglomeration [8]. The ultra-low sized particles of soot added and the hydrocarbons particles might form the first peak, while the second peak might be formed by larger carbonaceous particles. In this sense, when high levels of small particles appear, new larger particles are formed by this phenomenon, increasing the number of large particles at the PSD curve. These particles usually come from volatile organics particles adhered to a carbonaceous nucleus, existing the possibility of being detected by the smokemeter (Table 5.1). Hence, the higher value of FSN respect the other points. In addition, this phenomenon might be replicated at 1200 rpm and 1800 rpm with lower magnitude of the second peak due to the smoke measurements presented in Table 5.1 and the PSD curves showed in Figure 5.4 and Figure 5.5.

PSD curves for CDC operation shows the same curve than that observed at 1200 rpm. In this sense, the total number of particles seems to be very similar, with a peak located at the same mobility diameter of 60 nm.

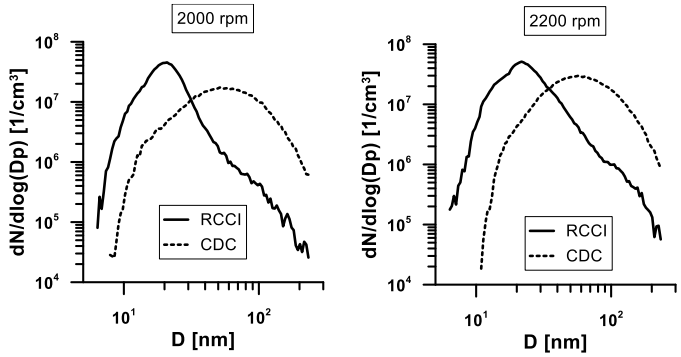

Figure 5.6. PSD at 2000 rpm and 2200 rpm.

Figure 5.6 presents the PSD curves for 2000 and 2200 rpm. Both RCCI PSD curves show big differences with the previous RCCI PSD curves observed at Figure 5.5, and also differ from those of CDC. The most relevant difference is that the second peak has disappeared. In this sense, only one peak is observed in both curves at 20 nm of mobility diameter in both engine speeds presented in the figure. Therefore, it is worthy to note that the phenomenon of coagulation observed at 1500 and 1800 rpm cases in not observed at these high engine speeds. Thus, low sized particles dominate the PSD at high engine speeds under RCCI.

PSD curves for CDC operation shows again the same trend that it has been observed at the other engine speeds. Thus, the total number of particles for the PSD peak seems to be slightly increased and the diameter where the PSD peak appears is kept constant around 60 nm.

From the nature of the particles standpoint, PSD analysis provides information about the mobility diameter of the particles and the number of particles corresponding with each diameter measured. Additionally, a nucleation or accumulation mode classification has been performed in order to identify the nature of the particles and the portion of representation for each mode type respect the total number of particles.

Figure 5.7 presents the particle classification in nucleation or accumulation mode, the total number of particles and the smoke emissions in FSN. Smoke emissions have been added to the graph in order to improve the understanding of the classification and observe the correlation existing between the smoke emissions and the accumulation mode particles emissions CDC PSD curves presented in Figure 5.4, Figure 5.5 and Figure 5.6, show the PSD peaks at a mobility diameter around 60 nm. Therefore, large sized particle domination of the PSD indicates that the majority of the particles have a carbonaceous origin. Consequently, the cutoff diameter used to limit as the nucleation mode as the accumulation mode has been 30 nm. This cutoff diameter ensures that the nature of the particles is kept in the correct particle counter. Thus, CDC classification is presented on the right graph. It is observed that the particle emission measured is dominated by large sized particles, which are provided by the soot produced during the combustion. Smoke emissions are also depicted in the figure and is directly related with the accumulation mode particles. As the smoke emissions increase with the engine speed, the number of accumulation particle increases as well, whereas the number of nucleation mode particles remains almost constant along the engine speeds tested.

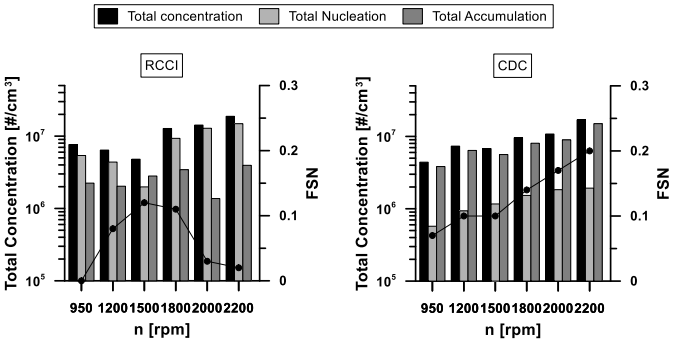

Figure 5.7. Particles mode classification for both combustion modes.

RCCI graph shows the classification of the total number of particles and the corresponding nucleation mode and accumulation mode particles. Considering the explanation given at the previous paragraph, the cutoff

diameter selected has been 30 nm. As it is depicted in Figure 5.7, the smoke emissions measurement and the total number of particles do not follow the same trend. Indeed, the smoke measurement presents the maximum value at 1500 rpm, and the total number of particles presents a minimum point. Therefore, it is possible to assume that RCCI is dominated by lower sized particles for all engine speeds. Nucleation mode particles are usually formed by volatile organic and sulfur compounds that are produced during the exhaust dilution. So that, smoke measurement is not able to detect this small particles where they are captured in the paper sample.

Comparing the total number of particles emitted by both modes, except at high engine speed that offers similar results, the number of particles is higher for RCCI than for CDC mode.

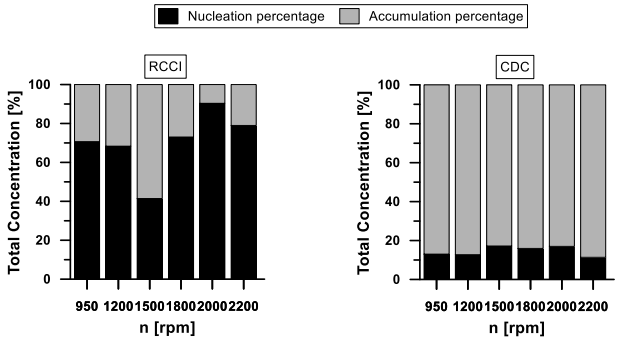

Figure 5.8. Concentration of nucleation and accumulation mode particles from the total number of particles.

Figure 5.8 shows the percentage of nucleation and accumulation mode particles respect to the total concentration of particles obtained. Big differences are found between the RCCI mode and the CDC mode, confirming that RCCI is dominated by the nucleation mode particles and CDC is dominated by accumulation mode particles.

Both combustion modes present a trend between the smokemeter results and the accumulation percentage depicted in the Figure 5.7 and Figure 5.8. As the smoke measurements increase, the percentage of

accumulation mode particles also increases. This trend might be explained by the diameter of the particles. At CDC mode, it is well-known the different correlations to convert the smoke measurements in soot mass as well as the nature and morphology of the particle. However, the nature of the particles and the correlations for RCCI are not accurately defined even more these big particles come from a coagulation phenomenon process.

5.3.2 Results under Dual-Mode Dual-Fuel (DMDF) concept

Following with the PSD and PN analysis, previous subsection has focused on the particles promoted by the RCCI concept. In order to enhance the comprehension of the DMDF concept, a dedicated study of the particles has been carried out. The methodology followed has been the same as the previous study. By contrast, the engine has been run from low to full engine load under DMDF operation (chapter 4). Apart from the emissions analysis, the present chapter also presents the main results in terms of emissions (Table 5.3 and Table 5.4). Table 5.3 and Table 5.4 also show the engine operation point in terms of engine speed, EGR rate and IMEP.

Table 5.3. Engine-out emissions and EGR rate for DMDF mode.

Speed	IMEP	EGR	ISNOx	ISCO	ISHC	Smoke
rpm	bar	%	g/kWh	g/kWh	g/kWh	FSN
1200	3.1	20.8	0.073	91.9	11.9	0
	6.3	19.7	0.051	20.7	7.2	0.08
	11.9	50.2	0.316	2.91	2.1	0.6
	17.3	45.8	0.351	8.15	2.0	0.37
	22.6	31.0	1.04	2.1	0.25	0.96

As it has been aforementioned, the strategy followed to perform the CDC operating points was based on replicating the stock combustion settings.

Main differences were observed at the intake air conditions due to the low pressure (LP) EGR loop respect from the high pressure EGR loop, not representing an issue as the results depicted shown. More information regarding the operation points can be observed in [9].

Table 5.4. Engine-out emissions and EGR rate for CDC mode.

Speed	IMEP	EGR	ISNOx	ISCO	ISHC	Smoke
rpm	bar	%	g/kWh	g/kWh	g/kWh	FSN
1200	3.1	29.6	2.86	1.8	0.53	0.04
	6.3	19.9	2.87	0.63	0.19	0.1
	11.8	4.5	5.94	0.19	0.19	0.07
	17.4	0	6.86	0.04	0.04	0.05
	22.8	0	8.62	0.23	0.03	0.1

Table 5.3 and Table 5.4 show the levels of EGR of both concepts. As it is observed, the difference of the EGR rate between both concepts is quite big, achieving up to a 50% of EGR rate for the DMDF concept. These differences are due to the combustion strategy. DMDF concept uses premixing dual-fuel strategies when the engine is running from low to medium-high engine load. This kind of strategies allow to use such a massive EGR rates without penalizing the smoke emissions in order to promote ultra-low NOx emissions. As it can be observed in Table 5.3, the EGR rate reduces as the load increases due to the switching from highly premixed to Dual-Fuel diffusion strategy. As the premixing component of the fuel is reduced, the EGR rate needs to reduce in order to avoid high levels of smoke emissions.

In order to provide additional information regarding the engine operating conditions, Figure 5.9 shows the injection settings, combustion duration, mixing time and the intake pressure used for both combustion concepts.

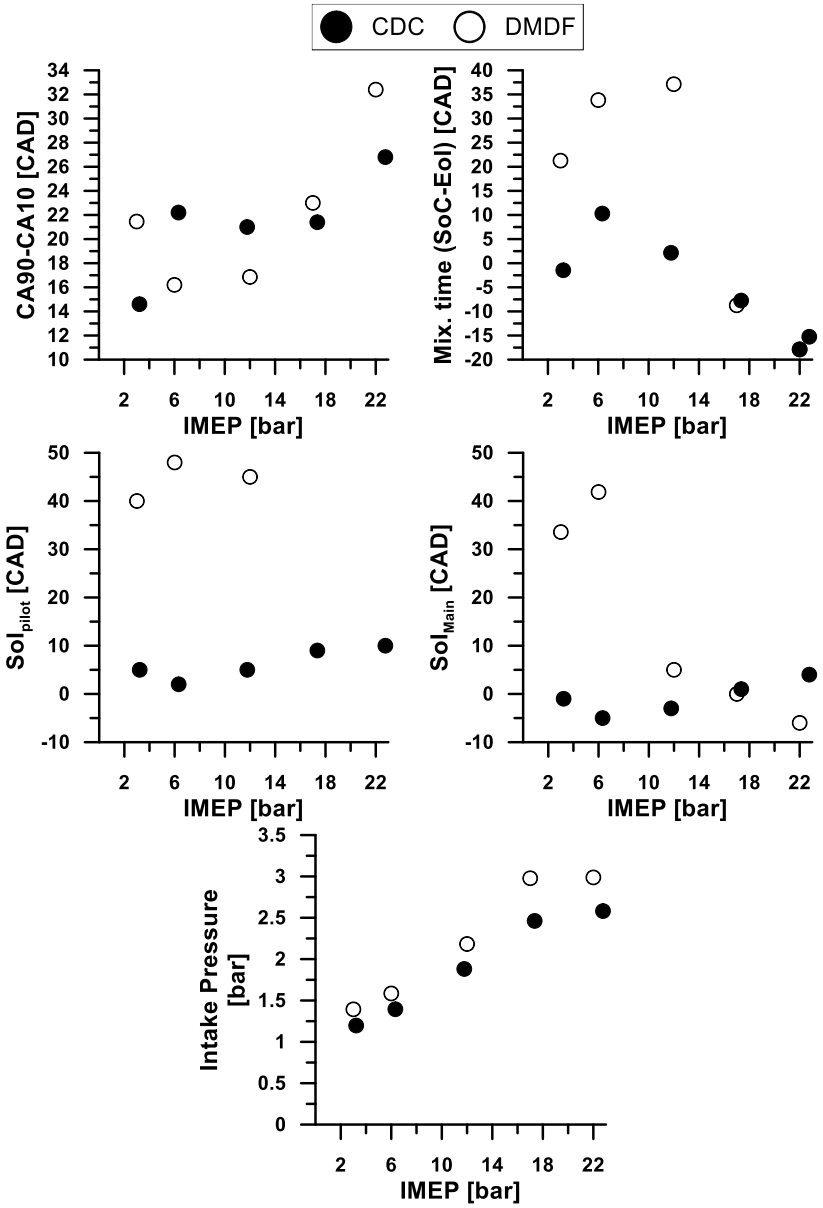

Figure 5.9. Combustion duration (CA90-CA10), mixing time, injection timings and intake pressure for the tested points.

The PSD measurements are depicted in Figure 5.12 and Figure 5.14. Figure 5.11 shows the total number of particles emitted by the combustion strategy of a size between 5-250 nm.

At low loads, smoke emissions for DMDF fully premixed are very similar than the smoke measured for CDC mode due to the OEM ECU calibration. These values are due to the higher mixing time observed at 3 and 6 bar IMEP for the fully premixed strategy (Table 5.3).

Regarding CDC case, smoke emissions for CDC are very low in this load range due to the ECU manufacturer's calibration (which is based in NOx emissions promotion instead of smoke). These reduced levels (around 0.12 FSN) are obtained due to the high bulk gas temperature which allows to burn all the soot formed during the combustion process, as it can be observed in Figure 5.10. By contrast, the NOx emissions are much bigger for CDC than for DMDF.

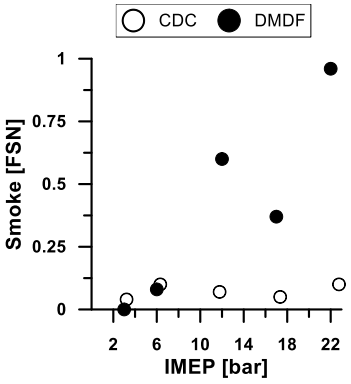

Figure 5.10. Smoke emissions for both combustion strategies.

At medium engine load (12 bar IMEP), big difference in smoke emissions between DMDF highly premixed and CDC operation mode are observed in Figure 5.10. CDC presents a better mixing time in Fig. 6 than DMDF, which reduces the local rich equivalence ratios. In addition, the EGR rates used are very low (Table 5.3 and Table 5.4), allowing the oxidation of the soot formed during the combustion process. DMDF highly premixed

strategy shows higher levels of smoke than CDC. Despite of having high values of mixing time (40 CAD) [9], the massive use of EGR rates (up to 50%) used should provoke a richer fuel equivalence ratio due to the lower oxygen available at the combustion chamber, producing soot formation.

At high engine load (from 17 to 22 bar IMEP), smoke emissions for CDC remain lower than for DMDF mainly diffusive operation mode. Low EGR rates allow a better oxidation of the soot formed during the combustion process, resulting in lower values of FSN that the ones observed at low load.

DMDF mainly diffusive produces more smoke than the CDC cases. This behavior is explained due to the combustion nature of the DMDF strategy. Mixing time observed in [9] is very similar than the mixing time observed for the CDC cases. The reason might be related with the diffusive nature of the DMDF strategy at high engine load. In addition, CDC cases recirculating exhaust gases (0% EGR rate), DMDF mainly diffusive uses EGR rates up to 40% as it is depicted in Table 5.3. Hence, a combination of negative mixing time and high EGR rates produces richer equivalence ratios, what enables soot formation. As a result, FSN measurements are much higher than for CDC.

FSN indicates, as it consists of a sample exhaust filter, the formation of black carbon. But the total amount of particles, including those which are formed by volatile organic species, are not represented with the FSN measurements. Therefore, lower FSN may not indicate lower total amount of particulates [10].

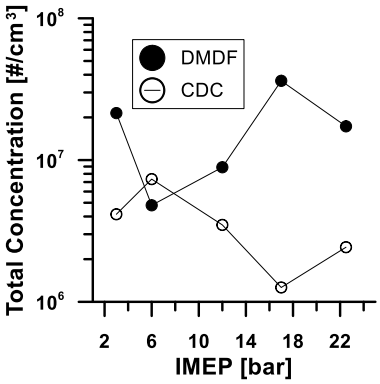

Figure 5.11. Total number of particles for both combustion modes.

From the particle size distribution (PSD) standpoint, Figure 5.11 shows the total number of particles obtained for each combustion mode. At first sight, it is clearly shown that the quantity of particles studied at this range is higher for the Dual-Mode concept than for CDC mode.

With the aim of improving the understanding of the total particle concentration observed in the previous figure, the particle size distribution for both modes have been depicted in Figure 5.12 and Figure 5.14.

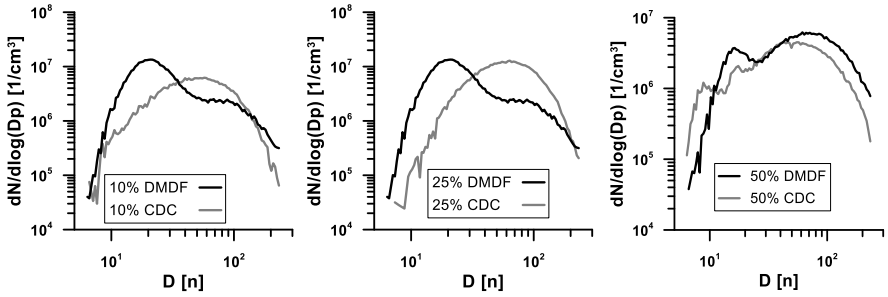

Figure 5.12. Particle size distribution for both concepts up to 50% engine load.

Figure 5.12 contains the particle size distribution (PSD) for 10%, 25% and 50% engine load operated under both combustion modes. The curves depicted show the quantity of particles measured respect to the scanning

mobility diameter of the particles. The PSD observed at low load under CDC operation mode reflects that the particles distribution is governed by the larger sized diameter particles. Under CDC operation, PSD curves present a peak of number of particles at 50 nm of mobility diameter. In this sense, large sized particles dominate the CDC operation distribution. Large sized particles usually refers to carbonaceous particles [11].

Regarding DMDF fully premixed operation, the PSD curve presents a dominant peak at 20 nm and a secondary peak at 80 nm of mobility diameter. Thus, low sized particles dominate DMDF fully premixed. However, the second peak observed at the DMDF fully premixed PSD curves is probably provoked by the coagulation phenomenon [8]. In this sense, when high number of small particles are formed, some part of the particles can coagulate giving as a result higher diameter particles and, thereby these particles might be not carbonaceous but organic volatile [11]. Hence, these particles would not be detected by the smokemeter providing low measurement FSN values.

DMDF highly-premixed is also presented in Figure 5.12 compared with the CDC curve. It presents a similar trend that the CDC curve observed at 10% and 25% engine load. PSD is also dominated by high sized particles around 50 nm of mobility diameter. DMDF highly-premixed PSD curve presents a bimodal shape. This curve has two peaks with the same order of magnitude. The first peak is observed below 20 nm of diameter and the second peak is located at the diameter of 70 nm. As the high sized particles observed are carbonaceous, the FSN measurement presents also a peak of 0.6, as it is observed in Figure 5.10. Despite of the mixing time for 12 bar IMEP in Table 5.3, the massive use of EGR and the second diesel injection moved closer to the TDC results in the late end combustion similar to the last part of the diffusion combustion. This phenomenon is clearly observed at the RoHR presented in Figure 5.13 for the highly-premixed curve (corresponding to the 12 bar of IMEP). This combination provides soot formation and, thereby high sized particles production.

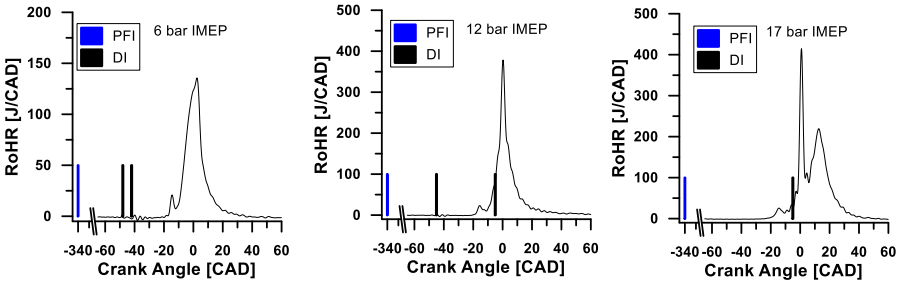

Figure 5.13. Rate of heat release and injection pattern for the DMDF concept.

Figure 5.14 presents the particles size distribution of the DMDF mainly diffusive mode and the CDC operation mode at 75% and 100% engine load. Both operation modes are dominated by the high sized particles.

Comparing both curves, DMDF mainly diffusive mode presents a curve peak at 80 nm for 75% engine load and at 100 nm at full load. CDC PSD curves present a peak at 70 nm at 75% engine load and at 50 nm at full load. For both modes, the size distribution is characterized by such a large particles, which suggests carbon particles. In Figure 5.15, smoke emissions are depicted and the values obtained are clearly correlated with the particle distribution.

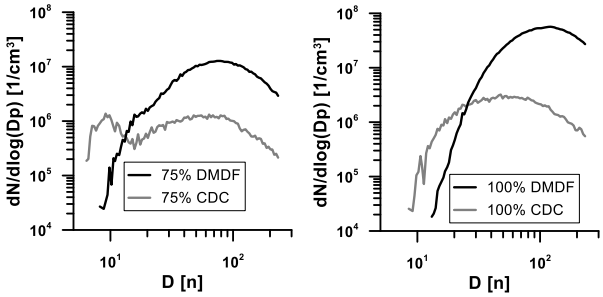

Figure 5.14. Particle size distribution for both concepts for 75% and 100% engine load.

Additionally to the PSD study, a classification between nucleation mode and accumulation mode has been carried out in order to try to differentiate the nature of the particles. Therefore, Fig. 13 presents the total number of particles measured and the classification of nucleation or accumulation mode. Additionally, the soot emissions in terms of FSN have been also added to the graph in order to complete the information scope of the particle emissions.

The criteria followed to classify particles in terms of nucleation mode or accumulation mode is the mobility diameter of the particle. Some authors define the nucleation mode size limit as 30 nm [11] due to the nature of the particle, which is mainly composed by volatile organic material. The other mode is accumulation, which contains particles between 40 nm to 1 µm in diameter, is mainly formed by soot with hydrocarbons adhered to the surface [11][12].

Figure 5.15 presents the classification of the particles in terms of nucleation or accumulation mode performed for both operation modes as well as the smoke emissions in FSN.

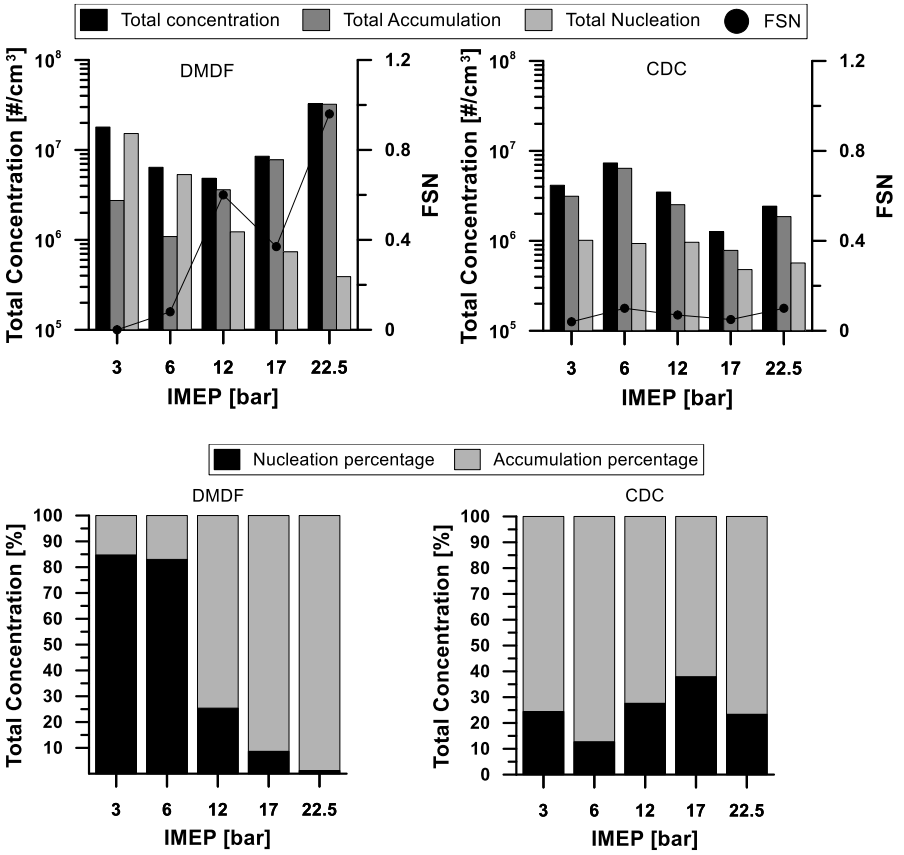

Figure 5.15. Classification of the nature of the particles and smoke emissions for both strategies.

As it is shown in Figure 5.12 and Figure 5.14, CDC PSD curves present the peaks of number of particles at the mobility diameter higher than 50 nm for all the engine load cases studied. As it can be observed in Figure 5.15, the FSN measured is directly related with the total amount of particles measured. The particle cutoff diameter used to limit both fields must be lower than 50 nm in order to distinguish properly the larger particles mainly formed by soot from the smaller particles mainly formed by volatiles. Therefore, the cutoff diameter selected for the CDC operation mode is 30 nm. In this sense, the number of particles counted of nucleation particles is much lower than the number of accumulation mode particles. In addition, FSN measurements are

corresponded with the trend observed by the accumulation mode particles presented in the figure. If FSN increases, the number of accumulation mode particles and, thereby the total number of particle, increases. However, nucleation mode particles remain constant for all the engine load cases.

Regarding the DMDF operation strategy, the particularly for each combustion mode defined in the previous chapter. Hence, two modes were defined as DMDF fully/highly premixed and Dual-Fuel diffusive strategies. From the PSD analysis, curve peaks have been identified at different mobility diameters. So that, the author considered that the cutoff diameter must be studied for each particular case in order to be as much accurate as possible. Following description tries to explain the criteria followed for the classification.

From this particular analysis, it can be concluded that the particles are mainly formed by volatiles. In addition, due to the high quantity of small particles, the coagulation phenomenon might occur producing a secondary peak at the PSD curve. Therefore, the cutoff diameter for this mode of combustion is 50 nm. In this sense, particles smaller than 50 nm are counted as nucleation mode particles and particles larger than 50 nm are counted as accumulation mode particles. As it is observed in Figure 5.15, the FSN values are very low (around 0 at 3 bar IMEP) and the accumulation mode particles also represent a small fraction of the total number of particles. Thus, nucleation mode particles represent most part of the total number concentration of particles. Comparing the total number of particles to CDC, DMDF fully premixed emitted higher number of particles.

DMDF highly premixed mode PSD analysis highlights that the double curve peak obtained presents a bigger quantity of large sized particles than the previous fully premixed and CDC mode. Thus, the cutoff diameter, since the peaks are observed at 20 nm and at 70 nm, has been fixed at 30 nm. Thus, nucleation mode particles are those which diameter is lower than 30 nm and accumulation mode particles are those which diameter is higher than 30 nm. At 12 bar IMEP (50% load) at Figure 5.15, the highly premixed point

shows higher number of accumulation mode particles, which corresponds with a smoke emissions peak. In this sense, large sized particles dominate the particles emission at highly premixed. Despite of having more FSN values than fully premixed mode, the number of particles is lower. These results should be consequence of the particle nature behavior moving from nucleation mode particles to accumulation mode particles. Thus, the number of particles have decreased while the diameter have increased.

DMDF mainly diffusive mode PSD analysis is summarized for 75% and 100% engine loads in Figure 5.15. Comparing DMDF results with CDC mode, results suggest a similar behavior due to the diffusive nature of the combustion. Thus, both combustion strategies are dominated by large sized particles. The cutoff diameter is 30 nm, due to the peaks observed at the PSD curves. DMDF PSD curves present a peak at 70 nm at 75% engine load, and a peak of 90 nm at 100%. In addition, both strategies are suitable to use the same cutoff diameter because of the PSD peak at 70 nm observed for CDC.

Nucleation mode particles represent a small fraction from the total quantity of particles at CDC mode. However, the difference between accumulation mode and nucleation mode at DMDF mainly diffusive is considerably due to the order of magnitude observed, surely related with the smoke emissions measured. At CDC, the smoke emissions is below 0.2 FSN, whereas at DMDF mainly diffusive the smoke emissions are around 0.8–1 FSN. Hence, the differences observed in Figure 5.15 justify the number of particles from nucleation and accumulation mode and the relation with the smoke measurements.

5.4 Engine mapping of particles size distribution and particle number under DMDF operation mode

Finally, a PSD and PN engine mapping has been performed for the DMDF concept. Hence, in order to explore the particle number and the PSD

analysis over the whole engine map, a dedicated study has been carried out [13]. This section presents several maps showing the total particle number and the particles promoted of nucleation and accumulation mode.

The analysis of the complete spectra is necessary to gain understanding on the particulate characteristics for the different combustion regimes. For this purpose, Figure 5.16 shows the effect of the engine load on the particle size distribution (PSD) at different engine speeds, measured with the scanning mobility particle sizer (SMPS). Cases at 10% and 25% correspond to the fully premixed RCCI regime, 50% load case corresponds to the highly premixed RCCI strategy, and 75% and 100% measurements come from the Dual-Fuel diffusive strategy.

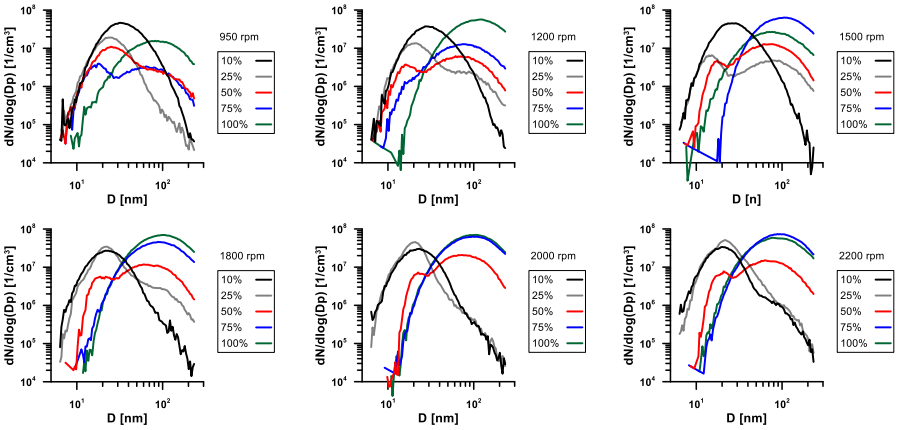

Figure 5.16. Particle size distribution for every engine speed at different engine speeds.

Comparing the different subfigures, it is seen that PSDs are mainly dominated by the combustion regime implemented (i.e., engine load), while the engine speed has little impact on them. As it has been observed at the previous sections, the fully premixed RCCI combustion is dominated by small particles (mobility diameter peak ≈30 nm), the dual-fuel diffusion mode is dominated by larger particles (mobility diameter peak ≈100 nm) and the

highly premixed RCCI regime shows a transitional PSDs, with two peaks of mobility diameter at around 20 and 80 nm. As found in the previous section, the increase of the particles diameter as load increases implies greater soot formation, which results in higher FSN values. This fact can be confirmed looking at Figure 5.10 and Figure 5.15, which shows the relationship between the smoke measurements in FSN units and the total quantity of bigger particulates. As it can be seen, the FSN measurements and the total quantity of bigger particulates follow the same trend, which means that effectively, these large particles are mainly formed by carbonaceous species (i.e., black carbon soot). In general, the fully premixed RCCI regime shows no bigger particles, while some amount of them can be identify in the highly premixed RCCI strategy. This is coherent with the findings reported by Storey et al. [10], which stated that RCCI particles appear to be composed of a solid carbon core, over which semi-volatile hydrocarbon species tend to condense.

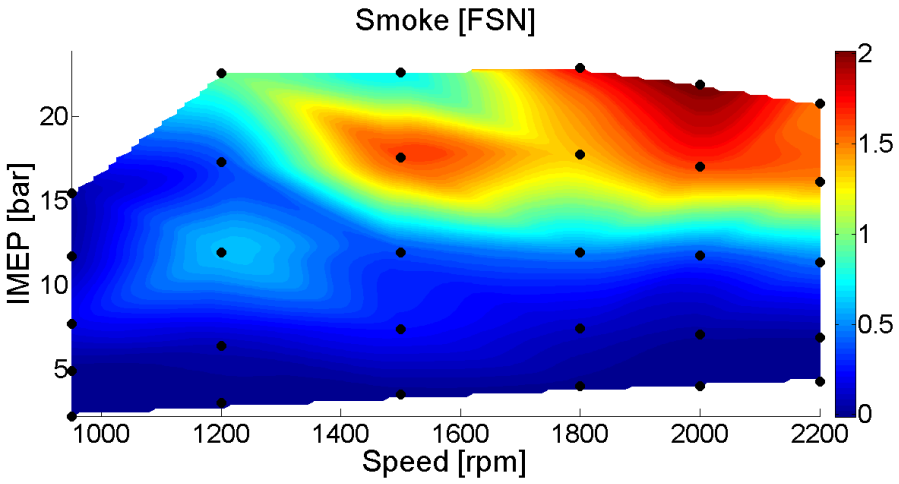

Figure 5.17. Smoke emissions for the DMDF concept.

Figure 5.17 shows the smoke emissions map and Figure 5.18 shows the total particle number map for the DMDF combustion strategy. Comparing qualitatively both figures, it is seen that the maps present greater similarities in the load region above 14 bar IMEP, where the diffusive dual-fuel strategy is applied. As it has been observed at the previous section, the higher FSN

values in this region suggest that particulates tend to be more diesel-like as load increases, i.e. mainly composed of elemental carbon. This thought is reinforced by the high coherence between the smoke meter and condensation particle counter (CPC) measurements. By contrast, less similarities between both maps are found in the region below 14 bar IMEP (fully and highly premixed RCCI strategies operate in this area). In this region, FSN cannot be related to the particulates measurement, since they are expect not to be of carbonaceous nature as it has been demonstrated previously along the present chapter.

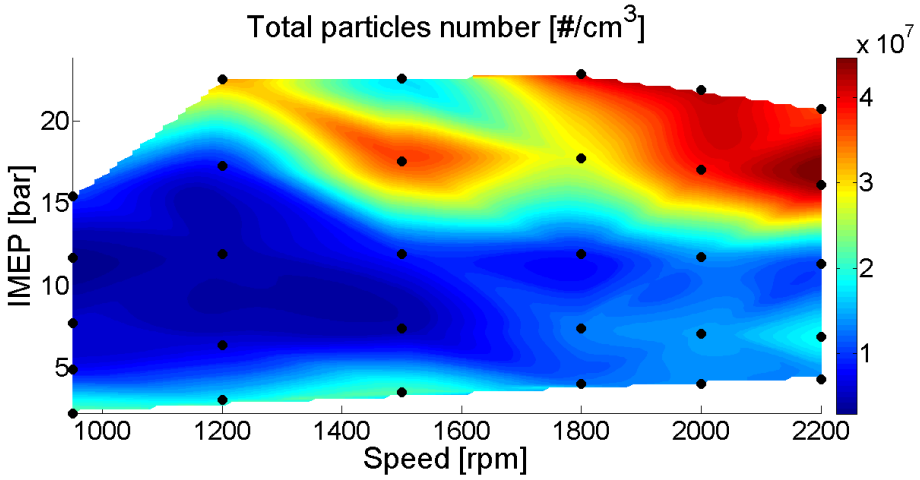

Figure 5.18. Total particle number for the DMDF concept.

Figure 5.19 shows the total particle number in the nucleation mode (mobility diameter <30 nm) and Figure 5.20 shows accumulation mode (from 30 to 250 nm). As it has been aforementioned, nucleation mode particles are primary composed of condensed hydrocarbon species, whose appearance is favored by the low temperature combustion process [7]. By contrast, accumulation mode particles contains elemental carbon species (i.e., soot particles) similar to those found during conventional diesel combustion [10],

and act as a sink for volatile species [14]. Considering this, both Figure 5.17 and Figure 5.18 allow to identify in a first approach the nature of the particles for each combustion mode. From the figures, it is seen that nucleation mode particles is dominant for the fully and highly premixed RCCI combustion mode, while accumulation mode particles is entirely confined in the high load region of the map, corresponding to the dual-fuel diffusion strategy.

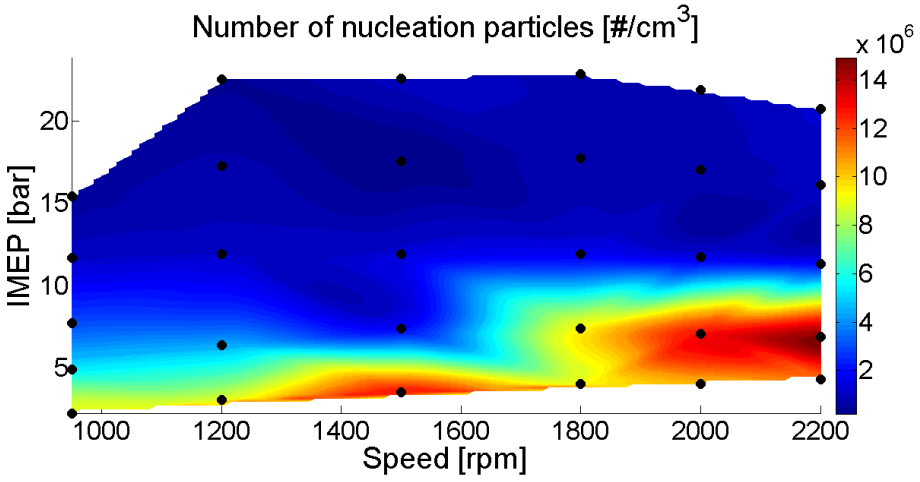

Figure 5.19. Number of nucleation mode particles for the DMDF concept.

Prikhodko et al. [15] demonstrated that conventional diesel oxidation catalysts are effective to reduce nucleation mode particles by diffusion [16]. In particular, the authors found that 35% of nucleation mode particles from RCCI were effectively removed by the DOC with inlet gas temperatures of around 250 °C. The same authors proved that using a diesel particulate filter (DPF) after the DOC, which is a standard aftertreatment layout for current diesel engines, the particulate conversion efficiency increased to near 99% due to the hydrocarbons absorption by the DPF. By contrast, the nucleation mode particles from RCCI were found to be not reduced by the DOC, as occurs during conventional diesel combustion.

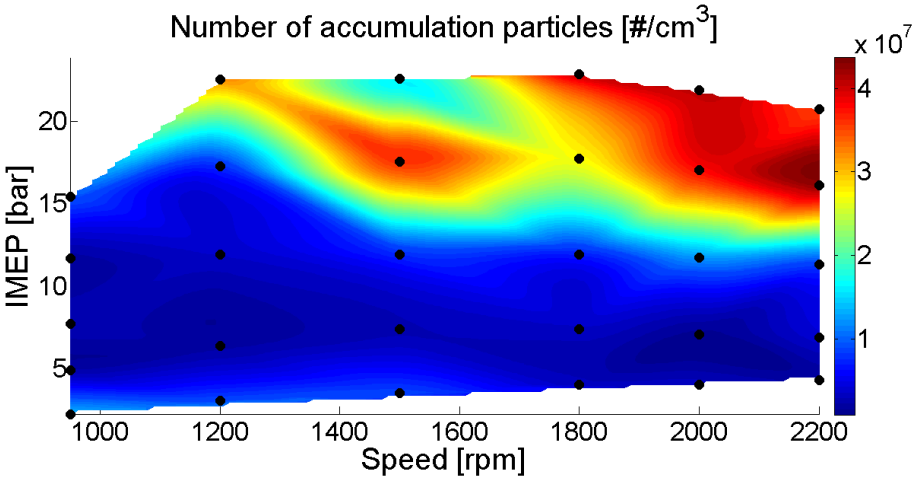

Figure 5.20. Number of accumulation mode particles for the DMDF concept.

To enhance the understanding of the particulates origin in each combustion mode, Figure 5.21 shows the gasoline fraction and Figure 5.22 shows the diesel mixing time used to cover the whole engine map. As it can be observed, the region above 14 bar IMEP shows mixing times between 0 and -20 CAD, which means the coexistence of the diesel injection and combustion processes during a certain period. This fact, together with the higher rate of diesel to gasoline injected (lower GF), explains the carbonaceous (high FSN) nature of the particulates in this portion of the engine map. By contrast, in the region below 14 bar IMEP, the mixing time values range from 20 to 40 CAD and gasoline fraction ranges from 65% to 95%. The combination of an extended mixing time and low amount of diesel fuel injected allows avoiding fuel-rich zones, and therefore the soot formation.

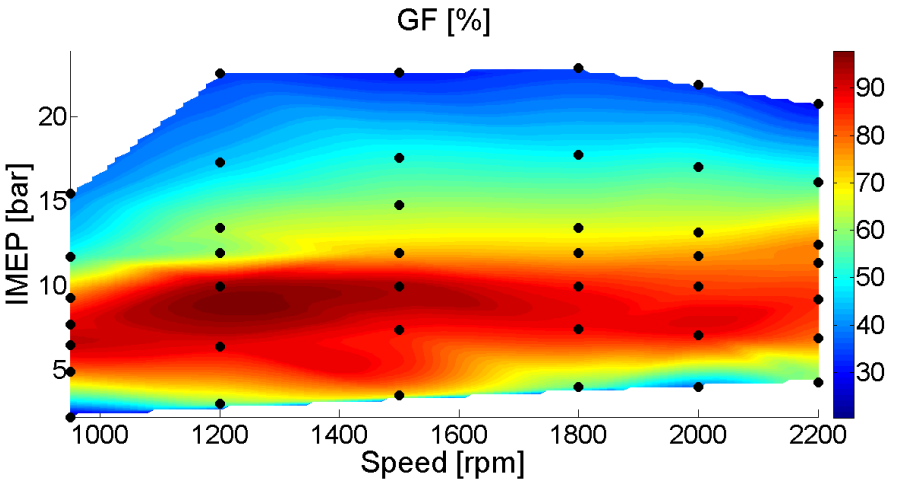

Figure 5.21. Gasoline fraction for the DMDF concept.

However, these conditions promote high levels of unburned HC species, which are prone to condense under low exhaust temperatures. This leads to an increase of the nucleation mode particles, characterized by a high amount of soluble organic fraction [17].

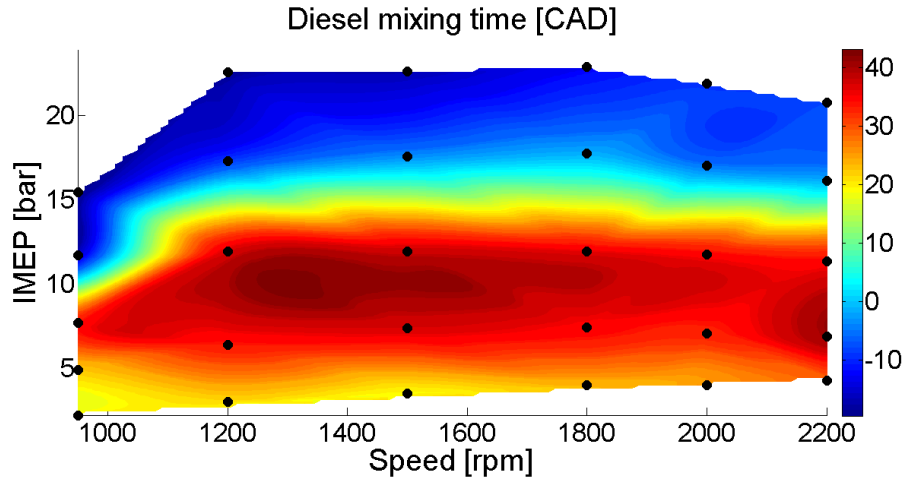

Figure 5.22. Mixing time for the DMDF combustion strategy.

5.5 Summary and conclusions

The present chapter is dedicated to the particle size distribution (PSD) and the particle number promoted by the DMDF concept. The study has been carried out by means of a scanning mobility particle sizer which is capable to measure particles from 5 to 250 nm.

The first part of the study has been focused on the particles emitted by the RCCI concept. Hence, the DMDF operates under RCCI from 10 to 40% engine load. It was selected the 25% engine load to sweep all engine speeds (950 rpm to 2200 rpm).

The second part of the study was to explore the particle emissions of the DMDF through low to full load. As it was aforementioned, the combustion strategy starts with fully premixed strategy and switches to highly premixed and mainly diffusive when the engine load increases. Therefore the evolution of the particle emissions was studied at 1200 rpm from low to full load.

The last part of the study focuses in the particle emissions over the whole engine operating map of an optimized DMDF concept. Thus, the engine range and load has been extended respect previous studies obtaining really interesting results in terms of particle nature and particle number for the whole operating range of the concept.

The most relevant conclusions obtained after the particle number and particle size distribution analysis are summarized as follows:

- PSD analysis presents a dependency between the total number particles and the engine speed for both combustion modes. Despite of the lower smoke values observed, DMDF concept promotes higher number of particles at high engine speeds than at CDC mode. This increase in the total amount of particles might be caused by the gasoline (high levels of CO and uHC

emissions), which produce more number of small particles than CDC mode.

- Smoke and total particle number maps were found to be similar in the region above 14 bar IMEP, provoked by the switching to diffusive dual-fuel strategy. This strategy leads to large carbonaceous nature particles typically found at CDC mode.
- No coherence was found between the smoke and the total particle number in the low region of the engine map operation. Hence, this behavior suggests that particles emitted during fully and highly premixed strategies operation might be mainly composed by soluble organic fraction coming from volatile species. Other possibility might be that these particle could come from increased solid particle cores, which also causes a discrepancy between the FSN and the total particle number. Hence, a dedicated study regarding the chemical composition of the particle would be interesting to assess the nature of the particle.
- DMDF concept operated under fully premixed strategy (RCCI) is dominated by small particles (diameter ≈ 30nm), the dual-fuel diffusive strategy is dominated by large particles (diameter ≈ 100nm), and the highly premixed strategy shows a mixed particle size distribution due to the transition nature of the strategy from fully premixed to dual-fuel diffusive nature. Hence, this intermediate strategy shows two main peaks of mobility diameters around 20 nm and 80 nm.
- Some large particles were also found for the fully premixed (RCCI) strategy. This finding is consistent with the literature, which describes the RCCI particle as a carbonaceous nucleus nature over which the volatile species tend to condensate due to a coagulation phenomenon.

5.6 Bibliography

[1] TSI Model 379020A: engine exhaust particle sizer spectrometer *Operation and Service Manual*.

[2] European Union official bulletin diary: CEPE number 83 regulation, 07 series. [2015/1038].

[3] Bermúdez V., Pastor, José V., López J. Javier, Campos D. "Experimental correlations for transient soot measurement in diesel exhaust aerosol with light extinction, electrical mobility and diffusion charger sensor techniques". Meas. Sci. Technol. 25, 065204, 2014.

[4] Benajes, J., Garcia, A., Monsalve-Serrano, J., and Boronat, V., "Particulates Size Distribution of Reactivity Controlled Compression Ignition (RCCI) on a Medium-Duty Engine Fueled with Diesel and Gasoline at Different Engine Speeds" SAE Int. J. Engines 10(5):2017, doi:10.4271/2017-24-0085.

[5] Kolodziej C., Wissink M., Splitter D. and Hanson, R. "Particle Size and Number Emissions from RCCI with Direct Injections of Two Fuels" SAE Technical Paper 2013-01-1661, 2013, doi:10.4271/2013-01-1661.

[6] Zhang, Y., Ghandhi, J., and Rothamer, D., "Comparison of Particulate Size Distributions from Advanced and Conventional Combustion - Part I: CDC, HCCI, and RCCI" SAE Int. J. Engines 7(2):820-834, 2014, doi:10.4271/2014-01-1296.

[7] Prikhodko, V., Curran, S., Barone, T., Lewis, S. et al., "Emission Characteristics of a Diesel Engine Operating with In-Cylinder Gasoline and Diesel Fuel Blending" SAE Int. J. Fuels Lubr. 3(2):946-955, 2010, doi:10.4271/2010-01-2266.

[8] Harris SJ, Maricq MM. "Signature size distributions for diesel and gasoline engine exhaust particulate matter" Journal of Aerosol Science, 2001-32-749, 2001.

[9] Benajes, J., Garcia, A., Monsalve-Serrano, J., and Boronat, V., "Gaseous emissions and particle size distribution of dual-mode dual-fuel diesel-gasoline concept from low to full load". Appl. Therm. Eng. 120, 138–149, 2017.

[10] Storey J., Curran S., Lewis S., Barone T., Dempsey T., Moses-DeBusk M., Hanson M., Prikhodko V., Northrop W., "Evolution and current understanding of physicochemical characterization of particulate matter from reactivity controlled compression ignition combustion on a multi cylinder light-duty engine". Int. J. Engine Res. (2016).

[11] Kittelson D.B., "Engines and nanoparticles: a review". J. Aerosol Sci. 29 (5/6) (1998) 575–588.

[12] Wang B., Mosbach S., Schmutzhard S., Shuai S., Huang Y., Kraft M., "Modelling soot formation from wall films in a gasoline direct injection engine using a detailed population balance model". Appl. Energy 163 (2016) 154–166.

[13] Benajes, J., Garcia, A., Monsalve-Serrano, J., and Boronat, V., "An investigation on the particulate number and size distributions over the whole engine map from an optimized combustion strategy combining RCCI and dual-fuel diesel-gasoline". Energy Conversion and Management, 140, 98–108, 2017.

[14] Abdul-Khalek I, Kittelson D, Brear F. "Diesel trap performance: particle size measurements and trends". SAE technical paper 982599; 1998, http://dx.doi. org/10.4271/982599.

[15] Prikhodko V, Curran S, Barone T, Lewis S, Storey J, Cho K, et al. "Diesel oxidation catalyst control of hydrocarbon aerosols from reactivity controlled compression ignition combustion". In: Proceedings of the ASME 2011 international mechanical engineering congress and exposition (vol. 9), Denver, CO, 11–17 November 2011, pp. 273–278. New York: ASME.

[16] Konstandopoulos A, Kostoglou M, Skaperdas E, Papaioannou E, Zarvalis D, Kladopoulou E. "Fundamental studies of diesel particulate filters:

transient loading, regeneration and aging". SAE technical paper 2000-01-1016, http:// dx.doi.org/10.4271/2000-01-1016.

[17] Jiang H, Wang J, Shuai S. "Visualization and performance analysis of gasoline homogeneous charge induced ignition by diesel". SAE technical paper 2005-01- 0136; 2005.

Chapter 6

Conclusions and suggestions for future work

Content

6.1 Introduction

This chapter represents the last chapter of the present investigation. The present thesis work contains a strong experimentalist charge that it have performed in a single-cylinder compression ignition engine derived from a medium-duty commercial engine. Regarding the combustion concept, Dual-Mode Dual-Fuel concept is based in dual-fuel premixed concept that corresponds to a low temperature combustion strategy. In particular, the reactivity controlled compression ignition (RCCI) is used as a starting point for the investigation, which provides the know-how of the dual-fuel strategies.

Hence, it summarizes the main conclusions of the different studies performed during the different chapters' investigations. A brief analysis of the conclusions obtained will provide the last section of this chapter with the suggestions for future works.

6.2 Summary and conclusions

This research has focused on improving the efficiency and reducing the most relevant engine-raw emissions of the compression ignition (CI) engines operated under conventional diesel combustion(CDC) mode. In order to achieve this outstanding target, the investigation has been performed by applying low temperature combustion (LTC) strategies, that are able to provide similar or better performance than diesel engines while the can reduce both NOx and smoke emissions simultaneously. Hence, the LTC break the traditional trade-off between NOx and soot existing at the CDC concept. Along the chapter 2, it has been presented the main advantages and disadvantages that provide the CDC mode and the alternative LTC concepts that could face the CDC challenges.

The literature review performed in chapter 2, presents the diesel combustion evolution along the history. A huge effort has been dedicated from the research community in order to improve the understanding of the

diffusive combustion phenomena in order to obtain better efficiency while the emissions are mitigated. In addition, the recent standard emissions limitations have forced the industry to add aftertreatment systems in order to promote clean exhaust flow emissions at the tail pipe. The LTC concepts have postulated as a feasible option in order to overcome the main challenges of the CDC concept. By contrast, despite of providing an excellent efficiency compared with the CDC (similar or even better), the existing dispersion cycle-to-cycle observed in these concepts provoke a poor combustion phasing control that limits the engine operation towards the full load. Hence, this weakness of the LTC concept has been investigated in order to improve the combustion process control by exploring the influence of the charge preparation or the fuel stratification at the combustion chamber. The most important conclusion was that it is possible to extend the engine operating range by using different reactivity fuels.

This dual-fuel combustion strategy was named as Reactivity Controlled Compression Ignition (RCCI). Hence, RCCI emerges as the most promising LTC due to the substantial improvement at the combustion phasing controlled compared with the previous LTC widely investigated. Indeed, the RCCI concept is able to maintain the reduced heat transfer due to the fast combustion process while it reduces both NOx and smoke emissions simultaneously. However, it also presents some issues. At low load operation it promotes excessively high levels of CO and unburned HC. Additionally, the exhaust gas temperature reached during the low load operation is extremely low, worsening the catalytic activity at the DOC aftretreatment element. During the high load operation, it provides excessive pressure rise rate that limits the full load range. Thus, despite of achieving very high GIE with ultra-low NOx and smoke emissions at medium loads conditions some actions need to be taken to overcome the weaknesses of the RCCI.

Another background generated at the second chapter regards to the PSD. Very few studies have been carried out at RCCI concept. Therefore, the exploration of the particles promoted by the RCCI concept results in a very special interest since the current EU VI standard limits the total number of particles.

Dual-Mode Dual-Fuel (DMDF) concept

The DMDF concept is aimed to solve the main issues found at the RCCI concept. The DMDF consists of a combination of dual-fuel combustion strategies that switches in function of the engine load. During the low load operation, the strategy used is a fully premixed as it can be found at the RCCI concept. Medium load uses a highly premixed strategy that allows controlling the combustion phasing with a controlled pressure rise rate. Finally, at full load operation, the concept switches to a mainly diffusive strategy igniting the combustion process with the LRF injection. In addition, the constraints in terms of emissions need to be relaxed for the CR15.3:1 tested in order to achieve the full load operation. Even relaxing the emissions constraints, the concept is able to provide low levels of NOx and smoke.

In order to explore the capabilities of the concept, it was used a SCE derived from a commercial EU VI engine. DMDF concept was implemented by using two different CR (12.75:1 and 15.3:1). The mechanical constraints were a maximum pressure of 190 bar and the pressure rise rate should not exceed 15 bar/CAD. The emissions constraints were not to exceed 0.4 g/kWh and the lowest smoke achievable. In addition, the NOx emissions constraint were relaxed when using a CR 15.3:1 in order to allow the operation of this concept up to full load. Despite of increasing the NOx emissions limitation, it is compliant with the EU VI limitation standard when the whole engine map is considered.

In this sense, the test campaign allowed to obtained the engine mapping of both compression ratios tested. The next step was to compare the results of both hardware configurations in order to determine which the best hardware configuration was. The criteria followed to determine which is the best compression ratio, it has been considered the fuel consumption, and the CO and unburned HC emissions. It is worthy to note, that due to the methodology followed to perform the test campaign, the NOx and smoke emissions as well as the maximum pressure and the pressure rise were not exceeding the self-imposed values. Therefore, it can be considered other parameters previously cited.

Thus, considering the fuel consumption, as it can be observed in chapter 4, the highest compression ratio tested improves the fuel consumption despite of promoting higher CO and unburned HC emissions in some ares of the engine map operation. Indeed, the CR15.3:1 promotes lower uHC during medium load operation than the CR12.75:1. However, the CR15.3 promotes higher CO emissions during the low load operation. The main reason that explains these differences might rely at the intake temperature, which was higher for the CR12.75 during the low load operation. Additionally, the uHC emissions are higher for the CR15.3:1 than for CR12.75:1 due to the higher combustion temperatures during the combustion process. Therefore, the higher combustion temperatures burn more fuel oxidizing better the CO. The rest portion of the engine map shows that both compression ratios promote similar values of CO emissions (results are quite close to 0).

As it has been explained during the second chapter, the temperatures at the exhaust play a key role when catalytic activity is required. Under all these considerations, the compression ratio of 15.3:1 tested resulted more interesting despite of reaching higher NOx emissions values during the full load operation.

PSD investigation on RCCI concept

The particle size distribution study (5-250nm) was performed with the compression ratio of 15.3:1. In order to explore the particle emissions under RCCI mode, the engine was operated at 25% engine load from 950 rpm to 2200 rpm. Thus, the engine was operated over the whole engine speed range under RCCI mode. The engine was also operated with the CR 15.3:1 under CDC in order to compare the particles promoted by both concepts. The study is fully detailed in chapter 5. Main results of the investigation suggest that the RCCI concept promotes higher number of particles than the CDC concept. However, both concepts present the same trend when the engine speed is modified. As the engine speed increases, the total number of particles increases as well. The CDC case shows a direct relation between the number of particles and the smoke emissions. As it has been observed, the higher the FSN, the higher the total number of particles. In particular, CDC strategy is

clearly dominated by accumulation mode particles, which means that the CDC promotes particles with a higher scanning mobility diameter with carbonaceous nature. The peak at the PSD curve can be found at around 60 nm.

On the other hand, the RCCI concept presents no relation between the FSN results and the total number of particles. The FSN increases when the engine speed is around 1500 rpm but it decreases when the engine speed increases. By contrast, the total number of particles continues increasing as in the CDC case. The PSD curves show a bimodal shape curve when the engine is running at these engine speeds, explaining the results depicted in the chapter 5. The particles promoted under RCCI are dominated by the nucleation mode particles. Nucleation mode particles are smaller and the nature of these particles is not carbonaceous, its origin comes from the soluble volatile fraction (SOF). The PSD curves observed in RCCI mode, present the peak of the curve at 20nm of diameter.

Thus, summarizing the main conclusions of the RCCI versus CDC PSD analysis, it is possible to state that the RCCI concept promotes around a 70% of nucleation mode particles against around 10% of nucleation mode particles for the CDC concept. These differences observed rely on the nature of the particles. Finally, the total number of particles is higher for the RCCI concept as it has been shown in chapter 5. During this investigation, no dedicated measurements were performed in order to obtain the total mass of the particles.

PSD investigation on DMDF concept

The PSD (5-250nm) analysis was performed for the DMDF concept. A first approach has been carried out by testing at a fixed engine speed (1200 rpm) and moving from low to full load. As it was done in the previous case comparing the RCCI and the CDC particles, the DMDF concept was compared against the CDC strategy. The CDC concept shows a clear consistent behavior regarding the type of particles emitted along the engine load tested. In this sense, the CDC is clearly dominated by the accumulation mode particles, showing a peak at 60nm of diameter.

On the other hand, the DMDF concept shows different trends depending on the engine load. As the load increases, the highest peak of the PSD curve moves from nucleation mode towards accumulation mode. hence, the peak at the curve goes from 20 nm to 100nm of scanning mobility diameter. This variation of the particle nature occurs due to the evolution of the injection strategy of the DMDF concept. During low load operation the strategy is the same that the RCCI concept strategy. However, when the engine load increases the injection strategy switches into a mainly diffusive strategy, which generates high local equivalence ratios promoting particles with carbonaceous nucleus typically found at CDC. This trend is also followed by the smoke emissions measurement in terms of FSN.

Finally, compared with the CDC mode, the DMDF promotes higher number of particles than CDC concept. In addition, from 50% engine load, the smoke measurements show a direct trend with the number of particles due to the lowest fully premixed of fuel quantity what moves the nucleation mode particles towards accumulation mode particles. Regarding the particle mass, it was not considered due to the equipment used and the objectives of the investigation.

PSD engine mapping under DMDF concept

The engine mapping has been performed in order to analyze the complete spectra of the particles in order to improve the comprehension of the particles emissions under DMDF operation. It is worthy to note that the DMDF concept combines different combustion strategies and uses two fuels over the whole engine map.

Main conclusions of the maps presented are that most relevant smoke emissions are promoted at high engine load and high engine speed (values close to 2 FSN in some engine operating points). Thus, the total number of particles, as it has been previously noted, increases with the engine speed and load. In this sense, the nucleation mode particles dominate the engine map when the engine load is below 7 bar of IMEP. On the other hand, accumulation mode particles dominates the upper side of the engine map, being predominant when the engine load is higher than 12 bar of IMEP and

more than 1200 rpm. Thus, between 7 to 12 bar of IMEP, the number of nucleation mode particles and accumulation mode particles is balanced due to the bimodal shape PSD curves found at the previous studies. This phenomenon also is explained due to the hybrid combustion strategy used for medium loads (highly premixed strategy).

Finally, in order to provide a global view of the work previously described, a graphical summary is presented in Figure 6.1.

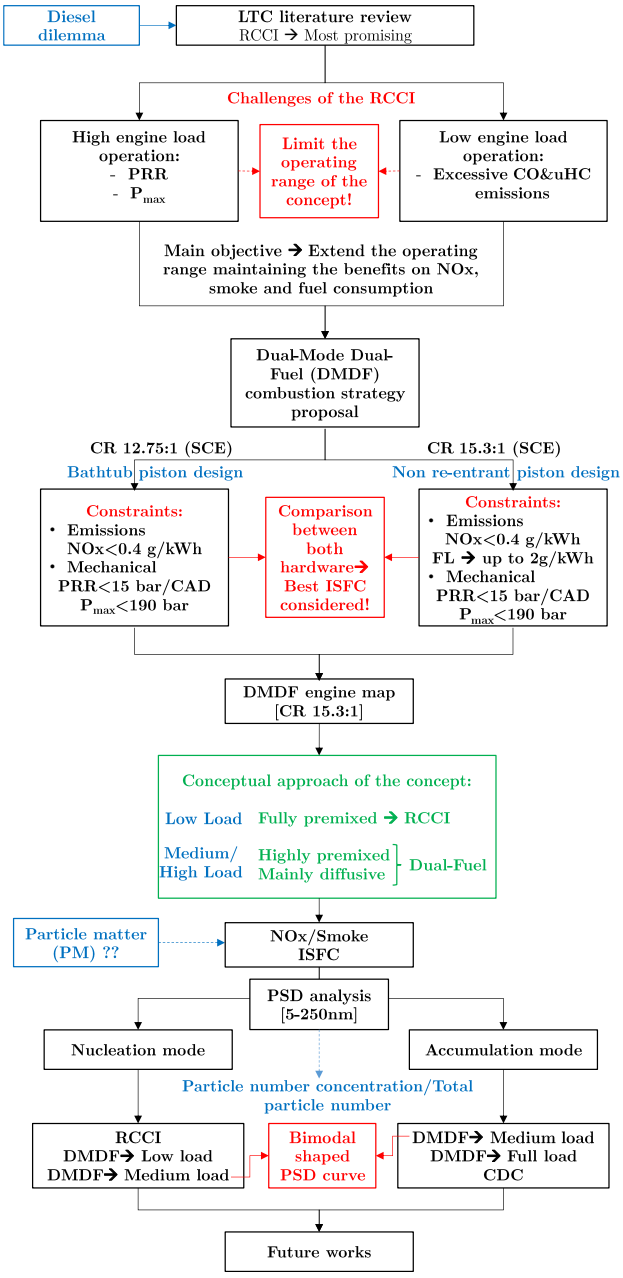

Figure 6.1. Graphical summary of the investigation carried out during the thesis work.

6.3 Suggestions for future work

Throughout the work carried out during the present investigation, some considerations about the achievements reached highlight some aspects that have been not deeply investigated due to the constraints in terms of time and tools. Hence, these studies might be performed in future investigations with the aim to complete the DMDF concept development.

These future works result from a combination of scientific interests as well as practical issues found during the investigation. The main suggestions are detailed as follows:

DMDF concept implementation in a multi-cylinder engine

Two engine maps have performed by using two different compression ratios under the DMDF concept. The results obtained are quite promising in terms of performance and emissions. In this sense, the engine mapping performed with the CR of 15.3:1 is the most promising due to the emissions and fuel efficiency considerations. Additional aspects such as exhaust temperatures would increase in a multi-cylinder engine improving the catalytic activity.

Thus, the implementation of the DMDF concept in a multi-cylinder engine results in a special interest in order to verify the challenges that would present the concept in a real engine. As it has been demonstrated along this work, the DMDF concept shows great potential to meet the current EU VI standard limitation under steady state conditions. However, the studies were performed in a SCE. The extrapolation of the concept into a production CI engine with the stock configuration would focused on the concept itself and the air management. The use of such a high EGR rates that require low EGR pressure loops presents a huge challenge for the turbocharger. In this sense, LP-EGR rates of 50% implies that the turbocharger has to boost at a given point 1.5 times more air mass flow than using HP-EGR or without EGR rate. Hence, the pumping work of the engine can drastically reduce the overall

efficiency of the engine mitigating the benefits of the concept. Additional effects such as EGR condensation and cooling are also important when a multi-cylinder engine is used.

Other important effects that appear when using a multi-cylinder engine is the cycle-to-cycle dispersion. Indeed, the fuel injected in the manifold or the EGR mixing is important in order to mitigate this variation. These questions could require a specific intake manifold with an improved design for the gasoline fuel injection or an improved EGR mixer in order to avoid the EGR dispersion. It is important to note that not only EGR is important to reduce the NOx emissions, but also it is important to adequate the reactivity of the air mixture in order to control the combustion phasing. If a huge dispersion appears, the mechanical constraints can occur overpassing the pressure rise rate and causing severe damage to the engine.

Total particle number and particle mass consideration

The study carried out during the present work only takes account of the particles between 5-250 nm. The particles emitted are usually inside the range of the diameters proposed for the current investigation. As the current standard emissions limitation limits also the total number of particles, the study performed would require to measure additional particles bigger than 250 nm. With the current study is possible to foresee the total number of particles emitted in a 13 modes cycle for instance due to bigger particles represent a small portion of the total particles promoted by the concept. In this sense, ensuring the whole range of particles could provide better results in order to explore if it is possible to meet the current standard limitations with or without EATS.

Additional considerations would be interesting regarding the particle mass correlations. Current diesel smoke measurements in FSN units (also happens with gasoline) use a set of correlations in order to convert the FSN into a particle mass. This conversion takes into account a specific volume and a given density of the particles promoted by the diesel (or gasoline) fuel.

The density was obtained experimentally as well as the correlation. The Dual-Fuel concepts have not any correlation in order to convert from FSN into particle mass. By contrast, the smokemeter mainly detects the carbonaceous particles and not the particles coming from SOF. Therefore, specific methodology and tests could be carried out in order to convert the total number of particles into a particle mass without weighting every particle.

Emissions speciation before/after the aftertreatment systems

The current investigation has focused on developing a low temperature combustion dual-fuel strategy based on the RCCI concept. Several self-imposed constraints have been used in order to obtain a combustion strategy that promote ultra-low values of NOx and smoke. In this sense, general emissions such as unburned hydrocarbons have been measured and considered during the investigation. However, the importance given to those pollutants was secondary compared with the relevance of NOx and smoke. The main reason for that is that current standard emissions limitations are extremely stringent with NOx and smoke emissions due to the existing trade-off between them at CDC mode. Hence, engine manufacturers are extremely concerned about mitigating these pollutants during the combustion process. Nonetheless, the complete study of the DMDF emissions implies a deep study regarding the uHC emissions as well as the different ways to mitigate them in order to meet the current standard emissions limitations.

Thus, the characterization of the nature, chemistry and aftertreatment considerations of the DMDF concept presents new research highlighting the importance of the fuels used, the portion of low reactivity fuel and other parameters such as the temperature during the combustion process. This study would help to determine the type of particular hydrocarbons that it is possible to find at the exhaust gases before and after the aftertreament system. The work in this topic might determine the factors that takes part on the hydrocarbons composition such as LRF portion or combustion peak temperature and the different parameters that might improve the reduction of the global hydrocarbons emissions. The reduction of the uHC emissions is

function of the hydrocarbons composition. Depending of the quantity of every hydrocarbon, the DOC required would be different (long hydrocarbons or short hydrocarbons chain) requiring different materials and light-off temperatures.

PSD analysis after the aftertreatment analysis

The present investigation analyzed the particles from the engine-out emissions. Despite the benefits of the DMDF concept in terms of NOx and smoke emissions, the aftertreatment system would not be totally removed. In addition, the EATS might be redesigned in order to optimize the whole power unit considering the whole package of elements. In addition, as it has been observed during the chapter 5, the premixed LTC strategies do not form particulate matter in the traditional pathways presented by the CDC concept. Thus, the characterization of the physicochemical properties of the particle matter acquires interest from the research community. Hence, improving the understanding of the size and composition of the particle matter would discover the sources of particle matter, which lead to new possibilities of mitigation pathways.

In this sense, the literature states that the conventional diesel oxidation catalysts are effective to reduce the nucleation mode particles by diffusion. The authors found that, under RCCI operation, 35% of nucleation mode particles from RCCI were effectively removed by the DOC catalytic stripping with temperatures at the exhaust around 250°C. By contrast, the particulate conversion efficiency reached up to 99% when using a DPF because of the adsorption of the hydrocarbons on the walls.

Therefore, a dedicated study considering the DOC and the DPF separately in order to explore the particles before and after these elements for the DMDF concept would be interesting in order to face future standard emissions limitations. Some considerations regarding the speciation of the hydrocarbons emissions could be also interesting. It has been demonstrated that the combination of particle matter and unburned HC products might

contain carcinogens elements. Finally, currently at the engine manufacture industry, the diesel DPF is widely known and it has been equipped in the vehicles for a long time. Gasoline DPF are being equipped recently due to the direct injected gasoline engines. However, the particulate filters required for these LTC dual-fuels strategies and multimode combustion strategies needs to be better understood.

Bibliography

[1] Amengual Rubén. "Bielas y álabes 1826-1914. Evolución histórica de las primeras máquinas térmicas a través de las patentes españolas". Oficina Española de Patentes y Marcas, 2008.

[2] Diesel R. "Internal combustion engine". US Patent Number 608845, 1898.

[3] Shrinivasa, U. "The evolution of diesel engines". Resonance. 2012.

[4] Carnot S. "Reflections on the Motive Power of Fire: And Other Papers on the Second Law of Thermodynamics". Dover Publications, 2005.

[5] European Commission. Transport. Statistical pocketbook, 2017. https://ec.europa.eu/transport/facts-fundings/statistics/pocketbook-2017_en.

[6] European Automobile Manufacturers' Association. "The Automobile Industry Pocket Guide 2014-2015". Technical report.

[7] Environmental Protection Agency. "Nitrogen Oxides (NOx), Why and How They Are Controlled". Technical report, 1999.

[8] Environmental European Agency. "Emissions of primary PM2.5 and PM10 particulate matter". Technical report.

[9] Regulation (EC) No 595/2009 of the European parliament and of the council of 18 June 2009 on type-approval of motor vehicles and engines with respect to emissions from heavy duty vehicles (Euro VI) and on access to vehicle repair and maintenance information and amending Regulation (EC) No 715/2007 and Directive 2007/46/EC and repealing Directives 80/1269/EEC, 2005/55/EC and 2005/78/EC.

[10] Engineer Commercial Vehicle. "Euro 6 the inside story". Technical report, March 2012.

[11] Selective Catalytic Reduction (SCR). Researchgate. More information in www.researchgate.net.

[12] AdBlue®. More information at https://www.vda.de/en.

[13] Commercial Vehicle Engineer, January 2010.

[14] Posada F., Chambliss S. and Blumberg K. "Costs of emission reduction technologies for heavy- duty diesel vehicles". ICCT, 2016.

[15] Johnson T.V. "Vehicular Emissions in Review". SAE Int. J. Engines, Vol. 5, 216-234, 2012.

[16] Gense N.L.J., Riemersma, Such C. and Ntziachristos L. "Euro VI technologies and costs for Heavy Duty vehicles". Technical report, Delft: TNO Science and Industry report, 56, 2006.

[17] Guide to the Volkswagen Emissions Recall. https://www.consumerreports.org/cro/cars/guide-to-the-volkswagen-dieselgate-emissions-recall-

[18] Dieselgate: Who? What? How? A study by Transport and Environment, 2016.

[19] Rupert Neate. "Meet John German: the man who helped expose Volkswagen's emissions scandal". The Guardian. 2015. More information at: https://www.theguardian.com/business/2015/sep/26/volkswagen-scandal-emissions-tests-john-german-research

[20] Hooftman N., Messagie M, Van Mierlo J and Coosemans T. "A review of the European passenger car regulations – Real driving emissions vs local air quality". Renewable and Sustainable Energy Reviews, 1-21, 2018.

[21] O'Kane S. "VW executive given the maximum prison sentence for his role in Dieselgate". The Verge. More information at: https://www.theverge.com/2017/12/6/16743308/volkswagen-oliver-schmidt-sentence-emissions-scandal-prison

[22] Luke John Smith. "Petrol and diesel car ban will go ahead in London this year - Ignore it and face £130 fine". Express. More information at https://www.express.co.uk/life-style/cars/944461/petrol-diesel-car-ban-London-UK-2018-fine.

[23] EC. Proposal for a regulation of the European Parliament and of the Council on the approval and market surveillance of motor vehicles and

their trailers, and of systems, components and separate technical units intended for such vehicles. Brussels; 2016.

[24] ICCT. Proposed new type-approval system for motor vehicles in the European Union. Berlin; 2016.

[25] ICCT. European vehicle market statistics. Berlin; 2016.

[26] European Parliament, Council of the European. Regulation (EC) No 595/2009 of the European Parliament and of the Council on type-approval of motor vehicles and engines with respect to emissions from heavy duty vehicles (Euro VI). Official Journal of the European Union 2009;188:1–13.

[27] Imtenan S, Varman M, Masjuki H, Kalam M, Sajjad H, Arbab M, et al. "Impact of low temperature combustion attaining strategies on diesel engine emissions for diesel and biodiesels: a review". Energy Convers Manage 2014;80:329–56.

[28] Splitter D, Wissink M, Hendricks T, Ghandhi J, Reitz R. Comparison of RCCI, HCCI, and CDC operation from low to full load, THIESEL 2012 conference on thermo- and fluid dynamic processes in direct injection engines; 2012.

[29] Neely G, Sasaki S, Huang Y, Leet J, Stewart D. "New diesel emission control strategy to meet US Tier 2 emissions regulations". SAE technical paper, 2005- 01-1091; 2005.

[30] Garcia A, Monsalve-Serrano J, Heuser B, Jakob M, Kremer F, Pischinger S. "Influence of fuel properties on fundamental spray characteristics and soot emissions using different tailor-made fuels from biomass". Energy Convers Manage, 108, 243–54, 2016.

[31] Bittle J.A., Knight B.M. and Jacobs T.J. "Heat Release Parameters to Assess Low Temperature Combustion Attainment". SAE Technical Paper, no 2011-01-1350, 2011.

[32] Inagaki K, Fuyuto T, Nishikawa K, Nakakita K, Sakata I. Dual-fuel PCI combustion controlled by in-cylinder stratification of ignitability. SAE technical paper, 2006-01-0028, 2006.

[33] Kokjohn S, Hanson R, Splitter D, Reitz R. "Fuel reactivity controlled compression ignition (RCCI): a pathway to controlled high-efficiency clean combustion". Int JEngine Res., 12, 209–226, 2011.

[34] Dec J. E. "A conceptual model of DI diesel combustion based on laser-sheet imaging". SAE Paper 970873, 1997.

[35] García J. M. Aportaciones al estudio del proceso de combustión turbulenta de chorros en motores Diésel de inyección directa. Tesis doctoral, Universidad Politécnica de Valencia, Departamento de Máquinas y Motores Térmicos, 2004.

[36] Musculus Mark P.B., Miles Paul C. and Pickett Lyle M. "Conceptual models for partially premixed low-temperature diesel combustion". Progress in Energy and Combustion Science, Vol. 39 no 2-3, pp. 246-283, 2013.

[37] Taylor C. F. The internal Combustion Engine in Theory and Practice Vol 2, 2 Ed. Revisada. The MIT Press, 1985.

[38] Payri González Francisco and Desantes José María. Motores de combustión interna alternativos. Editorial Reverté, España, 2011.

[39] Heywood J. B. Internal combustion engine fundamentals. McGraw-Hill Publishing, 1988.

[40] Espey C., Dec J. E., Litzinger T. A. and Santavicca D. A. "Planar laser rayleigh scattering for quantitative vapor-fuel imaging in a diesel jet". Combustion and Flame, Vol. 109 no 1-2, pp. 65-78, 1997.

[41] Kosaka H., Drewes V. H., Catalfamo L., Aradi A. A., Iida N. and Kamimoto T. "Twodimensional imaging of formaldehyde formed during the ignition process of a diesel fuel spray". SAE Paper 2000-01-0236, 2000.

[42] Bruneaux G. "Study of the correlation between mixing and auto-ignition processes in high-pressure Diesel jets". SAE Paper 2007-01-0650, 2007.

[43] Glassman I. and Yetter R. Combustion, 4 Ed. Academic Press, 2008.

[44] Dec J. E. and Tree D. R. "Diffusion-flame/wall interactions in a heavy-duty DI diesel engine". SAE Paper 2001-01-1295, 2001.

[45] Dec J. E. y Canaan R. E. "PLIF imaging of NO formation in a DI diesel engine". SAE Paper 980147, 1998.

[46] Dec J. E. y Kelly-Zion P. L. "The effects of injection timing and diluent addition on late-combustion soot burnout in a DI diesel engine based on simultaneous 2-D imaging of OH and soot". SAE Paper 2000-01-0238, 2000.

[47] Li T. and Ogawa H. "Analysis of the Trade-off between Soot and Nitrogen Oxides in Diesel-Like Combustion by Chemical Kinetic Calculation". SAE Int. J. Engines, Vol. 5, pp. 94-101, 2011.

[48] Neely G.D., Sasaki S., Huang Y., Leet J.A. and Stewart D.W. "New Diesel Emission Control Strategy to Meet US Tier 2 Emissions Regulations". SAE Technical Paper, no 2005-01-1091, 2005.

[49] Kamimoto T. and Bae M. "High Combustion Temperature for the Reduction of Particulate in Diesel Engines". SAE Technical Paper, no 880423, 1988.

[50] Y. Lee, K. Huh. "Analysis of different modes of low temperature combustion by ultra-high EGR and modulated kinetics in a heavy duty diesel engine". Appl. Therm. Eng. 70, 776–787, 2014.

[51] Y. Qian, Q. Zhou, X. Wang, L. Zhu, X. Lu. "Enabling dual fuel sequential combustion using port fuel injection of high reactivity fuel combined with direct injection of low reactivity fuels". Appl. Therm. Eng. 103 399–410, 2016.

[52] Hiroyasu, H., Hiroyasu, T., Miki, M., Jamiura, J., & Watanabe, S. (2003). "Genetic Algoritms Optimization of Diesel Engine Emissions and Fuel Efficiency with Air Swirl, EGR, Injection Timing and Multiple Injections". SAE Paper 2003-01-1853, 2003.

[53] García, A. Estudio de los efectos de la post inyección sobe el proceso de combustión y la formación de hollín en motores Diésel. Barcelona: Editorial Reverté S.A., 2011.

[54] Pickett L. M. and Siebers D. L. "An investigation of diesel soot formation processes using micro-orifices". Proceedings of the Combustion Institute, Vol. 29 no 1, pp. 655-662, 2002.

[55] Siebers D. L. and Pickett L. M. "Injection pressure and orifice diameter effects on soot in DI Diesel fuel jets". Proceedings of THIESEL conference, pp. 199-213, 2002.

[56] Pickett L. M. and Siebers D. L. "Non-Sooting, Low Flame Temperature Mixing-Controlled DI Diesel Combustion". SAE Paper 2004-01-1399, 2004.

[57] Huestis E., Erickson P. A. and Musculus M. P. B. "In-cylinder and exhaust soot in low temperature combustion using a wide-range of EGR in a heavy-duty Diesel engine". SAE Paper 2007-01-4017, 2007.

[58] Benajes J., Molina S., Novella R. and Belarte E. "Evaluation of massive exhaust gas recirculation and Miller cycle strategies for mixing-controlled low temperature combustion in a heavy duty diesel engine". Energy, Vol. 71, 355-366, 2014.

[59] Benajes J., Molina S., Martin J. y Novella R. "Effect of advancing the closing angle of the intake valves on diffusion-controlled combustion in a HD diesel engine". Applied Thermal Engineering, Vol. 29, 1947-1954, 2009.

[60] Belarte E. Estudio del proceso de combustión premezclada controlada por la reactividad del combustible en un motor de encendido por compresión. 2015.

[61] Splitter Derek A. and Reitz Rolf D. "Fuel reactivity effects on the efficiency and operational window of dual-fuel compression ignition engines". Fuel, Vol. 118 no 0, pp. 163-175, 2014.

[62] Kokjohn S. L., Hanson R. M., Splitter D. A. and Reitz R. D. "Fuel reactivity controlled compression ignition (RCCI): a pathway to controlled high-efficiency clean combustion". International Journal of Engine Research, Vol. 12, 3, 209-226, 2011.

[63] Manente V., Johansson B., Tunestal P. and Cannella W. "Effects of Different Type of Gasoline Fuels on Heavy Duty Partially Premixed Combustion". SAE International Journal of Engines, 2, 71-88, 2010.

[64] Benajes J., García A., Monsalve-Serrano J., Boronat V. "Dual-Fuel Combustion for Future Clean and Efficient Compression Ignition Engines". Applied Sciences 7(1):36, 2017.

[65] Benajes J., Molina S., García A., Monsalve-Serrano J. and Durrett R. "Performance and engine-out emissions evaluation of the double injection strategy applied to the gasoline partially premixed compression ignition spark assisted combustion concept". Applied Energy, 134, 90-101, 2014.

[66] Benajes J., Molina S., García A., Monsalve-Serrano J. and Durrett R. "Conceptual model description of the double injection strategy applied to the gasoline partially premixed compression ignition combustion concept with spark assistance". Applied Energy, 129, 1-9, 2014.

[67] Alperstein M., Swim W.B. and Schweitzer P.H. "Fumigation kills smoke-improves diesel performance". SAE Technical Paper, no 580058, 1958.

[68] Najafabadi MI, Aziz NA. "Homogeneous charge compression ignition combustion: challenges and proposed solutions," J. Combustion, 2013-783, 2013.

[69] Lu X., Han D. and Huang Z. "Fuel design and management for the control of advanced compression-ignition combustion modes". Prog Energy Combust Sci 2011-37-741, 2011.

[70] Bessonette PW, Schleyer CH, Duffy KP, Hardy WL and Liechty MP. "Effects of fuel property changes on heavy-duty HCCI combustion". SAE paper 2007-01-0191; 2007.

[71] Manente V, Tunestal P, Johansson B et al. "Effects of Ethanol and Different Type of Gasoline Fuels on Partially Premixed Combustion from Low to High Load". SAE Technical Paper 2010-01-0871, 2010.

[72] Singh AP, Agarwal AK. "Combustion characteristics of diesel HCCI engine: an experimental investigation using external mixture formation technique". Appl Energy 2012-25-99:116, 2012.

[73] Bessonette P, Schleyer C, Duffy K, Hardy W., Liechty M. "Effects of Fuel Property Changes on Heavy-Duty HCCI Combustion". SAE Technical Paper 2007-01-0191, 2007.

[74] Peng Zhijun, Zhao Hua and Ladommatos Nicos. "Effects of Air/Fuel Ratios and EGR Rates on HCCI Combustion of n-heptane, a Diesel Type Fuel". SAE Technical Paper, Vol. 2003-01-0747, 2003.

[75] Park H, Youn IM, Lim Y and Lee CS. "Influence of the mixture of gasoline and diesel fuels on droplet atomization, combustion and exhaust emission characteristics in compression ignition engine". Fuel Processing Technology 2013-106-392, 2013.

[76] Inagaki K, Fuyuto T, Nishikawa K, Nakakita K and Sakata I. "Dual-Fuel PCI Combustion Controlled by In-Cylinder Stratification of Ignitability". SAE Technical Paper 2006-01-0028, 2006.

[77] Kokjohn SL, Hanson M, Splitter D, Reitz RD. "Experimental Moodeling of Dual-Fuel HCCI and PCCI Combustion Using In-Cylinder Fuel Blending", SAE Technical Paper 2009-01-2647, 2009.

[78] Benajes J, Molina S, García A and Monsalve-Serrano J. "Effects of Direct injection timing and Blending Ratio on RCCI combustion with different Low Reactivity Fuels". Energy Conversion and Management, 99, 193-209, 2015.

[79] Benajes J, Molina S, García A and Monsalve-Serrano J. "Effects of low reactivity fuel characteristics and blending ratio on low load RCCI (reactivity controlled compression ignition) performance and emissions in a heavy-duty diesel engine". Energy, 90, 1261-1271, 2015.

[80] Benajes J, García A, Pastor J.M and Monsalve-Serrano J. "Effects of piston bowl geometry on Reactivity Controlled Compression Ignition heat transfer and combustion losses at different engine loads". Energy, 98, 64-77, 2016.

[81] Benajes J, Pastor José V, García A and Monsalve-Serrano J. "An experimental investigation on the Influence of piston bowl geometry on RCCI performance and emissions in a heavy-duty engine". Energy Conversion and Management, 103, 1019-1030, 2015.

[82] Desantes JM, Benajes J, García A and Monsalve-Serrano J. "The role of the in-cylinder gas temperature and oxygen concentration over low load reactivity controlled compression ignition combustion efficiency". Energy, 78, 854–868, 2014.

[83] Splitter Derek A., Kokjohn Sage L., Rein Keith, Hanson Reed M., Sanders Scott and Reitz Rolf D. "An Optical Investigation of Ignition Processes in Fuel Reactivity Controlled PCCI Combustion". SAE Technical Paper 2010-01-0345, 04 2010.

[84] Monsalve-Serrano J. Dual-Fuel compression ignition: Towards clean, highly efficient combustion. 2016.

[85] Prikhodko V., Curran S., Parks J. and Wagner R. "Effectiveness of Diesel Oxidation Catalyst in Reducing HC and CO Emissions from Reactivity Controlled Compression Ignition". SAE Int. J. Fuels Lubr. 6(2):2013, doi: 10.4271/2013-01-0515.

[86] Benajes J, García A Monsalve-Serrano J. and Boronat V. "A RCCI operational limits assessment in a medium duty compression ignition engine using an adapted compression ratio", Energy Convrsion and Management, 126, 497-508, 2016.

[87] Anand Nageswaran Bharat. "Optimization of the air handling system of a multi-cylinder light-duty engine running on reactivity controlled compression ignition- a simulation study, 2016.

[88] European Union official bulletin diary: CEPE number 83 regulation, 07 series. [2015/1038].

[89] Kittelson D. "Engine and Nanoparticles: a Review," Journal of Aerosol Science, 1998-29-575, 1998.

[90] Shi J, Harrison R, Brear F. "Particle size distribution from a modern heavy duty diesel engine," The Science of the Total Environment, 1999-235-305, 1999.

[91] Armas O., Gómez A., Mata C., Ramos A. "Particle size distributions from a city bus fuelled with ethanol–biodiesel–diesel fuel blends". Fuel 111, 393– 400, 2013.

[92] J. Storey, S. Curran, S. Lewis, T. Barone, T. Dempsey, M. Moses-DeBusk, M. Hanson, V. Prikhodko, W. Northrop, Evolution and current understanding of physicochemical characterization of particulate matter from reactivity controlled compression ignition combustion on a multi cylinder light-duty engine, Int. J. Engine Res. (2016).

[93] Benajes, J., Novella, R., Arthozoul, S., Kolodziej, C., "Injection Timing Effects on Premixed Low Temperature Combustion Particle Emissions from Light and Heavy Duty Diesel Engines," 14th ETH-Conference on Combustion Generated Nanoparticles, ETH-Zurich, Switzerland, August 1-4, 2010.

[94] Prikhodko V., Curran S., Barone T., Lewis S. "Emission characteristics of a diesel engine operating with in-cylinder gasoline and diesel fuel blending". SAE Int. J. Fuels Lubr., 946–955, 2010.

[95] Lucachick G., Curran S., Storey J., Prikhodko V., Northrop William F. "Volatility characterization of nanoparticles from single and dual-fuel low temperature combustion in compression ignition engines". Aerosol Sci. Technol. 50, 436–447, 2016.

[96] Northrop William F., Madathil Praveen V., Bohac Stanislav V., Assanis Dennis N. "Condensational growth of particulate matter from partially

premixed low temperature combustion of biodiesel in a compression ignition engine". Aerosol Sci. Technol. 45, 26–36, 2011.

[97] Kolodziej C., Wissink M., Splitter D., Hanson R. et al. "Particle size and number emissions from RCCI with direct injections of two fuels". SAE Technical Paper, 2013.

[98] Zhang Y., Ghandhi J., Rothamer D. "Comparison of particulate size distributions from advanced and conventional combustion – part I: CDC, HCCI, and RCCI". SAE Int. J. Engines, 2014.

[99] Northrop W., Bohac S., Chin J., Assanis D. "Comparison of filter smoke number and elemental carbon mass from partially premixed low temperature combustion in a direct-injection diesel engine". J. Eng. Gas Turbines Power 133, 102804, 2011.

[100] Curran S., Prikhodko V., Cho K., Sluder S., Parks J., Wagner R.et al. "In-cylinder fuel blending of gasoline/diesel for improved efficiency and lowest possible emissions on a multi-cylinder light-duty diesel engine". SAE technical paper 2010-01-2206, 2010.

[101] García A. " Estudio de los efectos de la post inyección sobre el proceso de combustión y la formación de hollín en motores diésel". Doctoral Thesis, Universitat Politècnica de València, CMT-Motores Térmicos, 2009.

[102] Molina S. A. "Influencia de los parámetros de inyección y la recirculación de gases de escape sobre el proceso de combustión en un motor Diésel". Tesis doctoral, Universitat Politècnica de València, CMT-Motores Térmicos, 2003.

[103] Novella R. "Estudio de la influencia de los ciclos Atkinson y Miller sobre el proceso de combustión y la formación de emisiones contaminantes en un motor Diésel". Tesis doctoral, Universidad Politécnica de Valencia, CMT-Motores Térmicos, 2009.

[104] Benajes J., Pastor J.V., García A., Boronat V., "A RCCI operational limits assessment in a medium duty compression ignition engine using an

adapted compression ratio". Energy Convers. Manage, 126, 497–508, 2016.

[105] Kakaee A.-H., Nasiri-Toosi A., Partovi B., Paykani A. "Effects of piston bowl geometry on combustion and emissions characteristics of a natural gas/diesel RCCI engine". Appl. Therm. Eng., 102, 1462–1472, 2016.

[106] Benajes J., Pastor J. V., García A., Monsalve-Serrano J. "An experimental investigation on the Influence of piston bowl geometry on RCCI performance and emissions in a heavy-duty engine". Energy Convers. Manage., 103, 1019–1030, 2015.

[107] Inagaki K, Fuyuto T, Nishikawa K, Nakakita K and Sakata I. "Dual-Fuel PCI Combustion Controlled by In-Cylinder Stratification of Ignitability". SAE Technical Paper 2006-01-0028, 2006.

[108] Kastner L.J. "An investigation of the airbox method of measuring the air consumption of internal combustion engines". Proceedings of the Institution of Mechanical Engineers, Vol. 157 no 1, pp. 387-404, 1947.

[109] "Measurement of intake air or exhaust gas flow of Diesel engines". SAE Standards J244, 1992.

[110] de Rudder K. "An approach to low-temperature combustion in a small HSDI diesel engine". Doctoral Thesis, Universitat Politècnica de València, Departamento de Máquinas y Motores Térmicos, 2007.

[111] Novella R. "Estudio de la influencia de los ciclos Atkinson y Miller sobre el proceso de combustión y la formación de emisiones contaminantes en un motor Diésel. Doctoral Thesis, Universitat Politècnica de València, Departamento de Máquinas y Motores Térmicos, 2009.

[112] Sherman M.T., Chase R., Mauti A., Rauker Z. and Silvis W. "Evaluation of Horiba MEXA 7000 Bag Bench Analyzers for Single Range Operation". SAE Technical Paper, 1999-01-0147, 1999.

[113] Sherman M.T., Mauti A., Rauker Z. and Dageforde A. "Evaluation of Mass Flow Controller Gas Divider For Linearizing Emission Analytical Equipment". SAE Technical Paper, 999-01-0148, 1999.

[114] Degobert P. Automobiles and pollution. SAE International, 1995.

[115] "Regulation (EC) No 595/2009 of the European Parliament and of the Council of 18 June 2009 on type-approval of motor vehicles and engines with respect to emissions 100 3. Tools and methodology from heavy duty vehicles (Euro VI) and on access to vehicle repair and maintenance information and amending Regulation (EC) No 715/2007 and Directive 2007/46/EC and repealing Directives 80/1269/EEC, 2005/55/EC and 2005/78/EC. Official Journal of the European Union, Vol. 52 no L275, pp. 1-14, 2009". http://eur-lex.europa.eu.

[116] Silvis W.M. "An Algorithm for Calculating the Air/Fuel Ratio from Exhaust Emissions". SAE Technical Paper, no 2016-04-05, 1997.

[117] Christian R., Knopf F., Jasmek A. and Schindler W. "A new method for the filter smoke number measurement with improved sensitivity". MTZ Motortechnische Zeitschift, 54, 16-22, 1993.

[118] Prikhodko V., Curran S., Barone T., Lewis S. "Emission characteristics of a diesel engine operating with in-cylinder gasoline and diesel fuel blending". SAE Int. J. Fuels Lubr., 946–955, 2010.

[119] Curran S., Prikhodko V., Cho K., Sluder S., Parks J., Wagner R.et al. "In-cylinder fuel blending of gasoline/diesel for improved efficiency and lowest possible emissions on a multi-cylinder light-duty diesel engine". SAE technical paper 2010-01-2206, 2010.

[120] Monsalve-Serrano J. Dual-Fuel compression ignition: Towards clean, highly efficient combustion. 2016.

[121] Benajes J., López J.J. and R. Novella A. García. "Advanced methodology for improving testing efficiency in a single-cylinder research diesel engine". Experimental Techniques, 32, 41-47, 2008.

[122] Payri F, Olmeda P, Martín J, García A. "A complete 0D thermodynamic predictive model for direct injection diesel engines". Appl Energy, 2011. http://dx.doi.org/10.1016/j.apenergy.2011.06.00.

[123] Lapuerta M., Ballesteros R. and Agudelo J.R. "Effect of the gas state equation on the thermodynamic diagnostic of diesel combustion". Applied Thermal Engineering, 26, 1492-1499, 2006.

[124] Woschni G. "A Universally Applicable Equation for the Instantaneous Heat Transfer Coefficient in the Internal Combustion Engine". SAE Technical Paper, no 670931, 1967.

[125] Payri F., Margot X., Gil A. and Martn J. "Computational Study of Heat Transfer to the Walls of a DI Diesel Engine". SAE Technical Paper, no 2005-01-0210, 2005.

[126] Degraeuwe B. "Contribution to the thermal management of DI Diesel engines". Doctoral Thesis, Universitat Politècnica de València, Departamento de Máquinas y Motores Térmicos, 2007.

[127] Torregrosa A., Olmeda P. and Degraeuwe B. and Reyes M. "A concise wall temperature model for DI Diesel engines". Applied Thermal Engineering, 26, 1320-1327, 2006.

[128] Martín J. "Aportación al diagnóstico de la combustión en motores Diésel de inyección directa". Doctoral Thesis, Universitat Politècnica de València, Departamento de Máquinas y Motores Térmicos, 2007.

[129] Nazemi M, Shahbakhti M. "Modeling and analysis of fuel injection parameters for combustion and performance of an RCCI engine". *Appl Energy* 2016;165:135–50.

[130] Splitter D., Hanson R., Kokjohn S., Wissink M. and Reitz R.D. "Injection Effects in Low Load RCCI Dual-Fuel Combustion". *SAE Technical Paper*, no 2011-24-0047, 2011.

[131] Yu S, Zheng M. Ethanol–diesel premixed charge compression ignition to achieve clean combustion under high loads. Proc Inst Mech Eng, Part D: *J Autom Eng* 2015.

[132] Payri F, Olmeda P, Martín J, García A. A complete 0D thermodynamic predictive model for direct injection diesel engines. *Appl Energy* 2011;88(12):4632–41.

[133] Payri F. and Desantes J.M. *Motores de combustion interna alternativos*. Editorial Reverté, 2011.

[134] Giakoumis E.G. "Cylinder wall insulation effects on the first- and second-law balances of a turbocharged diesel engine operating under transient load conditions". Energy Conversion and Management, Vol. 48 no 11, pp. 2925-2933, 2007.

[135] Shabir M.F., Authars S., Ganesan S., Karthik R. and Kumar Madhan S. "Low Heat Rejection Engines – Review". SAE Technical Paper, no 2010-01-1510, 2010.

[136] Kokjohn S., Hanson R., Splitter D. and Reitz R.D. "Fuel reactivity controlled compression ignition (RCCI): a pathway to controlled high-effciency clean combustion".International Journal of Engine Research, Vol. 12 nº 3, pp. 209-226, 2011.

[137] Monsalve-Serrano J. Dual-Fuel compression ignition: Towards clean, highly efficient combustion. 2016.

[138] Benajes J., García A., Monsalve-Serrano J., Balloul I., Pradel G. "An assessment of the dual-mode reactivity controlled compression ignition/conventional diesel combustion capabilities in a EURO VI medium-duty diesel engine fueled with an intermediate ethanol-gasoline blend and biodiesel". Energy Conversion and Management, Vol. 123, Pages 381-391, 2016.

[139] Benajes J., Molina S., García A., Belarte E., Vanvolsem M. An investigation on RCCI combustion in a heavy duty diesel engine using in-cylinder blending of diesel and gasoline fuels. Applied Thermal Engineering, Vol. 63, Pages 66-76, 2014.

[140] Yifeng Wang, Mingfa Yaoc, Tie Lia, Weijing Zhanga, Zunqing Zhengc. A parametric study for enabling reactivity controlled

compression ignition (RCCI) operation in diesel engines at various engine loads. Applied Energy, Vol. 175, Pages 389–402, 2016.

[141] TSI Model 379020A: engine exhaust particle sizer spectrometer *Operation and Service Manual*.

[142] European Union official bulletin diary: CEPE number 83 regulation, 07 series. [2015/1038].

[143] Bermúdez V., Pastor, José V., López J. Javier, Campos D. "Experimental correlations for transient soot measurement in diesel exhaust aerosol with light extinction, electrical mobility and diffusion charger sensor techniques". Meas. Sci. Technol. 25, 065204, 2014.

[144] Benajes, J., Garcia, A., Monsalve-Serrano, J., and Boronat, V., "Particulates Size Distribution of Reactivity Controlled Compression Ignition (RCCI) on a Medium-Duty Engine Fueled with Diesel and Gasoline at Different Engine Speeds" SAE Int. J. Engines 10(5):2017, doi:10.4271/2017-24-0085.

[145] Kolodziej C., Wissink M., Splitter D. and Hanson, R. "Particle Size and Number Emissions from RCCI with Direct Injections of Two Fuels" SAE Technical Paper 2013-01-1661, 2013, doi:10.4271/2013-01-1661.

[146] Zhang, Y., Ghandhi, J., and Rothamer, D., "Comparison of Particulate Size Distributions from Advanced and Conventional Combustion - Part I: CDC, HCCI, and RCCI" SAE Int. J. Engines 7(2):820-834, 2014, doi:10.4271/2014-01-1296.

[147] Prikhodko, V., Curran, S., Barone, T., Lewis, S. et al., "Emission Characteristics of a Diesel Engine Operating with In-Cylinder Gasoline and Diesel Fuel Blending" SAE Int. J. Fuels Lubr. 3(2):946-955, 2010, doi:10.4271/2010-01-2266.

[148] Harris SJ, Maricq MM. "Signature size distributions for diesel and gasoline engine exhaust particulate matter" Journal of Aerosol Science, 2001-32-749, 2001.

[149] Benajes, J., Garcia, A., Monsalve-Serrano, J., and Boronat, V., "Gaseous emissions and particle size distribution of dual-mode dual-fuel diesel-gasoline concept from low to full load". Appl. Therm. Eng. 120, 138–149, 2017.

[150] Storey J., Curran S., Lewis S., Barone T., Dempsey T., Moses-DeBusk M., Hanson M., Prikhodko V., Northrop W., "Evolution and current understanding of physicochemical characterization of particulate matter from reactivity controlled compression ignition combustion on a multi cylinder light-duty engine". Int. J. Engine Res. (2016).

[151] Kittelson D.B., "Engines and nanoparticles: a review". J. Aerosol Sci. 29 (5/6) (1998) 575–588.

[152] Wang B., Mosbach S., Schmutzhard S., Shuai S., Huang Y., Kraft M., "Modelling soot formation from wall films in a gasoline direct injection engine using a detailed population balance model". Appl. Energy 163 (2016) 154–166.

[153] Benajes, J., Garcia, A., Monsalve-Serrano, J., and Boronat, V., "An investigation on the particulate number and size distributions over the whole engine map from an optimized combustion strategy combining RCCI and dual-fuel diesel-gasoline". Energy Conversion and Management, 140, 98–108, 2017.

[154] Abdul-Khalek I, Kittelson D, Brear F. "Diesel trap performance: particle size measurements and trends". SAE technical paper 982599; 1998, http://dx.doi. org/10.4271/982599.

[155] Prikhodko V, Curran S, Barone T, Lewis S, Storey J, Cho K, et al. "Diesel oxidation catalyst control of hydrocarbon aerosols from reactivity controlled compression ignition combustion". In: Proceedings of the ASME 2011 international mechanical engineering congress and exposition (vol. 9), Denver, CO, 11–17 November 2011, pp. 273–278. New York: ASME.

[156] Konstandopoulos A, Kostoglou M, Skaperdas E, Papaioannou E, Zarvalis D, Kladopoulou E. "Fundamental studies of diesel particulate

filters: transient loading, regeneration and aging". SAE technical paper 2000-01-1016, http:// dx.doi.org/10.4271/2000-01-1016.

[157] Jiang H, Wang J, Shuai S. "Visualization and performance analysis of gasoline homogeneous charge induced ignition by diesel". SAE technical paper 2005-01- 0136; 2005.